C-TERMINAL SPLICE VARIANTS OF THE MU OPIOID RECEPTOR DIFFERENTIALLY REGULATE SIGNAL TRANSDUCTION AND LIGAND BIAS

A Dissertation

Presented to the Faculty of

Weill Cornell Graduate School of Medical Sciences

in Partial Fulfillment of the Requirements for the

Degree of Doctor of Philosophy

by

Ankita Narayan

January 2017

C-TERMINAL SPLICE VARIANTS OF THE MU OPIOID RECEPTOR DIFFERENTIALLY REGULATE SIGNAL TRANSDUCTION AND LIGAND BIAS

Ankita Narayan, Ph.D.

Cornell University 2017

The opioid field and the quest for the ideal analgesics with limited side effects has accumulated decades of research and thousands of new opioid compounds. However, in spite of the substantial advances in the understanding of opioid receptor pharmacology, the main stays of pain management remain to be mu analgesics such as morphine, fentanyl, and oxycodone, that exhibit the side effect profile - tolerance, dependence, constipation, respiratory depression, and euphoria resulting in abuse and addiction. The opioid response is mediated in conjunction by G protein and β-arrestin signaling pathways, where the G protein pathway is often linked to the therapeutic effect of the drug and the β-arrestin pathway is linked to the side effects. More recently, the field has focused on developing biased agonists that activate only the subset of signaling pathways important for the therapeutic effect while limiting the unwanted side effects. Much of the recent work in the field has explored ligand bias at only the MOR-1 variant. However, the mu receptor gene, Oprm1, shows extensive alternative splicing and more than 60 different splice variants have been identified across different species. In this study, we explored the differences across the C-terminal variants of the mu opioid receptor and how these differences at the tip of the C-terminal tail might impact its ability to stimulate G protein coupling, β-arrestin

recruitment, and ultimately, signal bias. In our comparisons across the the C-terminal variants, we were able to identify a C-terminal variant, MOR-1O which showed significant β-arrestin bias relative to MOR-1. The MOR-1O receptor variant contains exons 1, 2 and 3 like MOR-1, with splicing downstream of exon 3 where it has exon 7 instead of exon 4 in MOR-1. We were able to generate an exon 7 knockout mutant mouse model by introducing a stop codon at the 5'-end of exon 7 (E7) to stop translation at the end of exon 3 in variants that contain exon 7. Interestingly, the mE7M mice show a phenotype similar to the β-arrestin-2 KO mice. These mE7M mice have no substantial difference in analgesic sensitivity or physical dependence but develop no tolerance in response to morphine. This provides a strong support for our in-vitro findings and suggests the functional interaction between the E7-associated C-terminal tails and β-arrestin-2. These findings are critical because they not only provide a potential target for therapeutic intervention to alleviate the morphine effects, but also, provides additional insights regarding the mu opioid receptor variants and their signaling biases to better screen for future new opioid analgesics.

BIOGRAPHICAL SKETCH

The author, Ankita Narayan, grew up in New Delhi, India. Following graduation from Delhi Public School in 2006, she moved to Philadelphia, Pennsylvania. In 2010, she graduated from Drexel University magna cum laude with a Bachelor of Science in Biomedical Engineering. She conducted her undergraduate research in the laboratory of Dr. Janet Clark in the Pharmacology department of Drexel University College of Medicine. While at Drexel, Ankita also interned at Merck & Co. working on drug discovery in the Department of Endocrinology at West Point, Pennsylvania.

In 2011, Ankita moved to Boston, Massachusetts and started working as a Research Associate at the Department of Genetics in the Harvard Medical School. During her time at Harvard, she studied the role of serotonergic system in affecting aggressive behavior in mice. In 2012, Ankita moved to New York City and enrolled in the Neuroscience Graduate Program at Weill Cornell Graduate School of Medical Sciences. During her first year as a graduate student, she completed rotations with Dr. Teresa Milner and Dr. Daniel Heller. In 2013, Ankita joined Dr. Gavril Pasternak's laboratory at Memorial Sloan Kettering Cancer Center, where she conducted her thesis research.

Throughout her career, Ankita has sought not simply to become better educated, but also better rounded — a "whole" person. Her extensive background working in drug development has equipped her with a deep

understanding of the basic research and clinical trial processes that are involved in bringing new drugs to market. While being deeply embedded in the PhD program at Cornell, Ankita also augmented her scientific background with business knowledge through her work with healthcare start-ups and taking business courses.

LIST OF FIGURES

LIST OF TABLES

TABLE OF CONTENTS

Chapter I - Introduction

The G-protein Coupled Receptor

G-protein coupled receptors (GPCRs) constitute the largest family of cell surface receptors and are found in all eukaryotes. The diversity of GPCRs is represented by the multiplicity of stimuli to which they respond, as well as by the variety of intracellular signaling pathways activated by them. About half of all known drugs work through GPCRs, as they mediate the response to an enormous diversity of signaling molecules, including hormones, mediators and neurotransmitters. There are approximately 800 unique GPCRs, out of which, 460 have been predicted to be olfactory receptors (Fredriksson et al., 2003). Their primary function is to transduce extracellular stimuli into intracellular signal and are involved in the regulation of a wide variety of physiological processes like, the sensory perception of pain, light, cognition, inflammation and immunity.

Despite the chemical and functional diversity of signaling molecules that bind to them, all GPCRs have a similar structure. Most of the initial structural insights about GPCR structure came from the rhodopsin family. Rhodopsin was easily obtained in large quantities from the bovine retina and was much more stable than most other GPCRs. The concentration of rhodopsin in rod outer segments is about 3mM, which is orders of magnitude higher than that of typical hormone or neurotransmitter receptors (Stryer, 1986). Findlay and

Pappin first modeled rhodopsin in 1986 and soon after that, a number of other GPCR models were also published (Findlay et al., 1986; Burbach et al., 1992; Chou et al., 1992; Cronet et al., 1993).

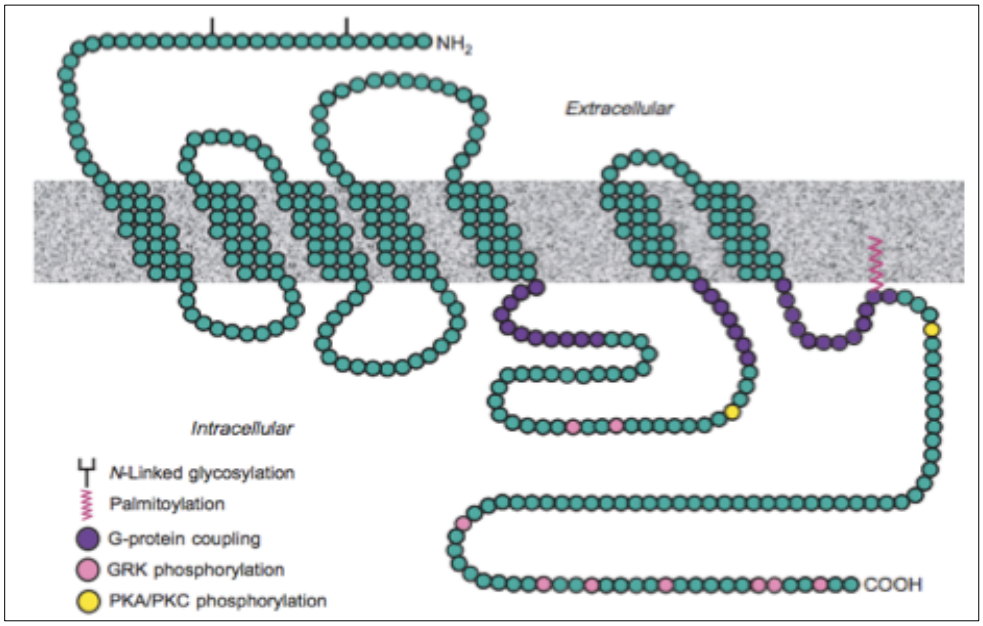

Figure 1 Seven trans-membrane receptor (Lefkowitz et al.,2000)

All GPCRs consist of seven trans-membrane (TM) segments with an extra-cellular amino terminus and an intra-cellular carboxyl terminus (Figure 1). The TMs are comprised of a single polypeptide chain that threads back and forth across the lipid bilayer. The TM segments show the greatest homology across GPCRs with the most differences at amino terminus, the carboxyl terminus and the intracellular loop spanning TM5 and TM6 (Pierce et al., 2002). Around this period of time in the 1980-90s, there was also a lot of ongoing effort towards developing amino acid similarity matrix methods. This enabled the characterization of the salient features of amino acid residues in the

proposed TMs and helical regions of the receptors (Attwood et al., 1991; Overington et al., 1992). These approaches helped provide a fingerprint for the helical regions of each GPCR and enabled clustering of the known receptor sequences into families and subtypes.

The GPCRs have been clustered into 5 sub-categories based on their sequence similarity: the rhodopsin family (701 members), the adhesion family (24 members), the frizzled family (24 members), the glutamate family (15 members) and the secretin family (15 members). The rhodopsin family of receptors have short N-termini and bind peptide, amine and lipid like molecules in a ligand-binding pocket defined by the TM regions of the protein (Nordström et al., 2009). The adhesion family is the second largest GPCR family. These receptors are characterized by long serine and threonine-rich N-termini. It has been speculated that these long N-termini have a role in cell-to-cell communication (Bjarnadottier et al., 2007). The frizzled receptors have long cysteine-rich N-termini that interact with the curly twisted Wnt protein and have a role in cell polarity. The Glutamate GPCRs are characterized by the "Venus Flytrap" mechanism, which is found in the N-termini and is crucial for ligand binding. In the Secretin family, all GPCRs have a hormone-binding domain (HBD) in their N-termini that interacts with peptide hormones (Schioth et al., 2007).

The β-adrenergic receptor for catecholamines became the prototype for the intense study of GPCRs, which lead to the unraveling of the structural basis of receptor function. A major part of the research that

ultimately led to the unraveling of the GPCR molecular structure came from the work of Earl Sutherland in the 1950s (Sutherland, 1971). Even though Sutherland's work focused on studying the mechanism of phosphorylase activation by epinephrine and glucagon and the discovery of the 'second messenger' system rather than the receptor function itself, he viewed the β-adrenergic receptor for epinephrine as a regulatory component of the adenylyl cyclase system. He explored the relationship between the receptors and enzyme catalytic activity by focusing particularly on the β-adrenergic stimulation of adenylyl cyclase. In 1970s, the study of membrane receptors was transformed by the development of radio-ligand binding studies, which permitted the direct study of the receptors for the first time. Once the radio-ligands were available, the challenge of purifying a functional adenylyl cyclase coupled receptor was undertaken.

Another crucial advancement came with the successful development of an affinity chromatography matrix, which was used to couple a β-adrenergic antagonist to agarose and purify the functionally active receptor. By 1982, the β2-adrenergic receptor was purified from amphibian erythrocytes and the β1-adrenergic receptor was purified from avian erythrocytes (Shorr et al., 1981; Shorr et al., 1982). Donnelly's three-dimensional model of the human β2-adrenergic receptor was used as the basis for construction of the GPCR models (Donnelly et al., 1989; Kobilka et al., 1992). These biochemical studies complemented Sutherland's work and also lead the way towards separating the concept of receptors from the catalytic moiety of

adenylyl cyclase and provided evidence that the receptors could be found in agonist-driven complexes with G proteins (Haga et al., 1977; Limbird et al.,1977; 1978).

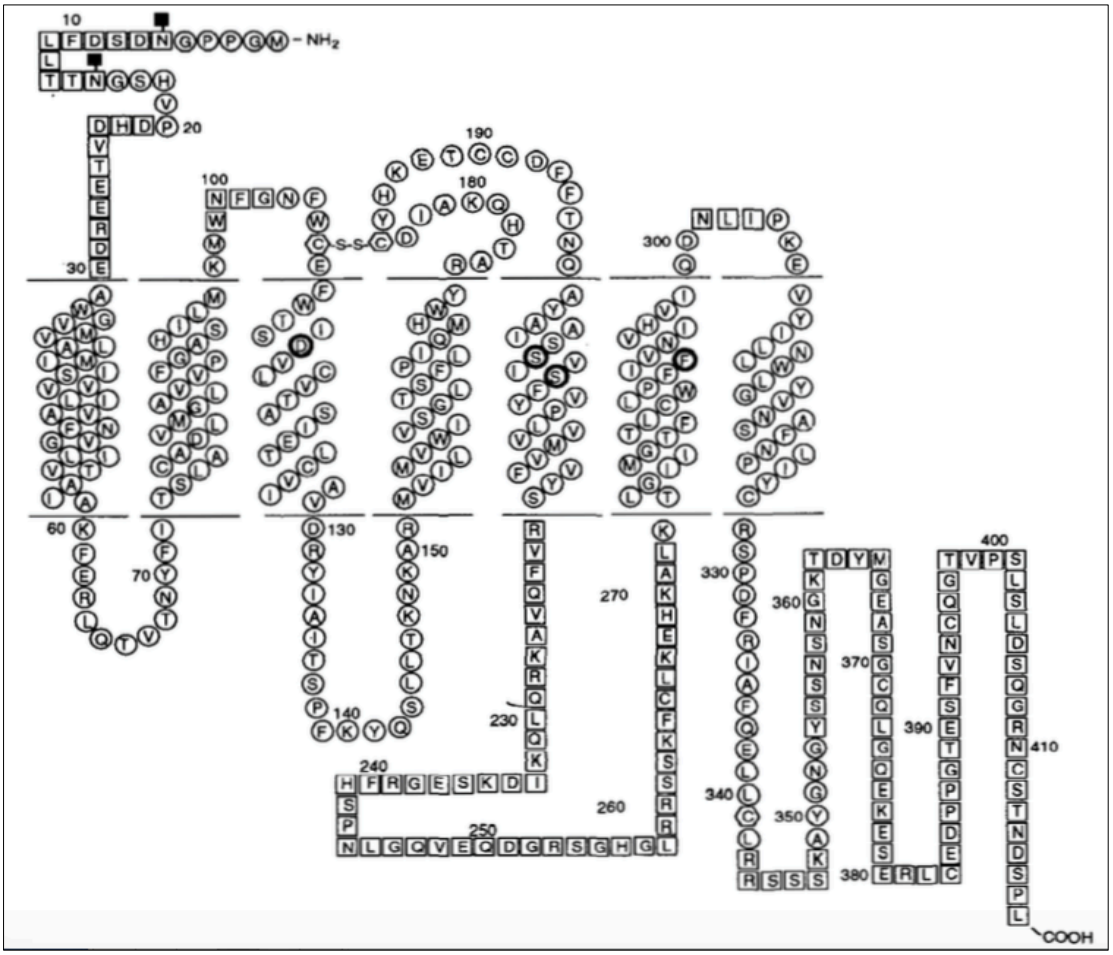

Figure 2 Primary structure of the hamster β2-adrenergic receptor showing the proposed topology of the seven transmembrane helices. The extracellular domain is at the top of the figure. Glycosylation sites are indicated with solid boxes. The boundaries of the eell membrane are represented by dashed lines. (Strader et al., 1994)

All GPCRs are glycoproteins that have at least one consensus sequence for N-linked glycosylation (Asn-X-Ser/Thr) in the extracellular domain. These putative glycosylation sites are usually

located near the N terminus of the protein, although occasionally there are potential sites in the second extracellular loop. Cloning and sequence determination of more members of β-adrenergic receptor family of receptor proteins showed that these receptors are characterized by seven hydrophobic stretches of 20-25 amino acids, predicted to form TM helices, connected by alternating extracellular and intracellular loops. Most of the primary sequence homology is contained in the hydrophobic TM regions of the GPCRs, whereas the hydrophilic loops show more divergence. The primary sequence identity in the TM domain of these receptors ranges from 85-95% for species homologs of a given receptor, 60-80% for related subtypes of the same receptor, 35-45% for other members of the same family and 20-25% for unrelated GPCRs (Strader et al., 1994).

GPCR Signal Transduction

The classical paradigm of GPCR signal transduction suggests that conformational changes in the receptor arise upon ligand binding. This allows it to couple to the heterotrimeric G proteins and regulate downstream effector molecules. However, the activation of a GPCR by its ligand also initiates the process of receptor desensitization. Desensitization is an adaptive process used by cells to arrest G protein signaling, potentially, preventing the harmful effects that could result from persistent receptor stimulation. Waning responsiveness to continuous or repeated stimulation constitutes the phenomenon of desensitization. Almost every GPCR undergoes desensitization, and

despite their diversity, most GPCRs use a universal mechanism involving the coordinated action of two families of proteins, the G protein coupled receptor kinases (GRKs) and the arrestins (Freedman et al., 1996; Ferguson, 2001).

G protein Signaling

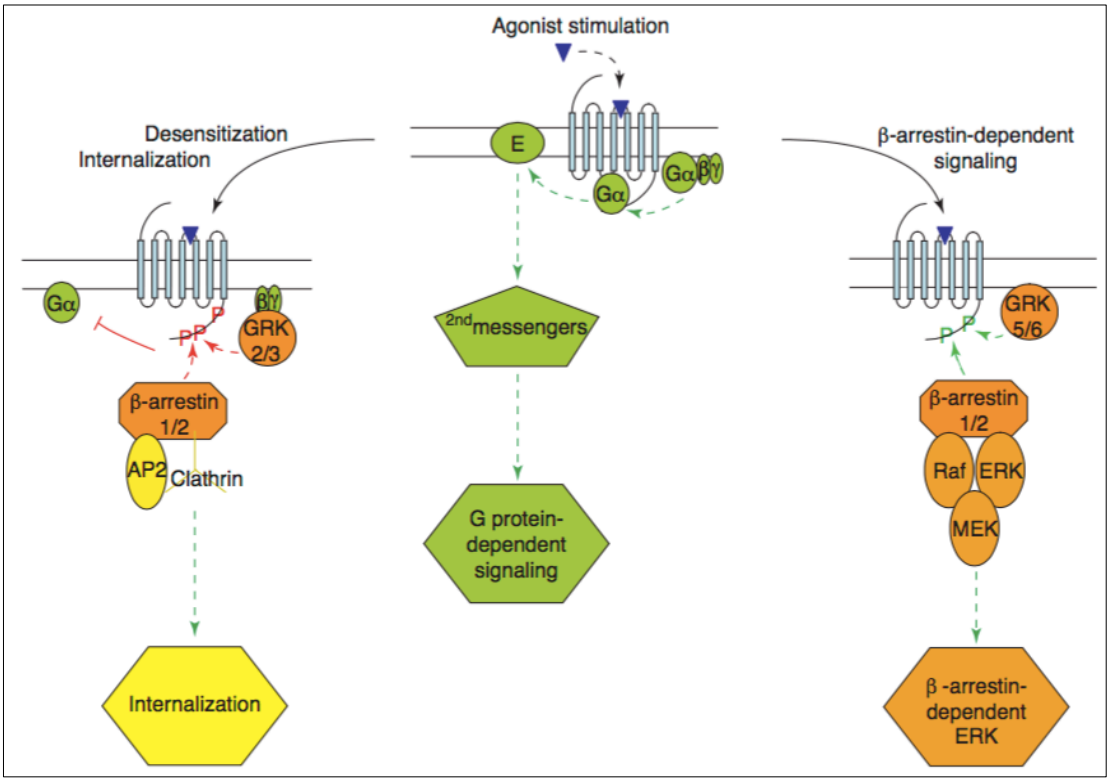

Figure 3 Schematic of GPCR signal transduction starts after agonist stimulation. Activated GPCR causes the dissociation of the heterotrimeric G protein that activates second messenger signaling. GRK 2/3 mediated β-arrestin recruitment leads to the internalization of the receptor and can also lead to desensitization. GRK 5/6 mediated β-arrestin recruitment leads to the activation of β-arrestin dependent ERK pathways and other kinases.

In the absence of an agonist, GPCRs exist in a low-affinity state. Agonist binding causes a conformational change that transforms GPCRs into a transient high-affinity complex comprising of the

agonist, activated receptor and the heterotrimeric GTP-binding proteins. The G proteins are attached to the cytoplasmic face of the plasma membrane, where they act as relay molecules while coupling the receptor to enzymes or ion channels (Pierce et al., 2002). The idea that guanine-nucleotide regulatory proteins functionally connect receptors with effectors was first conceived in 1971, by Martin Rodbell (Rodbell et al., 1971). However, it wasn't until 1987, that the G protein was purified and shown to be heterotrimeric, comprising of α, β and γ subunits (Gilman et al., 1987). The β and γ subunits remain associated in a tightly linked complex. The overall combination of α, β and γ subunits increases the combinatorial complexity of G-proteins. The α subunit is responsible for GTP and GDP binding and for GTP hydrolysis. So far, 16 α, 5 β and 12 γ proteins have been cloned. There are 4 main sub-families of the α subunit: $\mathbf{G_s}$ proteins cause the stimulation of adenylyl cyclase, $\mathbf{G_i}$ proteins cause the inhibition of adenylyl cyclase as well as the activation of G-protein-coupled inwardly rectifying potassium (GIRK) channels; $\mathbf{G_q}$ proteins couple to the activation of phospholipase Cβ; and $\mathbf{G_{12}}$ proteins couple to activation of Rho Guanine nucleotide exchange factors (GEFs) (Pierce et al., 2002).

In the basal state, the α subunit is bound to a GDP and the G protein is in its inactive state. The activated receptor acts as a Guanine nucleotide exchange factor (GEF) promoting the dissociation of GDP from the G protein and its replacement by GTP. The GDP-GTP exchange causes the dissociation of the heterotrimeric G-protein into α

subunits and βγ dimer, both of which can regulate separate effectors (Pierce et al., 2002).

Table 1 G protein subunits and their functional effectors. (Pierce et al., 2002)

G-protein subunits	**Effectors**
G_s	Adenylyl cyclase
G_{olf}	RGS-PXI, calcium channels, c-Src tyrosine kinases
G_t	cGMP phosphodiesterase
G_{gust}	Phosphodiesterases
$G_{i1,2,3}$	Adenylyl cyclase, c-Src tyrosine kinase
G_o	Rap1GAP1
Gz	Rap1GAP1
G_q, G_{11}, $G_{14,15,16}$	Phospholipase C, LARG RhoGEF
G_{12}, G_{13}	p115 RhoGEF, PDZ-RhoGEF, LARG RhoGEF
$G_{\beta\gamma}$	GIRK K+ channels, GRKs, Adenylyl cyclases, Phospholipases

Eventually, the α subunit acts as a GTPase and hydrolyzes the GTP back to GDP and re-associates with the βγ to reform an inactive G protein. The GTPase activity of the α subunit is enhanced by the binding of a second protein called the regulator of G protein signaling (RGS) proteins. There are about 25 RGS proteins encoded in the human genome, each of which is thought to interact with a particular set of G proteins (De Vries et al., 2000; Ross et al., 2000).

G proteins act by modulating the levels of cyclic AMP (cAMP). cAMP was first identified as a small intracellular mediator in the 1950s (Sutherland, 1971). It was while studying the mechanism of phosphorylase activation by epinephrine and glucagon that Sutherland succeeded in establishing the first cell preparations in which hormonal effects could be observed. These systems led him to the discovery of the 'second messenger' responsible for the actions of these hormones, cAMP, and to the enzyme responsible for its formation, adenylyl cyclase. Adenylyl cyclase is a large transmembrane protein with its catalytic domain on the cytosolic side of the plasma membrane. Once synthesized, cAMP is rapidly hydrolyzed by cAMP phosphodiesterases to adenosine 5'-monophosphate (5'-AMP). The normal concentration of cAMP inside the cell is about 10^{-7}M, but an extracellular signal can cause the cAMP levels to change by more than 20 folds in seconds (Lefkowitz et al., 2000).

All GPCRs that are coupled to stimulatory G_s proteins, activate adenylyl cyclase and increases cAMP concentration. Inhibitory G_i proteins inhibit adenylyl cyclase and usually act by directly regulating ion channels rather than by decreasing cAMP content. cAMP can directly activate certain types of ion channels. However, it exerts most of its effects by activating cAMP-dependent protein kinase (PKA). PKA catalyzes the transfer of terminal phosphate group from ATP to specific serines or threonines of selected target proteins, thereby regulating their activity. PKA consists of a complex of 2 catalytic and 2 regulatory subunits. The binding of cAMP to the regulatory subunits alters their

conformation, causing them to dissociate from the complex. The released catalytic subunits can also phosphorylate downstream substrates.

GRK-mediated regulation

G protein receptor kinases (GRKs) are known to phosphorylate the activated or the agonist-occupied conformation of the receptor, thereby, mediating homologous or agonist-specific desensitization. The agonist-occupied receptor gets phosphorylated after the GRK kinases are recruited to the plasma membrane and form a complex with the receptor. The GRKs are encoded by a family of seven genes, GRK1-GRK7. They have been divided into three subfamilies: the first consists of GRK1 and GRK7. GRK1 and GRK7 are confined to the retinal rods and cones, respectively. The second subfamily consists of the pleckstrin homology domain-containing GRK2 and 3, which interact with the βγ subunits of G proteins and phosphatidylinositol 4,5-bisphosphate. The third group consists of GRK 4, 5 and 6. These GRKs remain constitutively associated with the plasma membrane through covalent attachment of either fatty acids or isoprenes to their carboxyl termini. Although the GRKs do show some receptor specificity, they are present fairly widely distributed and regulate a large, overlapping portfolio of receptors (Moore et al., 2007).

GRKs phosphorylate the agonist-activated receptor at specific serine and threonine residues located in the C-tail and the third intracellular

tail. Phosphorylation by GRKs promotes binding of an arrestin molecule to the receptor while, also uncoupling the receptor from its respective G proteins. Several studies have suggested that GRK2 is often the major GRK associated with signal termination (Figure 3). However, the absence of subtype specific inhibitors for GRKs and the fact that GRK2 knockout mice are embryonically lethal has made determining the specificity of its action difficult to understand.

Table 2 GRK mutations and their functional consequences (Moore et al., 2007)

GRK	**Target GPCR**	**Phenotype**
GRK1	Rhodopsin	Prolonged response of retinal cells to light
GRK2	Unknown	Embryonic lethality
GRK2(-/+)	β_1/ β_2 - AR	Enhanced cardiac contractility to isoproterenol
GRK3	Odorant receptor Muscarinic	Olfactory supersensitivity, Enhanced airway response to methacholine
GRK5	M2 muscarinic D1 dopamine 5-HT1A, CXCR4	Enhanced hypothermia, hypoactivity, central cholinergic supersensitivity
GRK6	CXCR4	Impaired lymphocyte chemotaxis

Several studies have tried to use small interfering RNAs (siRNA) to inhibit individual GRKs to better understand their specific function. This approach helped characterize that GRK2 and -3 are primarily responsible for agonist- dependent receptor phosphorylation, β-arrestin recruitment and functional uncoupling, whereas GRK5 and -6 make lesser contributions to this outcome (Kim et al., 2005; Ren et al., 2005). Another recent siRNA study demonstrated that H1 histamine receptor desensitization is mediated by endogenous GRK2 but not GRK5 (Iwata et al., 2005). However, GRK5 and -6 have also been implicated in various examples of receptor desensitization in vivo and/or in vitro (Gainetdinov et al., 1999; Gainetdinov et al., 2003).

Second-messenger kinase regulation

Phosphorylation of GPCRs by other protein kinases like PKA, PKC and c-Src can also serve as negative feedback regulators and uncouple the receptor from its respective G proteins. They can also regulate heterologous forms of desensitization in which kinase activation by one type of receptor can lead to phosphorylation and desensitization of another receptor. For example, it was shown that in the β-adrenergic receptor, PKA mediated receptor phosphorylation switches the receptor away from G_s and enhances G_i coupling (Daaka et al., 1997; Zamah et al., 2002). This facilitates Gi-coupled pathways such as stimulation of the extracellular signal related kinase (ERK) and mitogen-activated protein kinase (MAPK) pathway.

ß-arrestin mediated signaling

The arrestins constitute of a four-member family. The arrestin 1 and arrestin 4 are expressed in the retinal rods and cones respectively. Arrestin 2 and 3 (also knows as β-arrestin 1 and 2), on the other hand, are present ubiquitously with highest levels of expression in the brain and spleen. The differential effects of visual arrestins and β-arrestins on GPCR endocytosis is influenced by the C-terminal tail of the molecule. β-arrestins, but not the visual arrestins, show affinity for clathrin in vitro. This happens through the binding of an LIEF

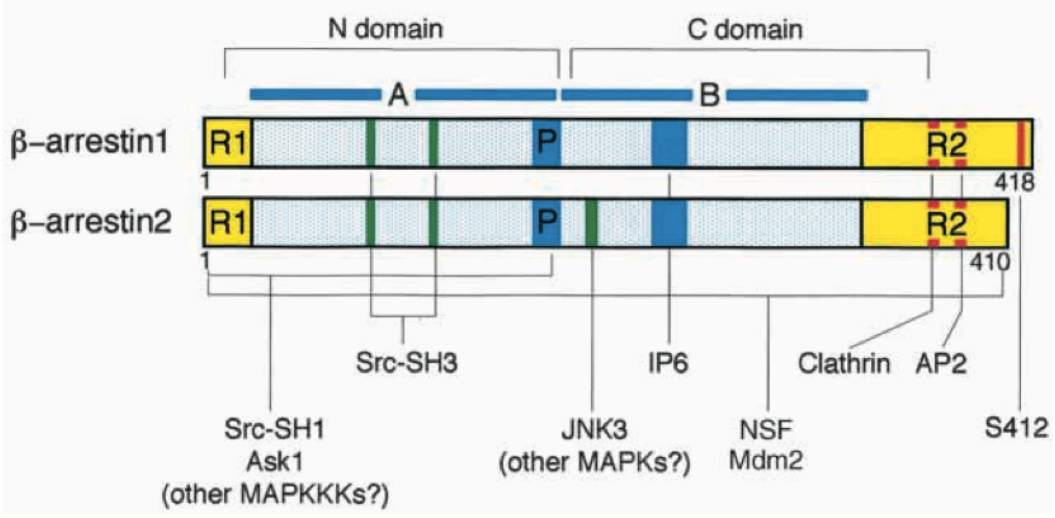

Figure 4 β-arrestin structure

sequence (residues 374-377 of β-arrestin2) to a N-terminal region of the clathrin heavy chain (residues 89-100) (Goodman et al., 1996; Krupnick et al., 1997). β-arrestin2 can also directly bind β2 adaptin subunit of the AP-2 adaptor complex. The AP-2 complex plays a

critical role in linking GPCRs to the clathrin endocytic machinery by binding to clathrin, dynamin, and EPS-15 and initiating receptor endocytosis (Kirchhausen, 1999).

Knockout animal models have been used to study the importance of β-arrestins in the regulation of GPCR function in vivo. It has been shown that a β-arrestin1 knockout animal is developmentally normal and exhibits normal cardiac parameters. However, the stimulation of the β-adrenergic receptor in this animal produces an exaggerated hemodynamic response (Conner et al., 1997). This indicates that β-arrestin1 plays a role in cardiac β-adrenergic receptor desensitization. Similarly, in a homozygous β-arrestin2 knockout animal, it has been shown that analgesic effect of morphine is prolonged in these animals with an inability to develop tolerance (Bohn et al., 1999; Bohn et al., 2000)

Table 3 β-arrestin mutation and their functional consequence

GRK	**Target GPCR**	**Phenotype**
Arrestin	Rhodopsin	Prolonged photoresponse in retinal rods
β-*arrestin 1*	β_1/ β_2 - AR	Enhanced contractility in response to isoproterenol
β-*arrestin 2*	Mu opioid CXCR4	Prolonged morphine analgesia and reduced tolerance Impaired lymphocyte chemotaxis

All members of the family can bind to agonist-occupied receptor that has been phosphorylated by GRKs. Arrestin binding is known to sterically block the receptor-G protein interaction and plays a critical role in the process of homologous desensitization. In addition to their role in GPCR desensitization, β-arrestins also act as adapter proteins that regulate endocytosis and target GPCRs to clathrin coated pits. This process of GPCR sequestration not only plays a role in desensitization of the GPCR in the continued presence of an agonist, but also, in receptor resensitzation and downregulation. β-arrestins are also known to bind to other proteins involved in signal transduction like the Src family kinases, ERK 1/2 and JNK3 MAP kinase cascades.

Desensitization of the receptor is a process that begins within seconds of agonist exposure and is initiated by phosphorylation of the receptor. Protein kinases like PKA and PKC, phosphorylate distinct serine and threonine residues in the C-terminal tail. As demonstrated with the β2-adrenergic receptor, the phosphorylation of C-tail by PKA, even in the absence of arrestins, is enough to impair receptor-G protein coupling (Benovic et al., 1985). The β2-adrenergic receptor kinases, GRK2 and GRK3, have C-terminal Gβγ subunit binding and pleckstrin homology domains, and they translocate to the membrane as a result of interactions between these domains and free Gβγ subunits and inositol phospholipids. The role of GRK phosphorylation is to increase the affinity of the receptor for arrestins (Lohse et al., 1993). There are several studies to suggest that receptor internalization and

dephosphorylation is required for the resensitization of many GPCRs (Sibley et al., 1986; Ferguson et al., 2001). With the β2-AR, it was seen that knocking out β-arrestin1/2 in a double knockout MEFs prevents the downregulation of the receptor (Kohout et al., 2001).

Even though arrestins play a role in the agonist-promoted internalization of a GPCR, the extent of β-arrestin involvement varies significantly depending on the receptor, agonist and cell type. For example, a study by Oakley et al. demonstrated that both β2-adrenergic receptor and vasopressin V2 receptor recruit β-arrestin. However, β2-adrenergic receptor recycles and resensitizes rapidly, whereas, V2R is known to recycle and resensitize slowly. This difference between the receptors was reversed when C-terminal tails of the two receptors was switched. These results indicated that the interaction of the β-arrestin with a specific motif in the C-tail dictates these effects (Oakley et al., 1999). Some of these differences could also be a result of differences in endogenous expression pattern of GRKs and β-arrestins and the availability of alternative pathways for GPCR endocytosis.

Mu Opioid Receptor

Clinical Relevance

Pain is a pervasive problem throughout medicine and opiates remain the most widely used analgesics in its treatment. Chronic pain affects more Americans than heart disease, cancer, and diabetes combined and is a major cause of visits to primary care physicians. Opioid alkaloids and related pharmaceuticals are the most effective analgesics for the treatment of acute and chronic pain and represent the largest market share of prescription pain medications (Melnikova, 2010). Out of the different classes of opioids, the mu receptor is the main opioid target for the management of pain. Opioid drugs such as morphine, fentanyl, and oxycodone are widely used clinically as powerful pain relievers. Due to their long history and proven efficacy, these mu opioids are the mainstay in the management of moderate to severe acute and chronic pain.

However, despite the efficacy and utility of these opioid analgesics, side effects such as respiratory depression, inhibition of gastrointestinal transit, addiction, physical dependence and tolerance limit the utility of most currently used opiates (Cherny et al., 2001). In addition to the side effects, prescription opioids are also currently the most commonly abused drugs in the United States. According to recent statistics, 44 people die from prescription opioid overdose each day, which is greater than deaths from heroin and cocaine combined

(Kochanek et al., 2015). The ability of opioids to alleviate pain as well as produce euphoria has led to elevated rates of opioid prescriptions, use, misuse, hospitalizations, overdoses, and abuse in the last decade. Not only that, major depression, post-traumatic stress disorder, and anxiety disorders are more prevalent in patients who suffer from chronic pain (McWilliams et al., 2003).

There is a significant unmet need for strong analgesic drugs with improved side effect profiles (Moskovitz et al., 2011). As a result, there is a lot of ongoing effort in the field to develop better analgesics that continue to provide the therapeutic pain relieving effect of opioids while minimizing some of the associated side effects. Decades of work in the opioid field has repeatedly demonstrated the heterogeneity of opioid receptor targets. We believe that a better understanding of the receptor multiplicity and their downstream signaling targets would facilitate the development of a new generation of opioid drugs that could provide pain relief with fewer side effects.

Discovery and Cloning of the Mu Opioid Receptor

In the early 1900s, physiologists such as Langley and Ehrlich first proposed the existence of entities understood as receptors, which bound and mediated the actions of drugs. The history of opioid receptor pharmacology, specifically, complements the history of the radioligand binding assay. The first proposal for the existence of opioid receptors came in the 1950s when several groups looked at the

structure-activity relationships of the opiates (Beckett et al., 1954; 1956; Portoghese, 1966). Subsequently, Goldstein et al. tried to use [^{3}H]levorphanol and its inactive enantiomer to demonstrate the existence of a stereo-selective receptor for opiates. They were, however, unsuccessful due to the low specific activity of the radioligand. It wasn't until 1973 that 3 groups - Pert and Snyder, Simon et al, and Terenius, individually demonstrated the existence of opioid receptors in the mammalian central nervous system using radioligand binding assays with [^{3}H]naloxone, [^{3}H]dihydromorphine and [^{3}H]etorphine respectively (Pert and Snyder, 1973; Simon et al., 1973; Terenius, 1973). The biologically active (-)-enantiomers of methadone, levallorphan, and levorphanol competed this binding with very high affinity while the inactive (+)- enantiomers exhibited dramatically lower affinity for the opioid binding site. This confirmed the identity of the site as the target mediating the physiological effects of opioid drugs.

Soon after the initial demonstration of opiate binding, additional studies revealed biochemical properties of opioids. Collier et al. reported the ability of opioid agonists to regulate the intracellular cAMP level in brain homogenates (Collier et al., 1974). Sharma et al. substantiated these finding in a cell line model using NG108-15 cells. Acute activation of the opioid receptor resulted in a Pertussis toxin (PTX) sensitive decrease in the intracellular cAMP levels. Chronic activation of the receptor, however, resulted in an increase of the cAMP levels when the agonist was removed (Collier, 1980). The inhibition of adenylyl cyclase regulated by the opioid receptor was mediated by Gi,

Go or Gz subunits. Pert et al. were further able to discriminate between agonist and antagonist binding to the receptor in vitro. They reported that sodium decreased agonist binding but increased antagonist binding (Pert et al., 1973).

Cloning of μ-OR happened in 1993 shortly after the cloning of the delta opioid receptor. Interestingly, it happened using a cDNA probe for mouse DOR-1 TM3 with low hybridization stringency. When this DOR cDNA was transfected into COS-7 cells, it conferred the μ-OR binding site that had sub-nanomolar affinity for [^{3}H]diprenorphine and nanomolar affinity for [D-A1a2,N-Me-Phe4,Gly-ol5]-enkephalin (DAMGO) (Chen et al., 1993). Further characterization of this binding site showed that binding was competed with high affinity by mu-selective small molecules such as naloxonazine, β-funaltrexamine, and cyprodime, while the delta- selective peptides DPDPE and DSLET and kappa-selective small molecule U50,488 had dramatically lower affinity. These COS-7 cells expressing MOR-1 when treated with DAMGO, showed a decrease in the steady state levels of cAMP after forskolin stimulation. Soon after this, a number of other labs also reported sequences of the mu receptor (Eppler et al., 1993; Fukuda et al.,1993; Thompson et al., 1993; Wang et al., 1993).

The mu receptor comprises of four exons yielding the seven TM structure of a traditional GPCR. The first exon encodes the N-terminus and the first TM domain while the second and third exons each encoded an additional three TM domains. The fourth exon is

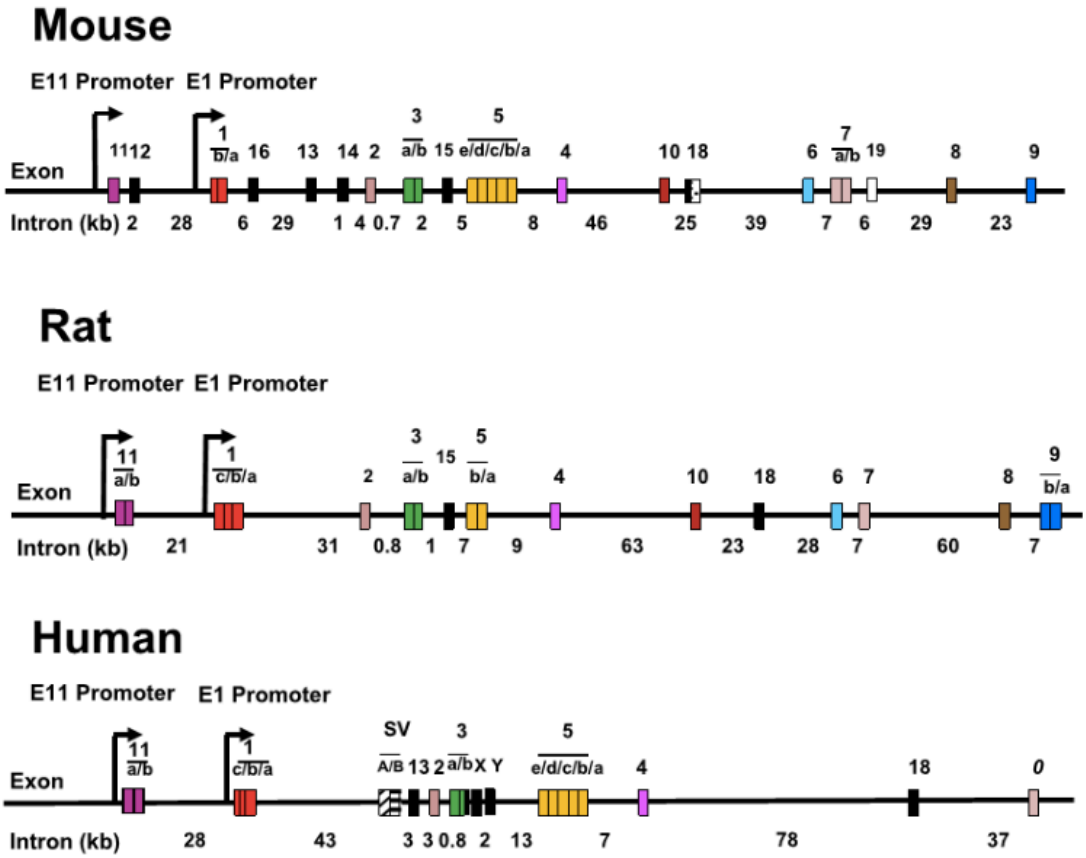

Figure 5 Gene Structure of Mouse, Rat, and Human Mu Opioid Receptor (OPRM-1). OPRM-1 undergoes extensive splicing, and exon structure is largely conserved across mammalian species. Boxes indicate exons and arrows indicate promoters. Genomic distances are indicated but are not to scale. Reproduced from (G. W. Pasternak & Pan, 2013).

responsible for coding only 12 amino acids at the tip of the intracellular C-terminus. Over the years, more than 60 splice variants have been isolated (Pasternak and Pan, 2013), out of which: there are 31 variants from mice (Doyle et al., 2006, 2007; Pan et al., 1999, 2000, 2005), 16 variants from rats (Zimprich et al., 1995, Pasternak et al., 2004; Xu et al., 2011;) and 19 variants from humans (Bare et al., 1994; Cadet et al., 2003; Pan et al., 2003; Pan, 2005; Choi et al., 2006; Xu et al., 2009).

Mu Opioid Receptor Multiplicity

The opioid field is unique with respect to the availability of extensive clinical data for a wide range of drugs even prior to the identification of the receptors. Clinicians have known for a long time that the opioids do not work equally well in every patient. Some patients respond better to certain drugs. The side effect portfolio also varies from patient to patient (Foley et al., 1985, 1996). In addition, opioids show incomplete cross-tolerance such that a patient who is highly tolerant to one mu opiate can be switched to another opiate at a lower dose (Cherny et al., 2001). These pharmacological observations cannot be reconciled with the existence of a single receptor and suggest the existence of multiple mu sites.

The first experimental evidence for multiple opioid receptors came from binding studies by Wolozin and Pasternak that revealed a second morphine binding site. They observed a biphasic displacement curves and non-linear Scatchard plots indicating heterogeneity in the mu binding site and named the two mu binding sites as mu1 and mu2 (Wolozin et al., 1981). It was proposed that the mu1 site binds opiates and enkephalins with high affinity (less than 1nM) and is irreversibly blocked by the antagonist naloxazone. The mu2 site, on the other hand, had lower affinity and selectively binds morphine with greater potency than several enkephalin analogs. In addition, it was also shown that mu1 and mu2 binding sites had distinct regional localization. Mu1 is thought to be associated with supraspinal

analgesia, whereas, mu2 is associated with respiratory depression and inhibition of gastrointestinal transit (Goodman et al., 1985, 1985a; Pasternak et al., 1983; Pasternak et al., 1986). Differences between the mu1 and mu2 sites were also demonstrated using [^{3}H]-DADL binding where it was observed that 80% of the binding did not correspond to classical mu or delta sites. The binding was sensitive to DAMGO and morphine and insensitive to DPDPE, confirming its mu-like nature (Clark et al., 1989). However, in the thalamus, both μ-OR and δ-OR selective ligands competed this binding with high affinity, which suggested [^{3}H]-DADL displayed selectivity for the mu1 site. The molecular identity of this site has not been identified.

Antisense mapping and Knockout Mice

Soon after the cloning of μ-OR, antisense knockdown studies were used to target receptor subtypes and understand the contribution of specific exons in the gene to the pharmacology. Antisense mapping involves the use of short oligodeoxynucleotides complementary to a targeted portion of mRNA to downregulate a gene product. These studies complement the antagonism studies but have the advantage of being more selective for the target gene. Depending on the abundance of the target mRNA, the antisense strategy typically reduces the protein levels by 25-50% and is reversible within 5 days after the final antisense treatment. This is consistent with estimates of approximately 3-5 day turnover times for opioid receptors (Ward et al., 1982; Standifer et al., 1994). However, a limitation of the antisense

strategy is that it requires multiple pretreatments with the antisense oligodeoxynucleotide.

Antisense studies of μ-OR supported previous pharmacological data indicating that not all mu agonists produce analgesia through the same molecular mechanism. For example, Morphine and M6G have similar affinity for the receptor; however, M6G is 100 fold more potent in its analgesic effects when given by an intracerebroventricular injection (Pasternak et al., 1987). Despite the presence of only one mu opioid receptor gene, the strict exon boundaries observed by antisense mapping suggests that alternative splicing could explain the pharmacological differences observed between morphine and M6G.

The Pasternak group utilized antisense oligonucleotides (ODNs) directed against the 5'-untranslated region of μ-OR clone (Rossi et al., 1994) and confirmed that the loss of these single genes alone was sufficient to impair analgesia of morphine. Rossi et al. demonstrated that antisense ODNs targeted to exons 1 and 4 blocked supraspinal morphine analgesia, while ODN's targeted to exons 2 and 3 failed to have any significant effect (Rossi et al., 1995). In contrast, supraspinal M6G analgesia was blocked by antisense ODNs targeted to exons 2 and 3 but not exons 1 and 4. Klein et al. observed similar results where exons 1 and 4 attenutated morphine but not heroin analgesia. Exon1 antisense also attenuated naloxone precipitated withdrawal from morphine and heroin (Klein et al., 2009). Another study in mice showed that ODNs against exon 2 blocked M6G, heroin, fentanyl and

etonitazine analgesia but had no effect on morphine (Rossi et al., 1996). With the subsequent discovery of mouse Oprm1 exons 6, 7, 8, 9, and 10, it was shown that antisense knockdown of these exons attenuated morphine but not M6G analgesia.

Multiple groups also examined endomorphin analgesia using antisense mapping and found some interesting results. Intrathecal antisense directed against exons 1 and 4 attenuated both endomorphin 1 and endomorphin 2 analgesia. Exon 8 antisense only attenuated endomorphin 1 analgesia and had no effect on endomorphin 2. Interestingly, however, supraspinal antisense directed against exon 1, but not exons 2 and 4, attenuated endomorphin 1 analgesia. Spinal and supraspinal endomorphin 1 and 2 analgesia were significantly attenuated by antisense directed against μ-OR exons 1, 2, 3, 4, 5, 7, 8, 9 but not exon 6 (Abbadie et al., 2002; Sanchez et al., 1999; Wu et al., 2002). Overall, these findings support the proposal that alternative splicing of the receptor leads to different receptor variants which regulate mu analgesics.

Mu Opioid Receptor Splice Variants

The mu opioid receptor gene Oprm1 has been identified in more than 30 vertebrate species ranging from non-mammalian vertebrates to humans (Figure 5). Mu opioid receptor gene homologues evolved early in vertebrate evolution, appearing first in teleosts as a gene comprised of 5 exons, each encoding a portion of the 7 TM domains that make up

the receptor (Herrero-Turrion & Rodríguez, 2008). Beginning in zebrafish, the introns separating exons 3-5 disappear to form a gene of 3 exons. A 4th exon was first seen in the chicken. This 4 exon structure is conserved across amphibian, reptile, and mammalian species, and share >71% amino acid identity. Exon 1 encodes for the extracellular N-terminal region as well as the first trans-membrane domain. Exon 2 encodes trans-membrane 2, 3 and 4. Exon 3 encodes trans-membrane 4, 5 and 6 as well as a significant portion of the C-tail. Exon 4 encodes the tip of the intracellular portion of the C-tail. Exon 4 is the major 3' exon in the C-terminus of MOR-1 in most species. Exon 11 is the major exon associated with 5' splicing. It has been identified in multiple mammalian species including rats and humans (Xu et al., 2009, Xu et al., 2011).

Although pharmacological approaches have distinguished between mu subtypes, only a single gene has been identified for the mu opioid receptor. The promoter associated with exon 11 is located upstream of exon 1 and has two active regions that are conserved in mouse and human (Xu et al., 2001; Xu et al., 2001) The promoter shares similarities with "housekeeping genes," as it contains high GC content and lacks a TATA box204. The gene is also under epigenetic control. The exon 1 promoter undergoes DNA methylation and histone modifications that can activate or silence the gene (Hwang et al., 2007; Hwang et al., 2009). The mouse OPRM1 gene contains at least 18 different exons spanning over 270 kb.

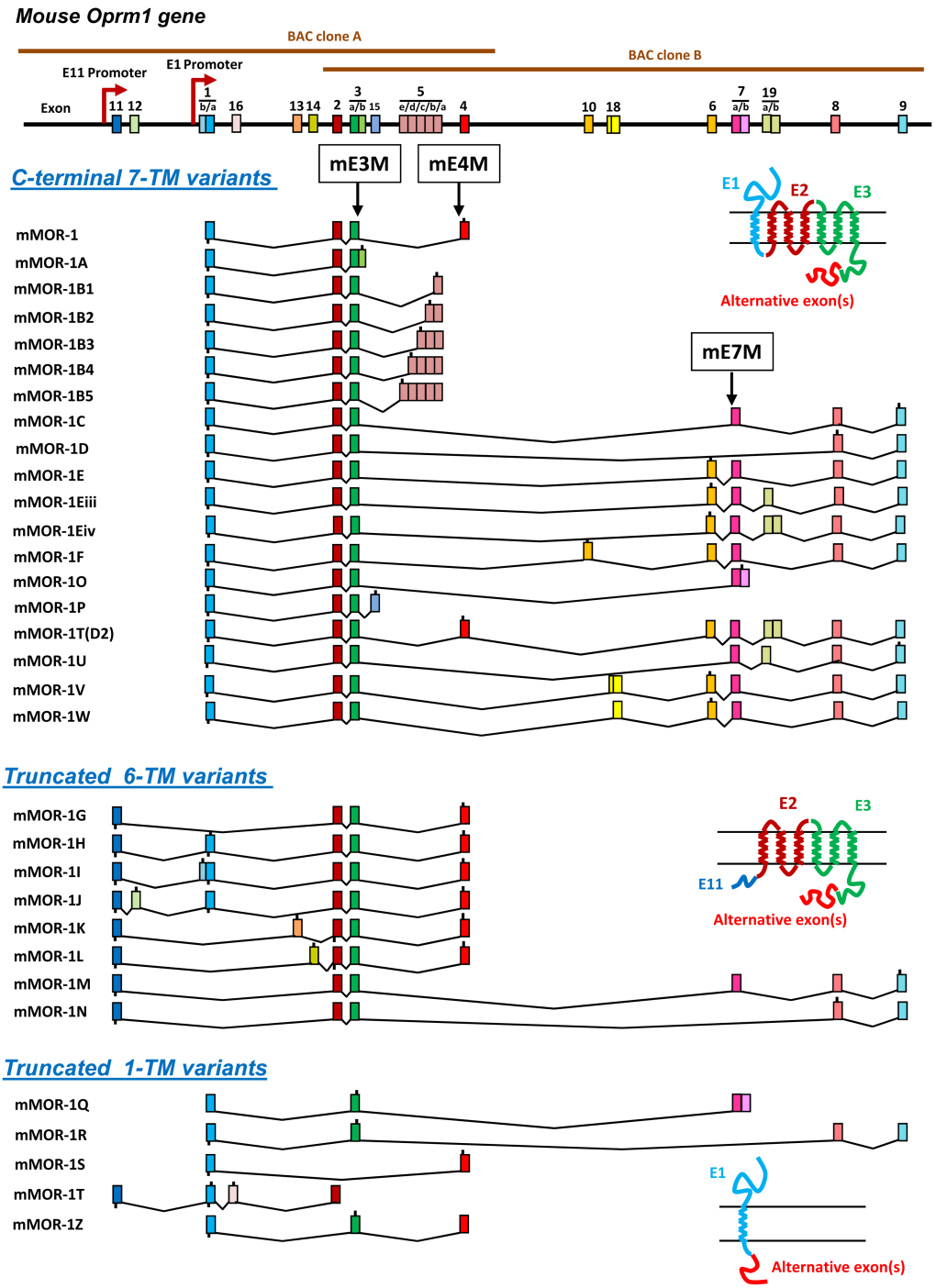

Figure 6 Mouse Oprm1 gene structure and alternative splicing. Oprm1 gene structure. Exons and introns are indicated by color-coded boxes and black horizontal lines, respectively. Promoters are showed by red arrows. Exons are numbered based upon the published data. Three classes of alternative splice variants, C-terminal full-length 7-TM variants, truncated 6-TM variants and truncated 1-TM variants, are indicated, and their predicted protein structures shown by cartoon inserts on right, in which color-coded structures match with corresponding color-coded exons (E). (Pasternak and Pan., 2013)

Three sets of μ-OR variants have been identified in rodents and humans. The first is the C-terminal variants. These are full-length 7TM variants that all contain exons 1,2, and 3 encoding the N-terminus and all the TM domains with splicing at the 3' end. The second set involves the exon-11 associated variants with splicing in the 5' end. Some of the exon-11 variants generate truncated 6TM receptor because of the absence of exon 1. The last set comprises the truncated variants with only a single TM domain encoded by exon 1.

C-terminal Splice Variants

C-terminal splice variants are all full-length variants that share exons 1, 2 and 3 with splicing downstream of exon 3. Although many of the variants share exon 3, the amino acid sequence downstream of exon 3 is unique for each variant due to reading-frame shifts or early termination. The length of the C-terminus in the C-terminal variants varies extensively with only 2 amino acids in mMOR-1B5 to 88 amino acids mMOR-1U. Since the MOR1 binding pocket is defined by TM 3, 5, 6 and 7; all of the C-terminal variants contain an identical binding pocket. As a result, all of the mu opioids have high affinity for all the C-terminal splice variants.

The splicing in rat and humans show some slight differences. For example, the alternative splicing of exon 5 generates 5 different variants in the mouse (mMOR-1B1 through mMOR-1B5), two variants in rats (rMOR-1B1 and rMOR-1B2), and five in humans (hMOR-1B1

through hMOR-1B5) with different C-terminal amino acid sequences depending on which splice site is used in exon 5 (Pan et al., 2005).

The splice variants are expressed in a very heterogeneous fashion. Some of the earlier studies examined the anatomical distribution of μ-OR mRNA in the brain. However, our current knowledge about the splice variants raises some questions regarding those results as most of the splice variants share some common exons. As a result, the mRNA probes might be labeling more than one species of mRNA (Mansour et al., 1994, Minami et al., 1995, Zhu et al., 1998). Regional differences in the expression pattern of these splice variants have also been established through semi-quantitative RT-PCR analysis. In mouse brain, it was shown that the thalamus has a higher level of expression of mMOR-1C and little expression of mMOR-1D and mMOR-1E mRNAs. The striatum and hypothalamus highly express mMOR-1E mRNA, whereas mMOR-1D has higher expression in the cortex, brain stem and periaqueductal gray.

Functional Differences

More than 20 different C-terminal splice variants of the mu receptor have been identified in mouse. The C-terminal splice variants of μ-OR differ in their regional distribution, agonist induced G protein coupling (as measured by [^{35}S]GTPγS binding), receptor phosphorylation, internalization and post-endocytic sorting. Spliced amino acid

differences at the C- terminus influence the ability of the opioids to activate the receptor independent of their receptor binding affinities.

Functional differences among the variants have been demonstrated using [^{35}S]GTPγS binding and adenylyl cyclase coupling. Zimprich et al. demonstrated that the functional coupling to adenylyl cyclase desensitizes at a slower rate in the MOR-1B variant, with a shorter C-tail, than in MOR-1. Pretreatment of the cells expressing the rMOR-1 variant showed a faster attenuation of the agonist induced inhibition of adenylyl cyclase in comparison to rMOR-1B variant. In addition to adenylyl cyclase, DAMGO induced desensitization measured as a decay of the opioid activated GIRK current, was also found to be much slower in MOR-1B than in the MOR-1 and MOR-1A variants (Oldfield et al., 2008). Another study in Human Embryonic Kidney 293 (HEK) cells showed similar results, where cells expressing the MOR-1B receptor desensitized at a slower rate during prolonged DAMGO exposure but re-sensitized at a faster rate than MOR-1 during agonist withdrawal. The same study also provided immunocytochemical evidence to show that DAMGO-induced internalization of MOR-1B happens much faster than that of MOR-1. Internalization is followed by rapid recycling of the receptor to the cell surface (Koch et al., 1998). Studies have shown in MOR-1, that the recycling of the receptor back to the cell surface following agonist-induced internalization is facilitated by the presence of an endocytic recycling sequence (Tanowitz et al., 2008)

The C-terminal differences of the variants are also associated with varying effects on efficacy and potency of the mu drugs. In Bolan et al., many mu opioids exhibited significant differences in their maximal stimulation relative to DAMGO across the different C-terminal splice variants of m μ-OR. β-endorphin stimulated [^{35}S]GTPγS binding in the MOR-1E expressing cells to a much greater degree (130%) than DAMGO, however in MOR-1C expressing cells, it displayed a maximal stimulation of only 44% (Table 4).

Table 4 Effects of opioids on [35S]GTPγS binding in MOR-1 splice variants. Adapted from Bolan et al., 2004

	MOR-1			**MOR-1A**		
	Ki	**EC50**	**% max**	**Ki**	**EC50**	**% max**
DAMGO	1.7 ± 0.4	68 ± 4	100	1 ± 0.3	70 ± 3	100
Morphine	5.3 ± 2.5	23 ± 2	102 ± 5	3.1 ± 0.5	19 ± 4	91 ± 2
M6G	6.4 ± 2.4	75 ± 18	122 ± 9	5 ± 1.5	114 ± 78	85 ± 9
Methadone	1.4 ± 0.1	73 ± 12	87 ± 9	0.7 ± 0.1	14 ± 3	90 ± 13
Fentanyl	2.3 ± 1.0	16 ± 2	145 ± 16	1.5 ± 0.6	60 ± 3	105 ± 23
β-Endorphin	8.4 ± 4.9	64 ± 7	97 ± 2	4.3 ± 1.0	111 ± 27	83 ± 3
	MOR-1C			**MOR-1D**		
	Ki	**EC50**	**% max**	**Ki**	**EC50**	**% max**
DAMGO	0.9 ± 0.2	62 ± 4	100	0.8 ± 0.2	62 ± 6	100
Morphine	2.7 ± 0.8	23 ± 5	75 ± 4	1.6 ± 0.2	82 ± 34	99 ± 3
M6G	4.5 ± 1.8	51 ± 9	63 ± 7	4.8 ± 0.9	93 ± 32	95 ± 1
Methadone	0.5 ± 0.1	57 ± 26	98 ± 5	1.4 ± 0.1	22 ± 1	102 ± 4
Fentanyl	1.2 ± 0.4	37 ± 17	86 ± 24	3.3 ± 1.5	49 ± 15	96 ± 1
β-Endorphin	5.8 ± 0.5	123 ± 19	44 ± 3	1.7 ± 0.5	73 ± 8	105 ± 6
	MOR-1E					
	Ki	**EC50**	**% max**			
DAMGO	0.6 ± 0.2	48 ± 4	100			
Morphine	2.4 ± 0.6	41 ± 13	116 ± 4			
M6G	5.6 ± 0.9	123 ± 87	90 ± 6			
Methadone	0.7 ± 0.3	25 ± 2	93 ± 5			
Fentanyl	1.2 ± 0.5	37 ± 16	90 ± 3			
β-Endorphin	4.9 ± 1.2	113 ± 25	130 ± 3			

The potency (EC50) of the drugs also varied among the clones with no correlation to [^{35}S]GTPγS binding and their binding affinity. DAMGO showed a 3 fold greater affinity in binding assays than morphine in MOR-1, but stimulated [^{35}S]GTPγS binding with a potency 3 fold lower than morphine in comparison. The most intriguing observation is that the relative efficacy of the drugs to each other varied from one variant to the other. In MOR-1, methadone stimulation was much lower than fentanyl, whereas in MOR-1C cells, methadone was far more efficacious than fentanyl.

To further add to the complexity of the signaling, the ability of these agonists to activate G proteins does not directly correlate with their ability to induce phosphorylation of the receptor, recruit β-arrestin and ultimately internalization. The amino acid differences in the C-terminal tail also lead to differences in potential phosphorylation sites among these variants. These differences have been shown to lead to significant implications in receptor pharmacology following agonist binding. The C-terminal tail is believed to be involved in recruiting intracellular proteins to the receptor signalosome, altering signaling and trafficking.

Signaling through β-arrestins is common to all GPCRs, however, the fate of the receptor- β-arrestin complex differs. β-arrestin signaling is mediated through a cluster of GRK-phosphorylated serine residues in the receptor carboxy terminal, which affects its ability to form a stable complex with β- arrestin (Schulz et al., 2004, Oakley et al., 2001).

Morphine bound receptor has low affinity for arrestins and undergoes limited receptor internalization in comparison to DAMGO (Groer et al., 2011; Haberstock-Debic et al., 2003).

The C-terminal splice variants differ in their agonist-selective membrane trafficking. Koch et al., have shown that MOR-1 and MOR-1C stably expressed in HEK cells exhibited phosphorylation, internalization and down-regulation in the presence of the mu agonist, DAMGO, but not in response to morphine. In contrast, MOR-1D and MOR-1E exhibited robust phosphorylation, internalization and down-regulation in response to both DAMGO and morphine. In addition, all the variants showed a similar desensitization pattern, measured during an 8-hour exposure to drug, and resensitization pattern, during a 50 minute drug withdrawal, in response to DAMGO. However, in response to morphine, MOR-1 and MOR-1C showed a faster desensitization and no resensitization as compared with MOR-1D and MOR-1E (Koch et al., 2001). Since phosphorylation and internalization of the receptor has been correlated with β-arrestin binding, these studies lay the ground for possible differences in arrestin recruitment pattern among the C-terminal splice variants.

In another study from our lab, we observed differences in the internalization pattern of the MOR-1 and MOR-1C variants in an in-vivo mouse model. The mice were treated with intracerebroventricular (i.c.v) DAMGO or Morphine. The internalization pattern was observed using brain slices treated with antibody against amino acids 410-430

in the murine MOR-1C or against amino acids 384-398 for MOR-1 immunoreactivity. It was observed that MOR-1C-like immunoreactivity was observed in the endosomes in the cytoplasm, following both DAMGO and morphine treatment. In contrast, DAMGO and not morphine, internalized MOR-1-like immunoreactivity (Abbadie et al., 2001).

N-terminal splice variants

The N-terminal splice variants were first identified by Pan et al in 2001, where they demonstrated the retention of M6G and heroin analgesia in Pintar's exon 1 knockout animal. The N-terminal variants are associated with the exon 11, which is an exon located 30kb upstream of exon 1 and contains an independent promoter region. A subset of the N-terminal variants skip exon 1 completely and lead to the formation of a truncated receptor with only 6TMs and lacking the first TM domain. Despite the truncation, these 6TM variants are expressed in a region-specific manner throughout the brain and spinal cord, albeit at lower levels relative to the full length MOR-1 (Abbadie et al., 2004; Ying-Xian Pan et al., 2001).

There was an initial contention that this truncated form of the receptor was unlikely to be functionally active as it did not share the 7TM architecture with the other GPCRs. However, the generation of the MOR exon 11 knockout animal confirmed the physiological relevance of these 6TM variants. The exon 11 knockout animal retained most of

the full length MOR variants, except the ones requiring exon 11 as well as exon 1. As expected, these animals showed a slight 20% reduction in the [^{3}H]-DAMGO sites as observed by the Bmax. Both, morphine and methadone, retained their full efficacy in these animals without significant loss of analgesic potency. However, mu agonists like, heroin, fentanyl and M6G showed a significant right-shift in their analgesic potency. This highlighted the importance of the exon 11-associated splice variants in the action of these drugs.

Taken together with the results from antisense mapping and reciprocal MOR exon 1 knockout animal from Pintar's group which expresses only truncated 6TM, the evidence overwhelmingly supports a model M6G and heroin act not only at the traditional mu receptors which mediate morphine's effects, but also a pharmacologically and genetically distinct population of receptors involving truncated 6TM receptors.

Phosphorylation sites at the μ-OR

Like any other GPCR, the C-tail of μ-OR gets phosphorylated after receptor binding and is involved in downstream signal transduction. The early mechanistic studies on receptor phosphorylation were done in 1996 that showed that phosphorylation of μ-OR is mediated via GRKs and not PKC (Zhang et al., 1996). The ability of the opioid ligand to induce phosphorylation is correlated to its efficacy. Full agonists such as DAMGO, etorphine induce high MOR-1 phosphorylation as

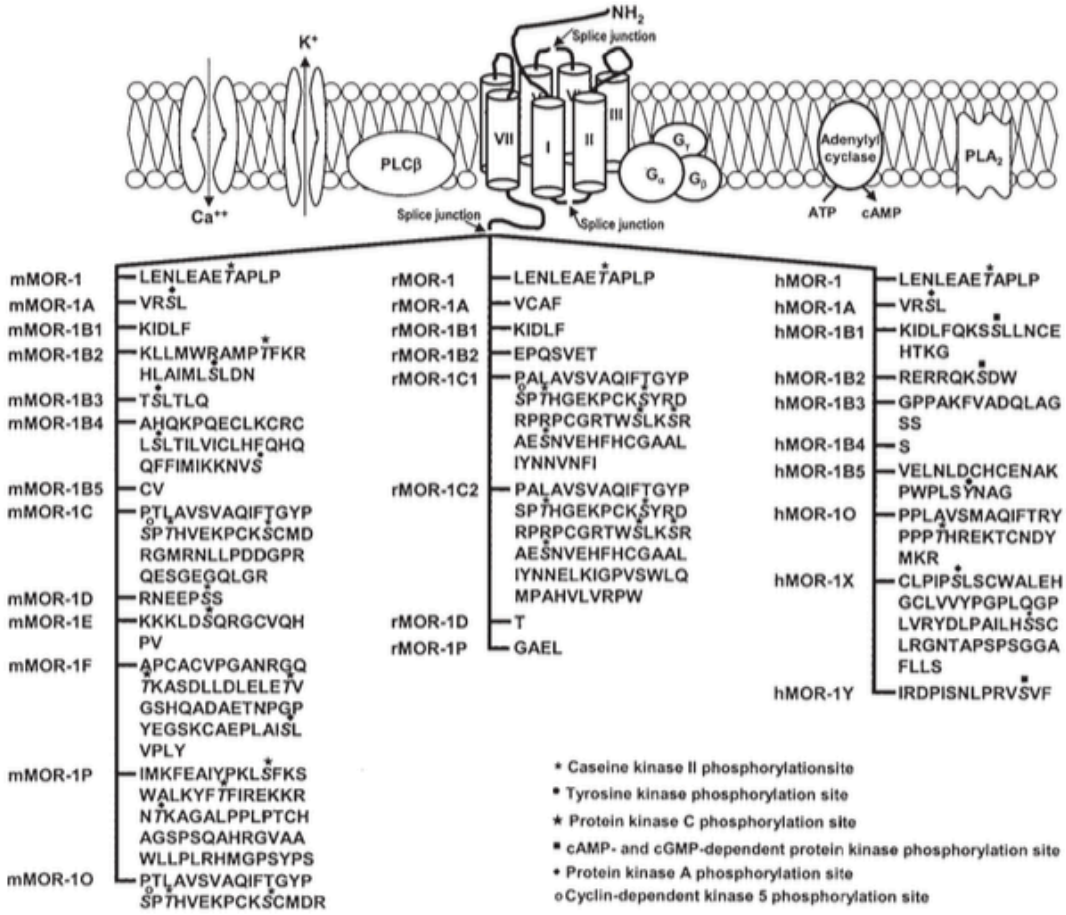

Figure 7 Predicted phosphorylation sites in the C-terminal Splice Variants of OPRM-1. Mouse, rat, and human c-terminal splice variant amino acid sequences are shown with symbols indicating predicted phosphorylation sites. Given the importance of phosphorylation in recruitment of b-arrestin, these differences are likely to have significant consequences on G- protein independent signaling and agonist bias. Reproduced from (Ying-Xian Pan, 2005).

against morphine. Arden et al. reported that morphine-receptor complex is a poor GRK substrate and therefore, induces lower levels of receptor phosphorylation in HEK293 cells (Arden et al., 1995). The morphine-induced receptor phosphorylation is through a cAMP-dependent protein kinase (PKA) mechanism whereas DAMGO-induced

phosphorylation is GRK dependent (Chakrabarti et al., 1998). Consequently, overexpressing GRK2 in HEK cells lead to high levels of receptor phosphorylation (Zhang et al., 1998). In CHO cells, however, Yu and colleagues reported that morphine was able to induce μ-OR phosphorylation without GRK overexpression (Yu et al., 1997). These findings show that one of the major caveats in trying to understand the MOR system is that the agonist induced phosphorylation as observed in cell models suffers from a system bias and is dependent on the levels of specific protein kinases present in the cellular system.

Initial experiments with deletion analyses were used to identify amino acid residues that are phosphorylated in MOR-1. Residues like Ser363 present in the C-tail showed basal phosphorylation even in the absence of agonist. Agonist induced the phosphorylation of 2 amino acid residues in the C-tail, Thr370 and Ser375 (Lau et al., 2011, Moulédous et al., 2015). Ser375 phosphorylation was shown to be much faster than Thr370 phosphorylation. The mutation of Ser375 to Ala reduced the rate and extent of receptor internalization, whereas mutation of Ser363 and Thr370 to Ala accelerated MOR-1 internalization kinetics (El Kouhen et al., 2001). Ser373, Thr370 and Ser375 lie in the exon 3 region and are all sites present in the conserved portion of C-tail. Additionaly, there is a Thr394 site that lies in the exon 4 region. Mutation of the Thr394 site to Ala in rMOR expressed in CHO cells results in the blunting of the agonist induced desensitization response (Pak et al., 1997). This could potentially link it to the β-arrestin mediated response. Deng et al. have also reported

GRK mediated Thr394 phosphorylation in the presence of agonists (Deng et al., 2000). However, other studies in HEK cells haven't been able to demonstrate phosphorylation of the Thr394 site. Some studies have also reported the phosphorylation of Tyr residues in addition to Ser/Thr sites but the results have been controversial.

Opioid receptor endocytosis is mediated by receptor phosphorylation and β-arrestin recruitment through the dynamin-dependent clathrin-coated pits pathway. β-arrestin recruitment as well as internalization of the receptor have been shown to be ligand dependent event. A number of studies have shown that agonist directed differences in β-arrestin2 recruitment are a function of the agonist's ability to phosphorylate μ-OR. For example, the DAMGO stimulated receptor shows higher levels of phosphorylation, β-arrestin recruitment as well as internalization in comparison to morphine (Bohn et al., 2004). Etorphine but not morphine is able to induce receptor endocytosis (Keith et al., 1996).

Interestingly though, it has been established that opioid receptor phosphorylation is not a prerequisite for receptor desensitization. Law and colleagues demonstrated that the time course of receptor phosphorylation is quite rapid in comparison receptor desensitization, as measured by adenylyl cyclase inhibition (Law et al., 2000). In addition, increasing the level of GRK expression increased the level of receptor phosphorylation but had no effect on the rate of receptor desensitization (El Kouhen et al., 1999, 2000; Law et al., 2000).

Crystal Structure

More recently, the crystal structure of μ-OR was solved in the presence of an antagonist. The authors used T4 lysozyme and the truncation of the N and C termini to facilitate crystallization of the receptor. It was confirmed that all opioid receptors belong to the class A rhodopsin-like subfamily of G protein-coupled receptors (GPCRs) with a common 7TM helical architecture. The crystal structure of MOR-1 was initially solved using the selective μ-OR antagonist β-FNA. The binding pocket of MOR-1 was exposed to the extracellular surface. The ligand covalently attached to the Lys233 side chain and made contact with TM 3, 4, 6 and 7. MOR-1 homodimerized through an association between TM1, TM2, and helix 8 located on the intracellular C terminus (Manglik et al., 2012).

Since then, the crystal structure of MOR-1 has also been solved in the agonist conformation. The receptor was bound by the morphinan BU72 and was stabilized in the agonist conformation using nanobodies (Huang et al., 2015). The nanobody created recognized MOR-1 bound to the selective agonist dmt-DALDA. As observed with the β-adrenergic, G protein binding was crucial for stabilizing MOR-1 in its agonist conformation. Interestingly, in comparison to the antagonist state, the agonist conformation of the receptor revealed no sodium ion, due to a rearrangement of the sodium binding site. This is consistent with previous findings that reflect that the sodium ion aids the allosteric stabilization of the inactive state of the receptor (Pert et

al., 1973). However, as with the previous study by Manglik et al., the receptor was truncated as the N terminus to facilitate crystallization. Therefore, the physiological relevance of these studies is ambiguous.

Biased Agonism

The classical idea of GPCR function relayed a two-state model where a receptor can exist in either an active or an inactive state. The drug action was described as a function of its affinity, potency and efficacy, where affinity is defined as the ability of the ligand to interact with the receptor as measured by a Ki value. Efficacy (Emax) is defined as the ability of the bound ligand to activate the receptor and produce a measurable response in the system and potency (EC50) refers to the amount of drug required to achieve the required biological response. More recent studies in GPCRs, however, support the idea of more than one active state or conformation of the receptor (Swaminath et al., 2004; Bokoch et al., 2010; Kahsai et al., 2011). The new evidence suggests that different ligands may be better at stabilizing one active state rather than another. This also sets forward the idea that the efficacies and potencies of the drug for these different active conformations of the receptors might vary and are not conserved among signaling pathways.

Biased agonism or functional selectivity refers to the ability of the drug to activate a selective cell signaling pathway yet show very little efficacy in activating another pathway, in a way that cannot be

explained by traditional models of receptor theory. Consequently, it has become an important potential drug property, as it allows the identification and development of ligands that may be better able to induce the therapeutic effects of the receptor while minimizing the adverse effects of drug treatment. Several recent studies provide examples of therapeutic applications of biased agonism at several different GPCRs, like, the parathyroid hormone receptors (Gesty-Palmer et al., 2009), GPR109A niacin receptor 2 (Walters et al., 2009), angiotensin II type 1 receptors (Zimmerman et al., 2012) as well as the MOR (DeWire et al., 2013).

Biased Agonism at μ-OR

Recent advances in the field allow for measuring multiple signaling outputs following activation of a receptor by a ligand, enabling the detection of ligand bias. There is an extensive body of work in the field that demonstrates agonist-determined differences in MOR-1 responsiveness to key signaling pathways, like the activation of G protein and specific Gα subunits, regulation by kinases and β-arrestins, as well as receptor internalization and desensitization.

G protein Coupling

Opioid receptors can couple to different inhibitory Gα subunits, like the $G\alpha_i$ and $G\alpha_o$. However, the agonist and the cellular system dictate the specific subunit that a ligand couples to. Massotte and colleagues examined the coupling efficiencies of agonists like DAMGO, morphine

and buprenorphine. They reported that in HEK293 cells, DAMGO fully activates $G\alpha_{i1}$ and only partially activates $G\alpha_{i2}$. Morphine stimulated both subunits and behaved as a partial agonist at both $G\alpha_{i1}$ and $G\alpha_{i2}$. Interestingly, Buprenorphine, which is a more potent analgesic than both DAMGO and Morphine acted as a partial agonist at both subunits (Massotte et al., 2002; Raehal et al., 2011). Another study compared DAMGO with other endogenous peptides like, Endomorphin-1, Endomorphin-2 and β-endorphin and showed that they are all equally efficient at recruiting $G\alpha_{i1}$ and $G\alpha_{oA}$. However, fentanyl, methadone, morphine and buprenorphine were partial agonists for both the subunits (Saidak et al., 2006).

Morphine and M6G, both agonists at the mu receptor, exhibit different signaling and analgesic profiles. M6G is 100 fold more potent analgesic than morphine. However, in binding assays, M6G labels the mu receptor less potently than morphine. Antisense studies have shown that an antisense probe targeting $G\alpha_{i2}$ blocks morphine analgesia but is inactive against M6G analgesia. Conversely, antisense blocking of $G\alpha_{i1}$ inhibits M6G analgesia without affecting morphine analgesia (Standifer et al., 1996). Although, it should be noted that the loss of function observed in these experiments does not necessarily imply a physical association of the specific Gα subunit to the receptor. It could be a result of an interruption anywhere along the response pathway. Studies have also shown that agonists induce differential G protein activation during short-term and long-term drug administration.

In rats, chronic morphine treatment results in a switch from the inhibitory $G\alpha_{i/o}$ coupling to $G\alpha_s$ coupling in the striatum, spinal cord and periaqueductal gray (Chakrabarti et al., 2005). This indicates that the different interacting receptor/Gα combinations may not be equivalent in terms of signaling efficiency and some of these combinations might better relay the structural changes induced by a given agonist.

Receptor Phosphorylation

Agonist binding induces recruitment of several protein kinases to the receptor that phosphorylate specific serine, threonine and tyrosine residues. However, the extent of receptor phosphorylation as well as the sites phosphorylated is ligand dependent. Using ^{32}P labeling in CHO-MOR-1, it has been shown that agonists like DAMGO, etorphine and methadone induce robust phosphorylation in comparison to morphine and buprenorphine (Yu et al., 1997). These findings have also been validated in HEK cell line using hemaglutinin-tagged (HA) receptor (Zhang et al., 1998; Koch et al., 2001; Schulz et al., 2004)

Koch and colleagues explored the differences in receptor phosphorylation among the C-terminal splice variants of the receptor, mMOR-1C, mMOR-1D and mMOR-1E in HEK293 cells. It was observed that MOR-1C, like MOR-1, showed higher levels of receptor phosphorylation in response to DAMGO in comparison to morphine. However, the agonist specific differences were obliterated in the

mMOR-1D and mMOR-1E variants and both DAMGO and morphine induced similar levels of receptor phosphorylation (Koch et al., 2001).

Recruitment of β-arrestins

β-arrestin recruitment has become one of the more popular segment within biased agonism at the MOR. β-Arrestin 2 knockout mice have enhanced and prolonged morphine analgesia with reduced morphine tolerance, respiratory depression and constipation (Bohn et al., 1999; Raehal et al., 2005). Several studies have connected β-arrestin recruitment to the MOR side effects and so there is a huge effort in the field to develop agonists that are biased against β-arrestin recruitment (DeWire et al., 2013; Van der Westhuizen et al., 2014). Several assays like the PathHunter (DiscoverX), which uses enzyme fragment complementation to quantitate β-arrestin2 recruitment, as well as bioluminescence resonance energy transfer (BRET) and fluorescence resonance energy transfer (FRET) assay are being rapidly used.

Agonists like morphine and heroin have been shown to be weak β-arrestin recruiters in comparison to DAMGO and etorphine (Zhang et al., 1998; Whistler et al., 1998; Bohn et al., 2004). Another study also confirmed that Met-Enkephalin, etorphine, DAMGO and fentanyl induced robust β-arrestin recruitment in comparison to morphine, oxycodone and buprenorphine (McPherson et al., 2010; Molinari et al., 2010).

Bohn and colleagues have developed a novel G protein biased agonist called herkinorin. Herkinorin has been demonstrated to be as efficacious as DAMGO at G protein coupling, ERK1/2 phosphorylation, cAMP inhibition in HEK293 as well as CHO cell lines expressing MOR-1. However, unlike DAMGO, herkinorin does not recruit β-arrestins (Harding et al., 2005; Groer et al., 2007; Xu et al., 2007). TRV130, is another G protein biased agonist that has been developed by Violin and colleagues (DeWire et al., 2013; Soergel et al., 2014; Viscusi et al., 2016).

Quantifying biased agonism

When trying to determine possible ligand bias, the methods for quantifying ligand bias are crucial. More so, because bias is usually not absolute and it is quite rare for an agonist at GPCR to fully activate one pathway and is completely inactive at another. As a result, the field is constantly evolving and several different approaches have been developed to quantify bias (Rajagopal et al., 2011; Kenakin et al., 2012, 2013). It is also important to consider that the observed response by a ligand at a signaling pathway is not solely determined by its affinity and efficacy. Rather, the observed response is a function of the differing coupling efficiencies of the signaling pathways referred to as system bias, as well as the differing conditions and sensitivities of the detection method called the observation bias.

Equimolar comparison:

The equimolar approach of quantifying bias was first proposed by Christopolous in 2010 (Gregory et al., 2010). It is a qualitative approach in which the data for a single ligand is collected in two different assays, such as a G protein assay and a β-arrestin assay. The responses of the two assays are then plotted against each other and the shape of the curve is used as a direct comparison of signaling through the two pathways. The concentration-response data are plotted against each other yielding a hyperbolic curve. One caveat with using just a hyperbolic curve is that it would suggest bias towards the assay that has a higher sensitivity. In order to avoid such a problem, the shape of the equimolar curve is normalized and compared to that of a reference balanced ligand. The bias of the test ligand is determined with respect to the balanced ligand.

Equiactive comparison:

Historically, it has been thought that all agonists activate the receptor by stabilizing a single active conformation of the receptor and that it is only the strength of the signal that varies and determines the observed efficacy. This model can also be referred to as the 'agonist potency ratio'. Potency of an agonist is the agonist concentration that produces 50% of the maximal response. This comparison can be performed using a formula for intrinsic relative activities proposed by Ehlert in 2008.

$$\beta = \log\left(\left(\frac{Emax,P1}{EC50,P1}\ \frac{EC50,P2}{Emax,P2}\right)_{lig} \times \left(\frac{Emax,P1}{EC50,P1}\ \frac{EC50,P2}{Emax,P2}\right)_{ref}\right)$$

The bias factor (β) is calculated as the logarithm of the ratio of intrinsic relative activities for a ligand at two different assays compared to a reference ligand where P1 and P2 denote the two signaling pathways 1 and 2, respectively (Figueroa et al., 2009).

In order for any of these bias quantifications to have any value in the drug discovery process, it is important that these ratios or calculations are valid in a system other than the test system i.e a monotonic relationship between receptor stimulation and cellular response. However, when this assumption is not valid, agonist potency ratios developed in one reference system become less useful for drug discovery.

Operational Model:

This approach is based on classic pharmacological model proposed by Black and Leff in 1983 and accounts for receptor reserve and shifts in agonist concentration-response curves. Until now, ligand bias was quantified by comparing the maximal effects (Emax) and potencies (EC50) of ligands in different signaling pathways. Although effective, these parameters don't account for differences in receptor reserve and signal amplification in different assays. Specifically assays with significant amplification, can lead to a false interpretation of bias

because both full and partial agonists can reach the same maximal response (Rajagopal et al., 2011).

We chose to use the operational model of Black and Leff to quantify the effective signaling by receptors. To compare the relative activity of agonists in the two pathways and identify the bias, we generated concentration response curve for each signaling pathway. In the operational model, the response of the system to ligand stimulation is based on receptor occupancy alone. τ is the coupling efficiency between the agonist/receptor complex and the downstream signaling partners.

$$E = Basal + \frac{(Emax - Basal)\tau^n[A]^n}{\tau^n[A]^n + ([A] + Ka)^n}$$

The caveat with using the operational model is that it assumes that the agonist-receptor complex has an identical affinity for separate signaling pathways. As proposed by Kenakin et al., instead of assuming an identical Ka value, the operational model can be modified to determine the transduction ratios (τ/Ka) of the agonists. (Kenakin et al., 2012; Van der Westhuizen et al., 2013; White et al., 2014).

$$E = Basal + \frac{(Emax - Basal)(\frac{\tau}{Ka})^n[A]^n}{(\frac{\tau}{Ka})^n[A]^n + (\frac{[A]}{Ka})^n + 1)^n}$$

τ incorporates agonist coupling, efficacy and receptor density in the system and Ka is the reciprocal of the conditional affinity of the agonist in the functional system. It has been shown that transduction

coefficients remain constant over large changes in receptor density (Kenakin et al., 2012)

$$\Delta \log\left(\frac{\tau}{Ka}\right) = \log\left(\frac{\tau}{Ka}\right) ligand - \log\left(\frac{\tau}{Ka}\right) Ref$$

$$\Delta\Delta \log\left(\frac{\tau}{Ka}\right) = \Delta \log\left(\frac{\tau}{Ka}\right) pathway\ 1 - \log\left(\frac{\tau}{Ka}\right) pathway\ 2$$

$$\text{Bias Factor} = 10^{\Delta\Delta\log\left(\frac{\tau}{Ka}\right)^n}$$

The log(τ/Ka) of each test ligand can then compared with the log(τ/Ka) of a reference ligand, like DAMGO, for both G protein activation and arrestin recruitment. It is ideal to use a reference ligand that has very similar EC50 value for both the G protein and arrestin pathways and displays full efficacy at both pathways. Ligand bias is quantified by comparing the relative activity of an agonist in one assay to the relative activity in another assay, using the same reference ligand. This method reduces to the observation or the system bias (Kenakin et al., 2013). Transduction coefficients are useful in comparing the relative signaling of ligands, but can be problematic when trying to measure the efficacy of agonists that produce maximal or no effects in a given signaling pathway, like Buprenorphine (Rajagopal, 2013).

Chapter II - Materials and Methods

In-Vitro Assays

Competition Binding Assay

Membranes from cells were prepared by manually lifting cells from the culture plates with a rubber septum into PBS. Cells were pelleted at 1,200g for 10 min and the pellet was resuspended in 20 volumes of TRIS buffer (50 mM; pH 7.4 at 25°C), potassium EDTA (1mM), sodium chloride (100mM), and phenylmethylsulfo- nylfluoride (10M). The homogenate was then incubated at 25°C for 15 min and centrifuged at 14,000rpm for 30 min. The resulting pellet was resuspended in 0.32M sucrose, homogenized, and aliquots were quick-frozen on dry ice. The membranes were stored at –70°C and retained their binding for at least 6 weeks.

Binding Studies: [^{125}I]-IBNtxA binding assays were carried out in Chinese Hamster Ovary (CHO) cells stably expressing mMOR-1 receptors. Cell membrane homogenates were prepared as previously described at a concentration of 3 - 10µg protein in a volume of 0.5 - 1ml of homogenate. Nonspecific binding was determined in the presence of levallorphan (1µM) and was subtracted from the total binding counts per million (cpm) to yield specific binding. Specific binding is reported. Binding was carried out for 90 min (equilibrium) at 25°C using 0.5 to 1ml of homogenate. Glass fiber filters were soaked

in 0.5% polyethyleneimine for at least 15 minutes prior to filtration to minimize nonspecific binding to the filters. KD, Bmax, and Ki values were calculated by nonlinear regression analysis (GraphPad Prism, San Diego, CA). Data is reported as mean and S.E.M. of at least 3 independent replicates.

[^{35}S]GTPγS Binding Assay

Stimulation of [^{35}S]GTPγS binding: [^{35}S]GTPγS assays were performed based upon published methods (Selley et al., 1998; Bolan et al., 2004; Pan et al., 2005). Membrane homogenates from CHO cells stably transfected with mMOR or its splice variants (200 µg protein) were incubated for 1 hour at 30°C with the indicated drug, [^{35}S]GTPγS (0.05nM) and GDP (60µM) in a final volume of 1ml assay buffer. The assay buffer contained Tris HCl (50 mM; pH 7.4 at 37°C), $MgCl_2$ (3mM), EGTA (0.2mM), NaCl (100mM), and a protease inhibitor cocktail (leupeptin, bestatin, aprotinin, and pepstatin). Nonspecific binding was assessed by the addition of 100µM cold GTPγS Binding was terminated by vacuum filtration through Whatman GF/C glass fiber filters which were rinsed 3 x 3ml with cold Tris HCl. Filters were cut out and 3ml of scintillation fluor (Liquiscint, National Diagonistics, Atlanta, GA) was added to each tube and incubated at room temperature for at least 3 hours before being counted on a Packard Tri-Carb TR-2900 liquid scintillation counter.

DiscoverX PathHunter assay

The PathHunter enzyme complementation assay was performed according to the manufacturer's protocol. Chinese Hamster Ovary (CHO) cells expressing MOR-1 tagged with a complementary β-gal donor fragment at the C-terminal region and β-arrestin-2 tagged with a complementary β-gal activator (EA) fragment were obtained from DiscoverX. When the receptor is activated, the β-arrestin-2 translocates to the active receptor and forms a functional enzyme. The cells were maintained in F-12 media with 10% fetal calf serum + Penicillin + Streptavidin. The media was supplemented with 800µg G418 and 300µg Hygromycin for cell selection. For the arrestin assay, the cells were plated at 2500 cells/ well in a 384 well plate. The next day, the cells were treated with the agonist compound for 90min at 37°C and β-arrestin-2 recruitment was measured using the PathHunter detection kit and read for chemiluminiscence on a Tecan plate reader.

Phospho-ERK1/2 Western

HEK-293 cells stably expressing a N-terminus hemagglutinin (HA) - tagged mouse MOR-1 or MOR-1O were assessed for agonist-induced ERK1/2 phosphorylation. Cells were serum-starved at 37°C under 5% CO2 for 30 min before drug treatment. For these assays, the cells were treated with PBS, 1µM DAMGO, Buprenorphine and Fentanyl. Cells

were stimulated for 5 minutes in the presence of agonists, and cell lysates were prepared on ice in lysis buffer. The Lysis buffer constituted 20mM Tris-HCl, pH 7.5, 150mM NaCl, 2mM EDTA, 0.1% SDS, 1% NP-40, 0.25% deoxycholate, 1mM sodium orthovanadate, 1mM PMSF, 1mM NaF, with Complete Mini, EDTA-free protease inhibitor cocktail tablet (Roche Diagnostics, Indianapolis, IN). Protein levels were determined with the use of the detergent-compatible protein assay system (Bio-Rad Laboratories, Hercules, CA), and 20 g of protein was loaded per lane on 10% Bis-Tris gels for gel electrophoresis (Bio-Rad Laboratories or Invitrogen, Carlsbad, CA). Proteins were transferred to polyvinylidene fluoride (PVDF) membranes (Immobilon P; Millipore, Billerica, MA) and blocked in 5% milk for 1 hour at room temperature. After blocking, the blots were incubated with antibody for total or phosphorylated ERK1/2 (anti-phospho ERK1/2 antibody 1:1,500 dilution, #4370, Cell Signaling or an anti-total ERK1/2 antibody 1:1,000 dilution, #4695, Cell Signaling) overnight at 4°C. Total ERK1/2 levels were used to normalize the overall phosphorylation of ERK1/2 between samples. Chemiluminescence was detected and quantified using the BioRad imaging device and Prism software (GraphPad Software, Inc., San Diego, CA).

Bias Factor Calculation

We chose to use the operational model of Black and Leff to quantify the effective signaling by receptors. To compare the relative activity of

agonists in the two pathways and identify the bias, we generated concentration response curve for each signaling pathway. In the operational model, the response of the system to ligand stimulation is based on receptor occupancy alone. τ is the coupling efficiency between the agonist/receptor complex and the downstream signaling partners.

$$E = Basal + \frac{(Emax - Basal)\tau^n[A]^n}{\tau^n[A]^n + ([A] + Ka)^n}$$

The caveat with using the operational model is that it assumes that the agonist-receptor complex has an identical affinity for separate signaling pathways. As proposed by Kenakin et al., instead of assuming an identical Ka value, the operational model can be modified to determine the transduction ratios (τ/Ka) of the agonists. (Kenakin et al., 2012; Van der Westhuizen et al., 2013; White et al., 2014).

$$E = Basal + \frac{(Emax - Basal)(\frac{\tau}{Ka})^n[A]^n}{(\frac{\tau}{Ka})^n[A]^n + (\frac{[A]}{Ka})^n + 1)^n}$$

τ incorporates agonist coupling, efficacy and receptor density in the system and Ka is the reciprocal of the conditional affinity of the agonist in the functional system. It has been shown that transduction coefficients remain constant over large changes in receptor density (Kenakin et al., 2012)

$$\Delta \log\left(\frac{\tau}{Ka}\right) = \log\left(\frac{\tau}{Ka}\right) ligand - \log\left(\frac{\tau}{Ka}\right) Ref$$

$$\Delta\Delta \log\left(\frac{\tau}{Ka}\right) = \Delta \log\left(\frac{\tau}{Ka}\right) pathway\ 1 - \log\left(\frac{\tau}{Ka}\right) pathway\ 2$$

$$\text{Bias Factor} = 10^{\Delta\Delta\log(\frac{\tau}{Ka})^n}$$

The log(τ/Ka) of each test ligand can then compared with the log(τ/Ka) of a reference ligand, like DAMGO, for both G protein activation and arrestin recruitment. It is ideal to use a reference ligand that has very similar EC50 value for both the G protein and arrestin pathways and displays full efficacy at both pathways. Ligand bias is quantified by comparing the relative activity of an agonist in one assay to the relative activity in another assay, using the same reference ligand. This method reduces to the observation or the system bias (Kenakin et al., 2013). Transduction coefficients are useful in comparing the relative signaling of ligands, but can be problematic when trying to measure the efficacy of agonists that produce maximal or no effects in a given signaling pathway, like Buprenorphine (Rajagopal, 2013).

In-Vivo Assays

Morphine analgesia

A radiant-heat tail-flick assay was used to test for analgesia. The animals were tested 30 min post-injection with a maximal latency of 10 seconds to minimize tissue damage. The results are reported as the percentage of maximum possible effect (%MPE), which is calculated as [(latency after drug baseline)/(10 – baseline latency)*100]. For the dose

response studies, animals were treated with 1, 2, 4, 8, 16 or 32 mg/kg dose of morphine. ED50 values were determined using nonlinear regression analysis (GraphPad Prism 6).

Morphine tolerance and physical dependence studies

Tolerance in the targeted mice on B6 background and CD-1 mice was induced by twice-daily injections with morphine (10 mg/kg, s.c.) for 5 days. Tolerance in the targeted mice on 129 background was induced by twice-daily injections with escalating doses of morphine (s.c., day 1, 10 mg/kg; days 2 & 3, 20 mg/kg; days 4 & 5, 40 mg/kg). Morphine analgesia was examined on Days 1, 3 and 5. Morphine dependence was determined on day 5 with naloxone (s.c., 1 mg/kg for mice on B6 background and 30 mg/kg for mice on 129 backgrounds and CD-1 mice) injection 3 hours after the last morphine treatment to precipitate withdrawal. The number of jumps within 15 min immediately following the naloxone injection was used for the measurement of withdrawal.

Statistical analyses

Statistical analysis was carried out using GraphPad Prism 6. A one-way ANOVA with post hoc Bonferroni's multiple comparisons test was used if more than two groups were compared, and a two-way ANOVA with post hoc Bonferroni's multiple comparisons test was used if two independent variables were compared. Data are represented as the means ± SEM of at least three independent experiments. Statistical

significance was set at $p < 0.05$. For the in-vivo experiements, all mice were randomized and assigned to groups. Some, but not all, experiments were performed under blinded conditions.

Chapter III - Results

The opioid field and the quest for the ideal analgesics with limited side effects has accumulated decades of research and thousands of new opioid compounds. However, in spite of the substantial advances in the understanding of opioid receptor pharmacology, analgesics such as morphine, fentanyl, and oxycodone, that target the mu opioid receptor and exhibit the side effect profile - tolerance, dependence, constipation, respiratory depression, and euphoria resulting in abuse and addiction, remain the mainstays of pain management.

The history of opioid pharmacology has revolved around discovering and exploiting receptor heterogeneity to maximize the desired therapeutic effects while minimizing off-target side effects. This began with first splitting opioid receptors into the different subclasses, mu, delta and kappa. And then evolved into understanding the different subtypes under these subclasses. More and more studies have revealed the existence of homo- and heteromeric signaling complexes comprised of multiple GPCRs, which exhibit unique properties from their component receptors and may be specifically targeted by drugs (Gomes et al., 2004, 2013; Jordan & Devi, 1999; Yekkirala et al., 2009). In this study, our approach has been to reconcile the pharmacologically defined opioid receptor subtypes with the extensive alternative splicing observed for the mu opioid receptor gene.

The Oprm gene has been mapped to be greater than 250 kb long and has at least 18 different exons (Pan et al., 2001). The gene shows extensive alternative splicing and more than 60 different splice variants have been identified. Specifically, the C-terminal splice variants sub-family of receptors consist of exons 1, 2 and 3 with alternative splicing downstream of exon 3 (Figure 8). Since these variants share the first 3 exons, they encode for all the 7 TM domains as well as a significant portion of the C-tail. As a result, these receptors have an identical binding pocket encoded by transmembrane 2, 3, 5 and 7. They selectively label mu opioids in binding assays and are antagonized by mu opioid-selective antagonists. The only difference among these variants is at the tip of the C-tail (Rossi et al., 1994, 1995a,b, 1996, 1997; Pasternak and Standifer, 1995; Schuller et al., 1999).

Opioid receptors are known to couple to the inhibitory G proteins (Gi/Go) family in an agonist dependent manner (Childers, 1991; Standifer and Pasternak, 1997). However, the sensitivity profile of mu analgesics vary significantly, with $Gi\alpha_2$ implicated in morphine analgesia and $Gi\alpha_1$ involved in M6G analgesia (Standifer et al., 1996). Additional G protein α-subunits have also been implicated in opioid analgesia. This diversity of mu opioid receptors and the differing G proteins involved with mu opioid actions raises the question of whether or not the G protein interactions of some of these Oprm splice variants may differ due to structural differences at the tip of the C-terminus.

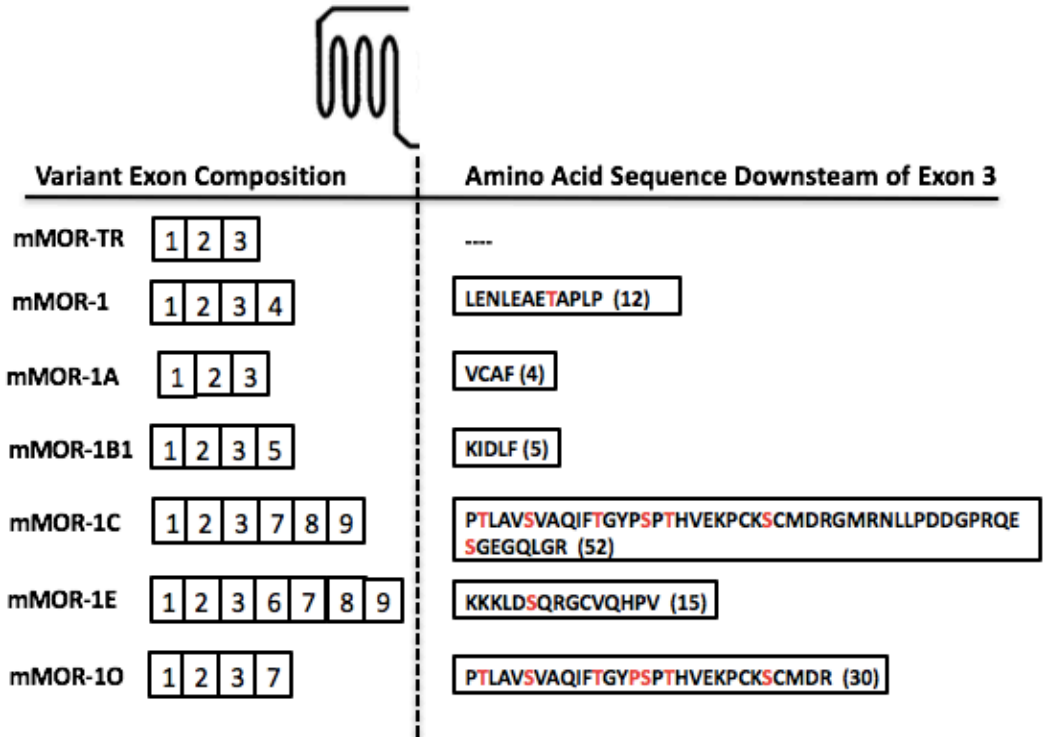

Figure 8 Schematic showing the Oprm gene structure and the C-terminal splice variants. All of these variants contain exons 1, 2 and 3 with splicing downstream of exon 3. Exons are represented in boxes and are numbered based on when they were reported. Exons and introns are represented by boxes and horizontal lines, respectively. Translational start codons and termination codons are indicated by heavy vertical lines.

Some of this has already been demonstrated. The C-terminal splice variants of μ-OR differ in their regional distribution, agonist induced G protein coupling (as measured by [^{35}S]GTPγS binding), receptor phosphorylation, internalization and post-endocytic sorting. Functional differences among the variants have been demonstrated using [^{35}S]GTPγS binding and adenylyl cyclase coupling. Zimprich et al. demonstrated that the functional coupling to adenylyl cyclase desensitizes at a slower rate in the mMOR-1B variant than in mMOR-1. This is due to rapid resensitization and recycling of mMOR-1B to the plasma membrane (Koch et al., 1998). However, different mu

agonists differentially bias this receptor recycling process. DAMGO induced desensitization, measured as a decay of the opioid activated GIRK current, is much slower in mMOR-1B than in the mMOR-1 and mMOR-1A variants. However, all three splice variants undergo rapid desensitization in response to morphine (Oldfield et al., 2008).

Our current approach has been to better understand how the differences at the C-terminus of the receptor affect its interaction with the downstream signaling pathways. This understanding of the downstream molecular targets would eventually help in optimizing and discovery better opioid analgesics.

Part I - C-terminal splice variants differentially regulate G protein pathways

In the current study, we expanded the number of C-terminal variants and series of opioids to screen for the stimulation of [^{35}S]GTPγS binding while simultaneously using a cell line that allowed for a comparison between the stimulation of the G protein and β-arrestin pathways. We used the cell lines developed for the DiscoverX PathHunter assay. These are CHO cells expressing the μ-OR tagged with a complementary β-gal donor fragment (called the prolink (PK) fragment) at the C-terminal region. The β-arrestin-2 is tagged with a complementary β-gal activator (EA) fragment. It is an enzyme complementation assay that leads to a functional β-gal formation upon agonist induced β-arrestin-2 recruitment to the receptor.

We tested 6 C-terminal splice variants with varying C-terminal tails, mMOR-1-PK, mMOR-1A-PK, mMOR-1B1-PK, mMOR-1C-PK, mMOR-1E-PK and mMOR-1O-PK, along with a control receptor MOR-TR-PK. The control receptor MOR-TR-PK has exons 1, 2, 3, with nothing downstream of exon 3. These C-terminal splice variants differ at the tip of the C-terminus with differences in length of the C-tail, specific amino acid residues at the tail, along with, conformation and potential phosphorylation sites at the C-tail. We attempted to study the effect of adding amino acids downstream of exon 3 in its ability to recruit G proteins.

The μ-OR clonal cell lines were selected based on expression level of the clone using [^{125}I]-IBNtxA competition binding assay and saturation studies. We picked the clones with relatively high and similar expression levels across the 7 different constructs (Figure 9).

We first wanted to confirm that these DiscoverX splice variants clones show similar affinities for a number of mu agonists, as previously published in Bolan et al., 2004. This would ensure that the extra PK fragment at the C-terminus of these variants was not interfering with drug interaction. We did competition binding assays with 2 DiscoverX clones, mMOR-1-PK and mMOR-1O-PK, which are the clones with the highest and lowest expression level and compared it with a regular mMOR-1 clone without the additional prolink fragment, also expressed in CHO cells. The DiscoverX constructs are indicated with a PK (prolink) to differentiate them from the non-modified receptor variant, mMOR-1 expressed in CHO cells.

We observed that the addition of the prolink fragment at the C-terminal tail of the receptor had no effect on the binding affinity of several mu agonists for the receptor. We saw this in both mMOR-1-PK and mMOR-1O-PK receptor variants (Figure 10, 11). Next, we chose to examine the functional differences among the C-terminal variants by measuring their ability to stimulate [^{35}S]GTPγS binding. [^{35}S]GTPγS binding is an in-vitro assay that serves an estimation of the agonist induced G protein coupling across the receptor variants. Since the

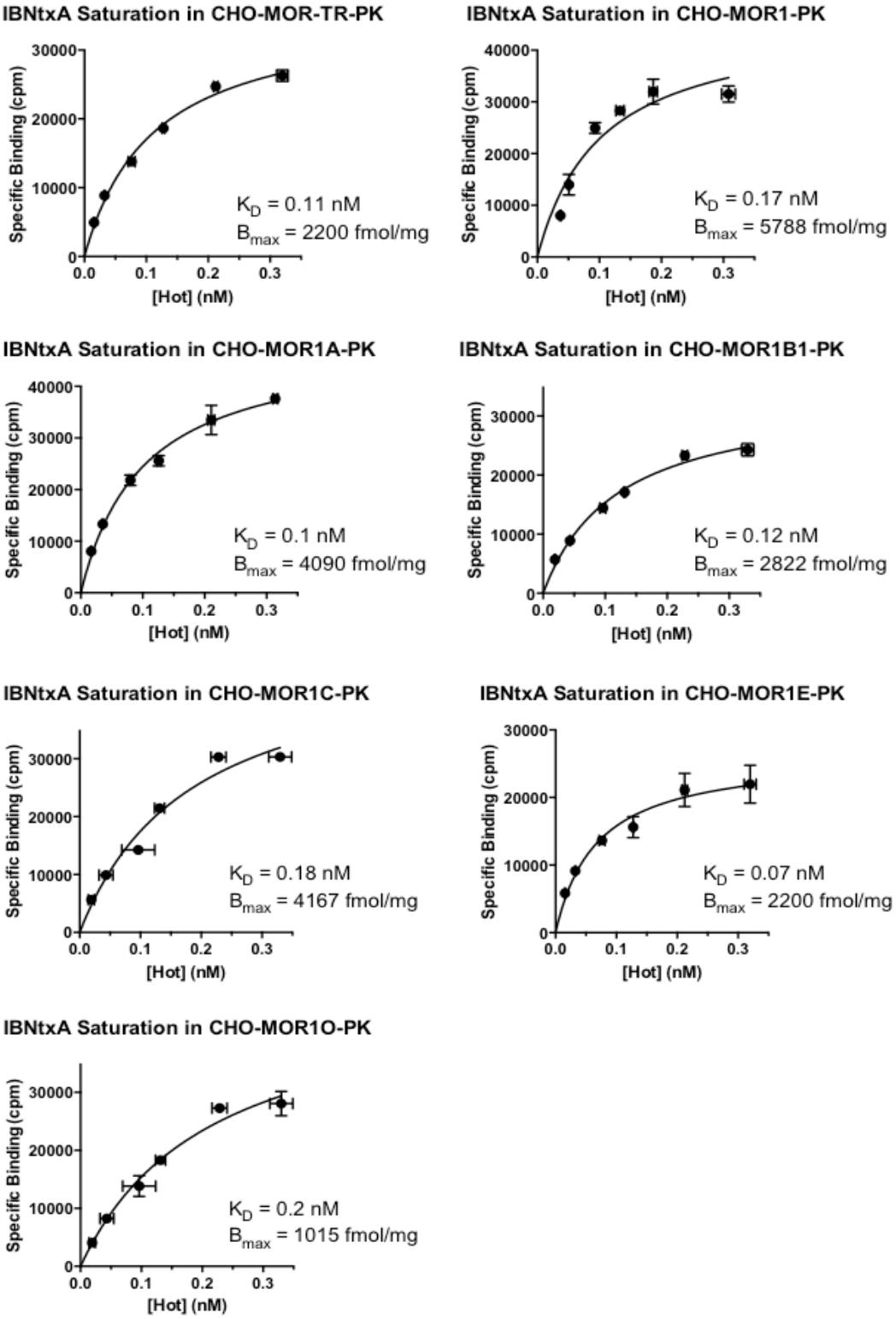

Figure 9 Saturation binding experiments represent the expression level of the receptor variants in the DiscoverX cell lines. 6 different C-terminal variants were characterized along with the control receptor MOR-TR-PK which is truncated after exon 3. Results are the mean ± S.E. of at least three independent experiments.

receptors in the DiscoverX cell lines have seemingly high expression levels, we first wanted to check if the endogenously expressed levels of G proteins in these cells lines might be rate limiting in [^{35}S]GTPγS binding assay. The receptor in a [^{35}S]GTPγS binding assay can interact with more than one G protein, therefore, a skewed receptor : G protein ratio could impact the ability of the receptor in activating G proteins. For this purpose, we used the DiscoverX cell line with the highest expression level, CHO-MOR-1-PK and compared its efficacy and potency in the [^{35}S]GTPγS binding assay to the CHO-MOR-1 cell line (Figure 12). We noticed that even though the expression level of the clones had no significant impact on the potency (EC50) of the mu agonists, it does seem that the CHO-MOR-1 cell line is more effective (Emax - % basal stimulation) in the [^{35}S]GTPγS binding assay. This difference could be a combined response to the difference in receptor expression level in the 2 clones as well as the signal amplification in the [^{35}S]GTPγS binding assay. As a result, we have normalized all the Emax values to % DAMGO stimulation at the receptor variant to eliminate any inherent biases due to differences in receptor expression level. This allows us to carefully characterize the response of the drugs across the different variants while eliminating any system bias.

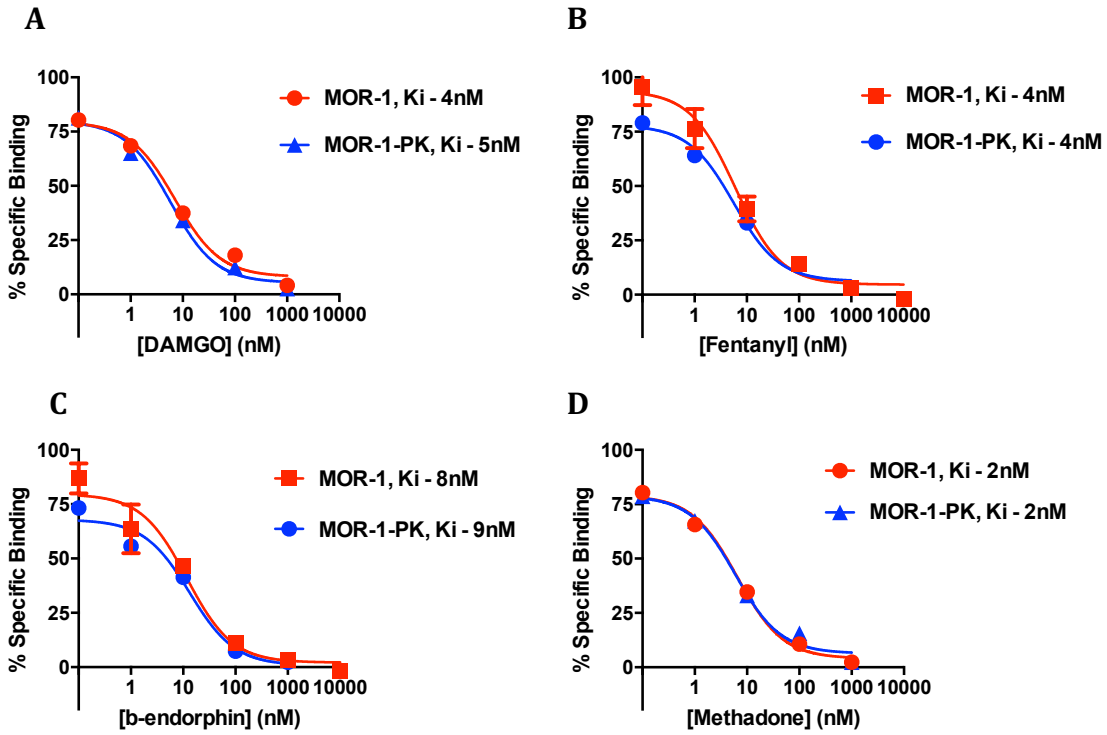

Figure 10 Competition binding curves in engineered CHO cell lines stably expressing MOR-1 and MOR-1-PK receptor variants. The DiscoverX variant is represented by MOR-1-PK. Competition binding curves was generated for 4 mu agonists, **A.** DAMGO, **B.** Fentanyl, **C.** b-Endorphin and **D.** Methadone. The Ki values were calculated on GraphPad Prism using non-linear regression analysis. The binding studies depict that the additonal prolink fragment at the C-terminus tail of the receptor has no significant effect on the affinity of the mu agonists for the receptor variant. Results are the mean ± S.E. of at least three independent experiments.

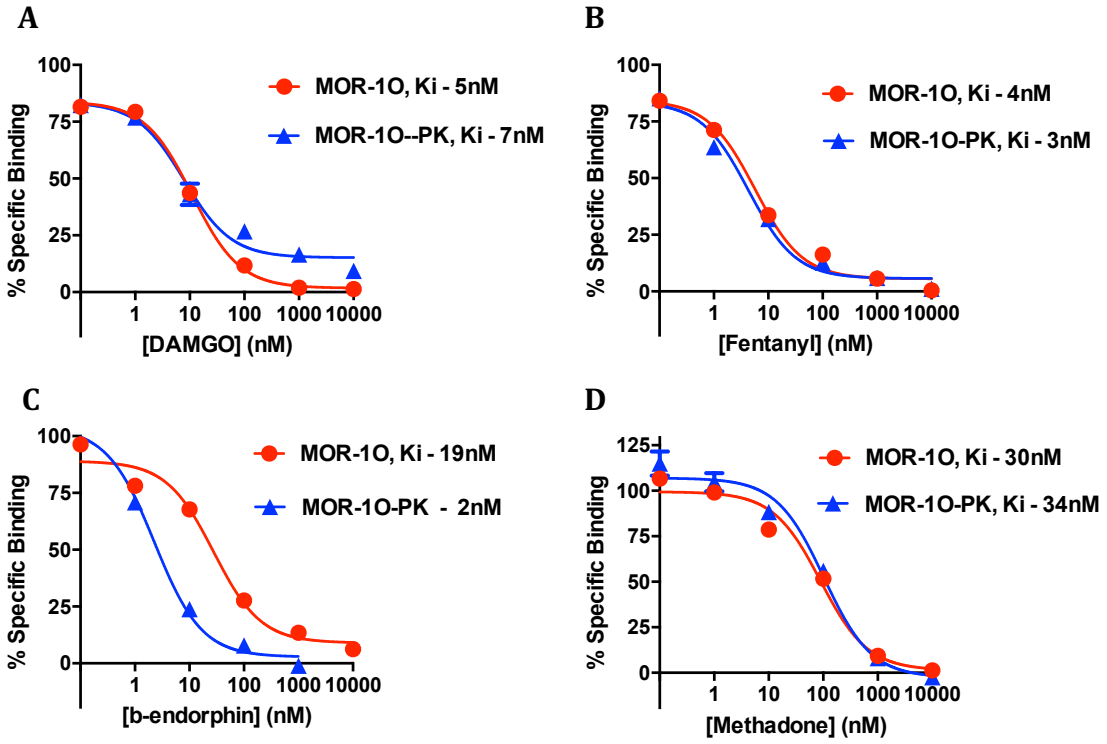

Figure 11 Competition binding curves in engineered CHO cell lines stably expressing MOR-1O and MOR-1O-PK receptor variants. The DiscoverX variant is represented by MOR-1O-PK. Competition binding curves was generated for 4 mu agonists, **A.** DAMGO, **B.** Fentanyl, **C.** b-Endorphin and **D.** Methadone. The Ki values were calculated on GraphPad Prism using non-linear regression analysis. The binding studies depict that the additonal prolink fragment at the C-terminus tail of the receptor has no significant effect on the affinity of the mu agonists for the receptor variant. Results are the mean ± S.E. of at least three independent experiments.

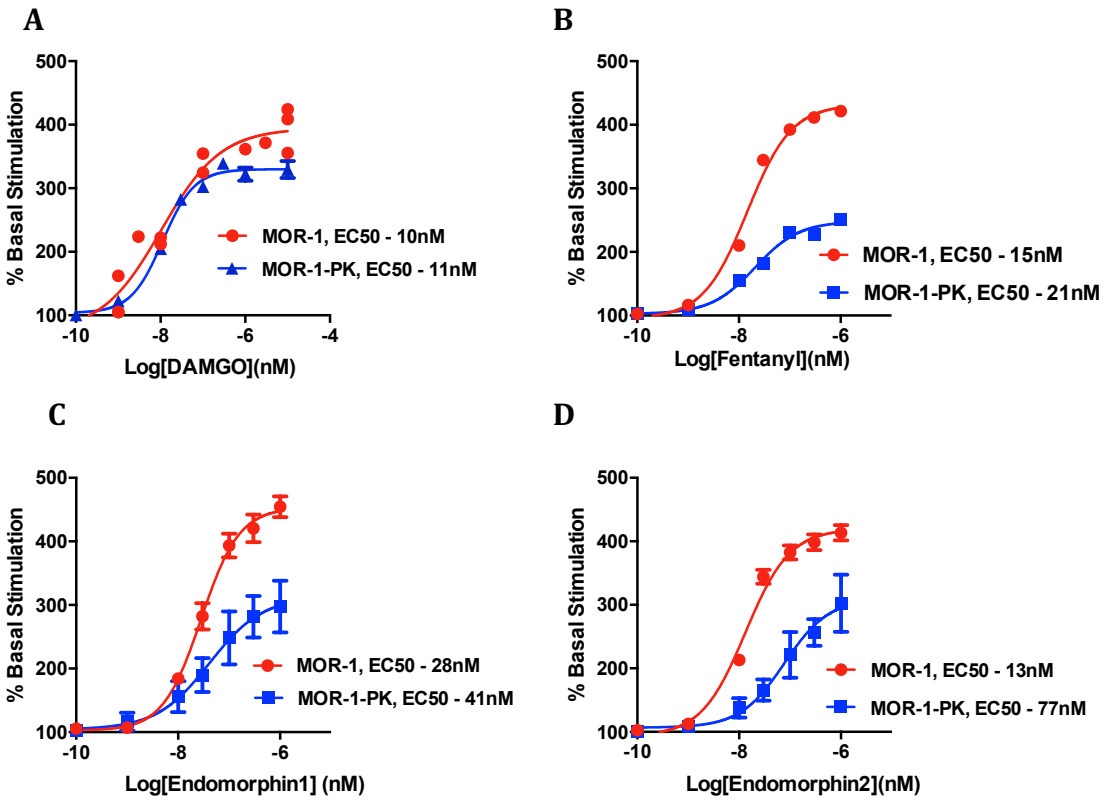

Figure 12 [^{35}S]GTPγS binding curves to observe the role of the difference in receptor expression level in these assays. We used the DiscoverX MOR-1-PK cell line with the highest receptor expression level and compared with CHO-MOR-1 cell line. A comparison of the [^{35}S]GTPγS binding curves were generated for 4 mu agonists, **A.** DAMGO, **B.** Fentanyl, **C.** Endomorphin1, **D.** Endomorphin2. The EC50 values were calculated on GraphPad Prism using non-linear regression analysis. Results are the mean ± S.E. of at least three independent experiments.

After optimizing the assay, we tested the 6 C-terminal variants, mMOR-1-PK, mMOR-1A-PK, mMOR-1B1-PK, mMOR-1C-PK, mMOR-1E-PK and mMOR-1O-PK, along with the control variant mMOR-TR-PK in their ability to stimulate [^{35}S]GTPγS binding in response to 9 different mu agonists. The ability of the various mu opioids to stimulate [^{35}S]GTPγS binding varied markedly. However, the differences among the splice variants and among the drugs in the stimulation of [^{35}S]GTPγS followed no predictable pattern. Some opioids were as efficacious as full agonists in cells expressing one variant and then showed low efficacy as a partial agonist in another. We observed significant differences in both the potency and maximal stimulation of the drug across variants, with the most differences observed in the mMOR-1O variant.

In response to DAMGO, the mMOR-1 (14nM) variant was more than 10 fold potent in triggering the maximal effect (Emax) of the drug in comparison to mMOR-1C (217nM) and mMOR-1O (166nM). The Emax and EC50 values are shown in Table 5. We compared the response of the variants to the control truncated exon 3 receptor to understand how the addition of few or more amino acids at the tip of the C-terminus affects the interaction of the receptor with other G proteins. Interestingly, the mMOR-TR response to β-endorphin was significantly right shifted while the other C-terminal variants with longer C-tails were significantly more potent in inducing the β-endorphin response (Figure 12). For example, with the addition of as few as 4 amino acids

in its C-tail, mMOR-1A was almost 20 fold more potent inducing the β-endorphin response in comparison to the control receptor.

The length of the C-tail, however, did not have a direct relationship with the efficacy of the drug. A longer C-tail does not always lead to better drug efficacy. For example, most of the C-terminal variants with their different C-tails show no marked differences in response to morphine except mMOR-1O. The mMOR-1O receptor was significantly less potent and effective in the [^{35}S]GTPγS assay in comparison to the control receptor and mMOR-1. Similarly, in response to Endomorphin1, the mMOR-1 receptor was again significantly more potent than the mMOR-1O receptor in the [^{35}S]GTPγS assay.

Endomorphin2, another potent peptide agonist at the mu receptor, had differences in both maximal stimulation as well as potency of the drug. At the mMOR-1A receptor, Endomorphin2 receptor was a full agonist that stimulated the receptor response at 124% of DAMGO. However, it was a partial agonist with a maximal efficacy of only 66% of DAMGO at the mMOR-1O receptor. In addition to the difference in efficacy, the drug was also two fold more potent at the mMOR-1A receptor in comparison to the mMOR-1O receptor. This is interesting because the mMOR-1A C-tail has 4 additional amino acids downstream of exon 3, whereas, mMOR-1O has an even longer C-tail with 30 additional amino acids.

Both mMOR-1C and mMOR-1O receptor variants have exon 7 at the C-tail and overlap in 30 amino acids downstream of exon 3. In addition to exon 7, mMOR-1C also contains exons 8, 9 and an extra 22 amino acids in the C-tail. In spite of the similarity in between these 2 variants, mMOR-1C is much more effective (188% of DAMGO) than mMOR-1O (101% of DAMGO) in triggering the G protein pathway in response Methadone. Met-Enk-Arg-Phe, another peptide, had a very diverse signaling profile across the variants. The peptide was significantly more potent in some variants like, mMOR-1E (7nM), mMOR-1 (14nM) and mMOR-1A (13nM), in comparison to other variants like, mMOR-1C (71nM) and mMOR-1O (84nM).

Although these assays do not provide sufficient evidence into why these C-terminal differences lead to differences in ability of the receptor to activate and signal through the G protein pathway, there can be a number of possibilities. As mentioned earlier, all of these C-terminal variants share the 7TM domains and differ only in the amino acid sequence at the very tip of the C-terminus. One possible reason for the observed differences across receptor variants could be that these alternatively spliced sequences contain differential phosphorylation sites that influence their function. Secondly, the lengths of the spliced C-terminal tails vary markedly. Although, we didn't find a directly proportional relationship between the length of the C-tail and the signaling from the receptor, we anticipate that the sequences and length of the alternatively spliced regions may modify the structure of the receptor and impact its ability to interact with

other protein complexes. Furthermore, it has been shown that in addition to the C-terminal tail, the third intracellular loop of the GPCRs is involved in G protein coupling, binding of calmodulin and arrestin. The differences in the C-tail across the receptor variants may influence their interaction and steric interference with the other regions of the receptor, and in specific, the third intracellular loop. The C-terminus has been implicated in the binding of arrestins and may be important in distinguishing between two classes of GPCRs (Oakley et al., 2000).

One potential caveat and limitation with the interpretation of these results is that these findings are dependent on assay conditions and the cell line used. Mu opioid receptors have been shown to interact with the Gi/Go family of G protein subunits (Traynor et al., 2002). However, the CHO cells that we used in the [^{35}S]GTPγS assay express all the G subunits implicated in opioid analgesia, with the exception of Gia1. Since the expression of this specific G protein differs between the cell line we used and endogenous expression in the brain, it is possible that the correlation of specific Ga subunit we are observing in our assays is different. We anticipate the differences to not be that significant as the GPCRs are known to recruit G proteins other than those they normally use depending on availability and expression, and the CHO cells used in our assays should still provide insights into the functional differences among the C-terminal variants (Shapira et al., 2000).

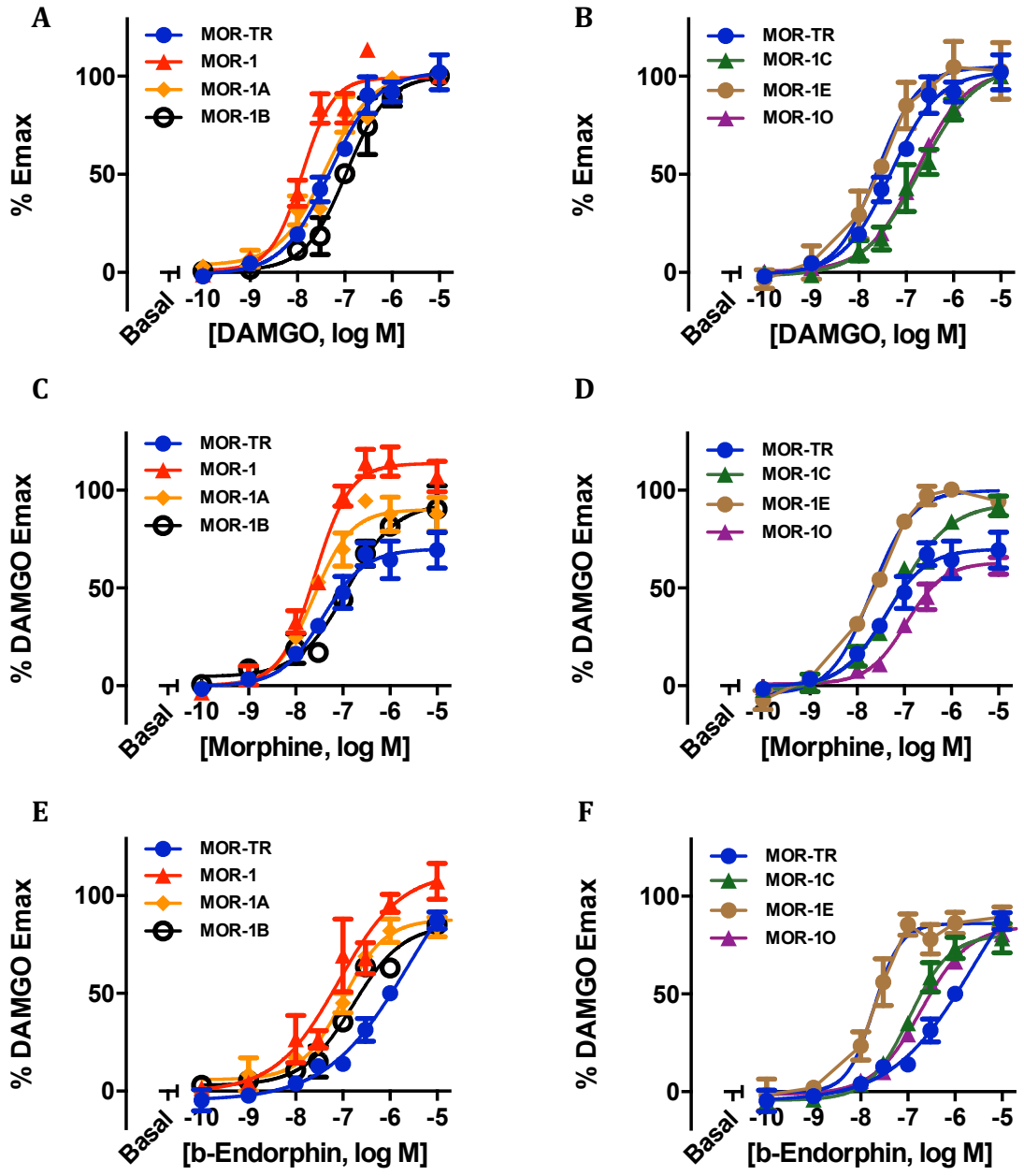

Figure 13 [^{35}S]GTPγS binding curves to compare the response of several mu agonists across the various C-terminal splice variants in the G protein assay.
Left panel: variants mMOR-TR, mMOR-1, mMOR-1A and mMOR-1B
Right panel: variants mMOR-TR, mMOR-1C, mMOR-1E, mMOR-1O
A comparison of the [^{35}S]GTPγS binding curves were generated for 3 mu agonists, **A. and B.** DAMGO, **C. and D.** Morphine, **E. and F.** b-Endorphin. The data was analyzed on GraphPad Prism using non-linear regression analysis. Results are the mean ± S.E. of at least three independent experiments.

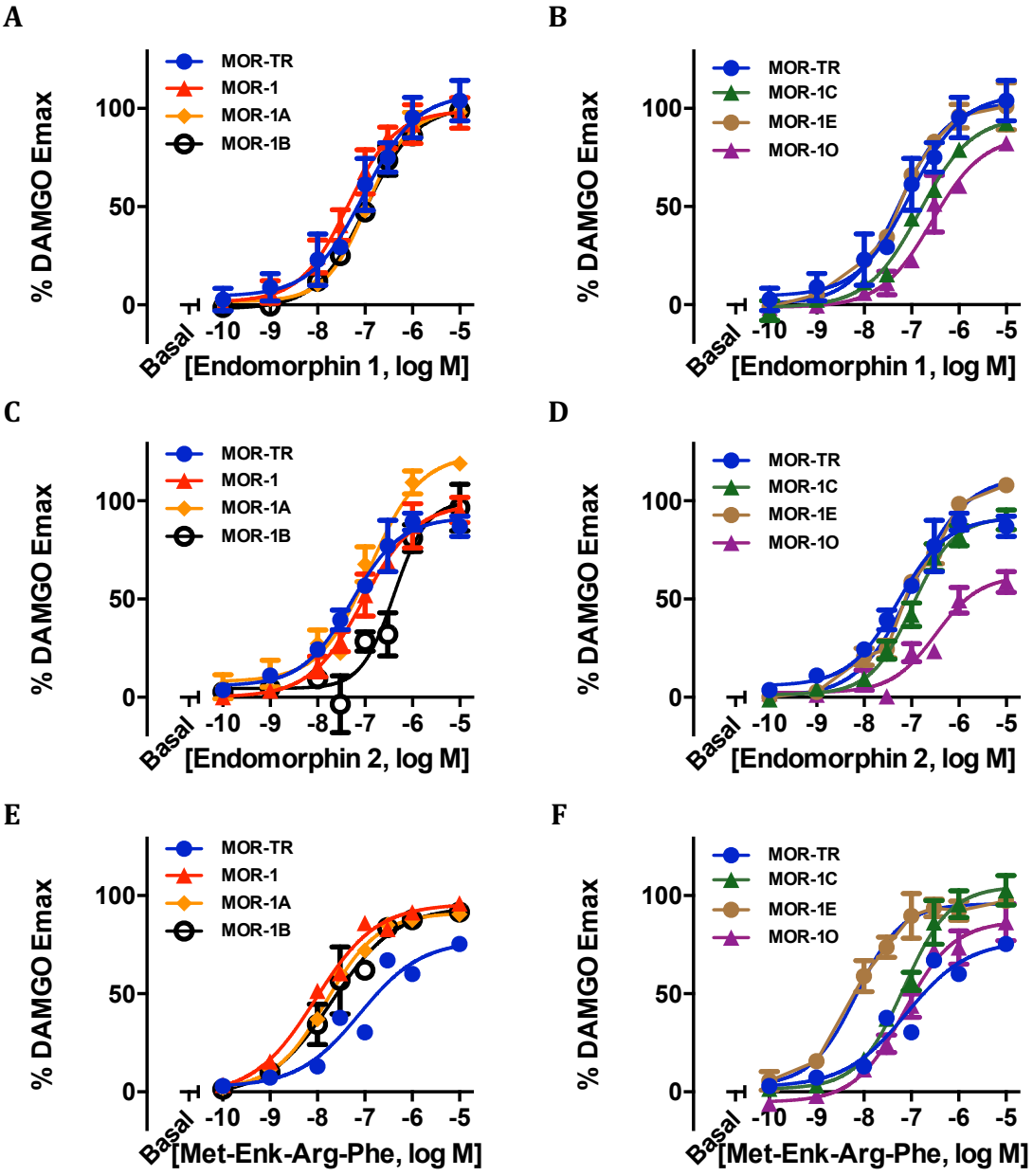

Figure 14 [^{35}S]GTPγS binding curves to compare the response of several mu agonists across the various C-terminal splice variants in the G protein assay. **Left panel**: variants mMOR-TR, mMOR-1, mMOR-1A and mMOR-1B **Right panel**: variants mMOR-TR, mMOR-1C, mMOR-1E, mMOR-1O A comparison of the [^{35}S]GTPγS binding curves were generated for 3 mu agonists, **A. and B.** Endomorphin 1, **C. and D.** Endomorphin 2, **E. and F.** Met-Enk-Arg-Phe. The data was analyzed on GraphPad Prism using non-linear regression analysis. Results are the mean ± S.E. of at least three independent experiments.

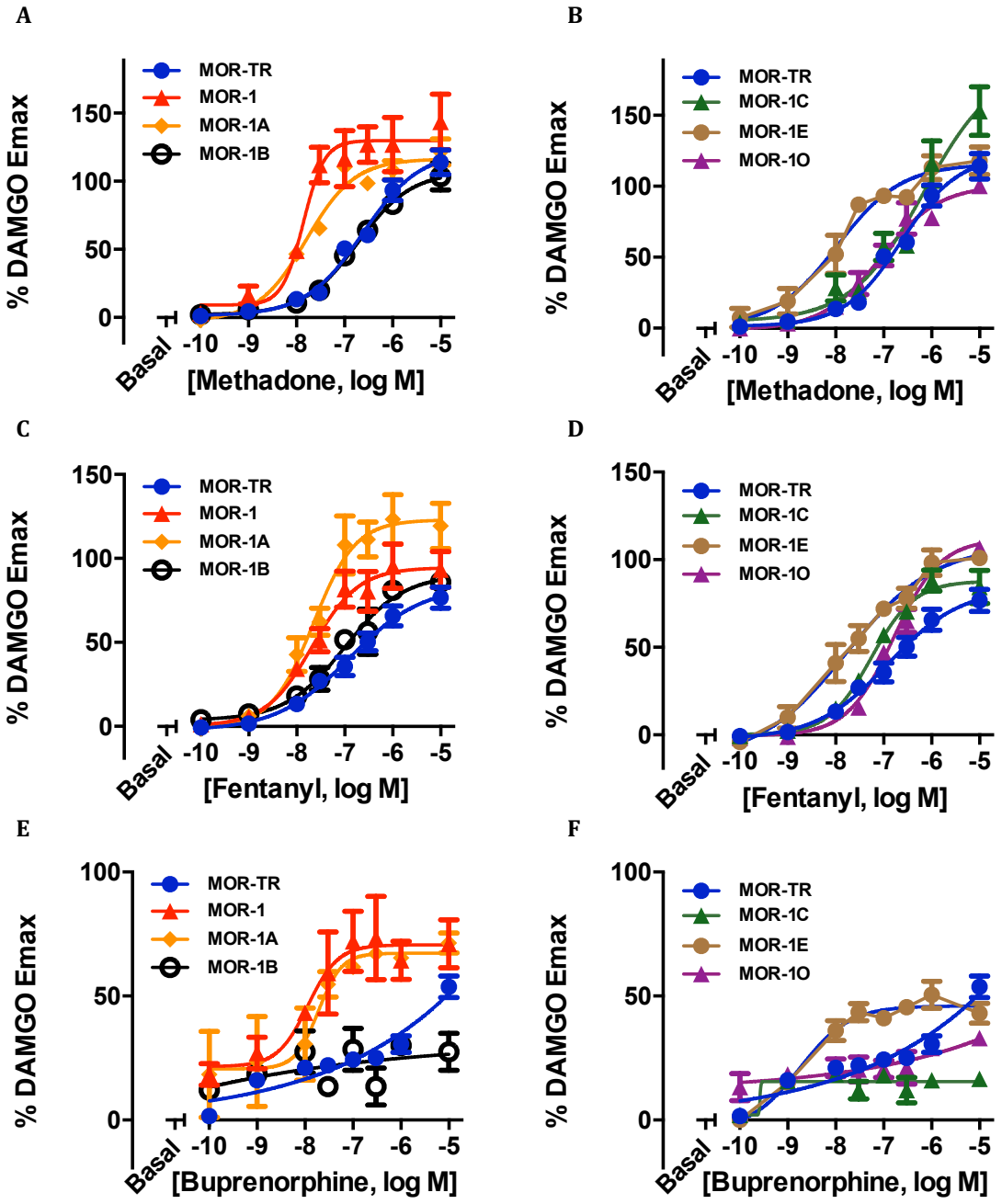

Figure 15 [^{35}S]GTPγS binding curves to compare the response of several mu agonists across the various C-terminal splice variants in the G protein assay. **Left panel**: variants mMOR-TR, mMOR-1, mMOR-1A and mMOR-1B **Right panel**: variants mMOR-TR, mMOR-1C, mMOR-1E, mMOR-1O A comparison of the [^{35}S]GTPγS binding curves were generated for 2 mu agonists, **A. and B.** Methadone, **C. and D.** Fentanyl, **E. and F.** Buprenorphine. The data was analyzed on GraphPad Prism using non-linear regression analysis. Results are the mean ± S.E. of at least three independent experiments.

Table 5 Effects of opioids on [^{35}S]GTPγS binding in MOR-1 splice variants. [^{35}S]GTPγS binding was performed with membranes (200µg) from stable cell lines containing the indicated cDNAs. 6 different C-terminal variants were characterized, mMOR-1, mMOR-1A, mMOR-1B1, mMOR-1C, mMOR-1E and mMOR-1O along with the control receptor MOR-TR-PK which is truncated after exon 3. Ki and EC50 values were calculated on GraphPad Prism using non-linear regression analysis. Analysis of variance followed by Bonferroni's post-hoc test was performed to determine whether there were any significant differences between the receptors for the indicated drug. Results are the mean ± SEM of at least three independent experiments. For each variant, the data was normalized using stimulation of 10µM DAMGO. The data is reported as % Emax DAMGO to normalize for difference in receptor expression level across variants as well as the variability in basal stimulation from assay to assay.

MOR-TR			**MOR-1**		
Ligands	G protein activation		Ligands	G protein activation	
	Emax (% of DAMGO)	EC_{50} (nM)		Emax (% of DAMGO)	EC_{50} (nM)
DAMGO	100	49 ± 5	DAMGO	100	14 ± 2
Morphine	72 ± 9	42 ± 8	Morphine	112 ± 10	30 ± 4
b- Endorphin	137 ± 14	2830 ± 781	b- Endorphin	108 ± 9	91 ± 40
Endomorphin1	110 ± 15	124 ± 56	Endomorphin1	99 ± 9	44 ± 8
Endomorphin2	93 ± 3	52 ± 2	Endomorphin2	99 ± 8	95 ± 14
Met-Enk-Arg-Phe	120 ± 6	80 ± 5	Met-Enk-Arg-Phe	98 ± 2	14 ± 5
Methadone	120 ± 6	244 ± 7	Methadone	125 ± 12	25 ± 11
Fentanyl	86 ± 12	180 ± 87	Fentanyl	95 ± 12	21 ± 1
Buprenorphine	50 ± 12	7 ± 4	Buprenorphine	71 ± 13	7 ± 4

Table 5 continued. Effects of opioids on [^{35}S]GTPγS binding in MOR-1 splice variants. [^{35}S]GTPγS binding was performed with membranes (200µg) from stable cell lines containing the indicated cDNAs. 6 different C-terminal variants were characterized, mMOR-1, mMOR-1A, mMOR-1B1, mMOR-1C, mMOR-1E and mMOR-1O along with the control receptor MOR-TR-PK which is truncated after exon 3. Ki and EC50 values were calculated on GraphPad Prism using non-linear regression analysis. Analysis of variance followed by Bonferroni's post-hoc test was performed to determine whether there were any significant differences between the receptors for the indicated drug. Results are the mean ± SEM of at least three independent experiments. For each variant, the data was normalized using stimulation of 10µM DAMGO. The data is reported as % Emax DAMGO to normalize for difference in receptor expression level across variants as well as the variability in basal stimulation from assay to assay.

MOR-1A			**MOR-1B-1**		
Ligands	G protein activation		Ligands	G protein activation	
	Emax (% of DAMGO)	EC_{50} (nM)		Emax (% of DAMGO)	EC_{50} (nM)
DAMGO	100	39 ± 15	DAMGO	100	115 ± 30
Morphine	90 ± 9	26 ± 0.3	Morphine	96 ± 15	70 ± 17
b- Endorphin	90 ± 5	95 ± 27	b- Endorphin	85 ± 3	152 ± 25
Endomorphin1	104 ± 4	88 ± 24	Endomorphin1	102 ± 3	123 ± 34
Endomorphin2	124 ± 4	138 ± 20	Endomorphin2	100 ± 13	356 ± 95
Met-Enk-Arg-Phe	94 ± 3	13 ± 2	Met-Enk-Arg-Phe	92 ± 4	33 ± 16
Methadone	118 ± 7	27 ± 11	Methadone	108 ± 13	207 ± 71
Fentanyl	123 ± 14	23 ± 3	Fentanyl	91 ± 3	143 ± 52
Buprenorphine	70 ± 3	16 ± 5	Buprenorphine	29 ± 6	52 ± 9

Table 5 continued. Effects of opioids on [^{35}S]GTPγS binding in MOR-1 splice variants. [^{35}S]GTPγS binding was performed with membranes (200µg) from stable cell lines containing the indicated cDNAs. 6 different C-terminal variants were characterized, mMOR-1, mMOR-1A, mMOR-1B1, mMOR-1C, mMOR-1E and mMOR-1O along with the control receptor MOR-TR-PK which is truncated after exon 3. Ki and EC50 values were calculated on GraphPad Prism using non-linear regression analysis. Analysis of variance followed by Bonferroni's post-hoc test was performed to determine whether there were any significant differences between the receptors for the indicated drug. Results are the mean ± SEM of at least three independent experiments. For each variant, the data was normalized using stimulation of 10µM DAMGO. The data is reported as % Emax DAMGO to normalize for difference in receptor expression level across variants as well as the variability in basal stimulation from assay to assay.

MOR-1C			**MOR-1E**		
Ligands	G protein activation		Ligands	G protein activation	
	Emax (% of DAMGO)	EC_{50} (nM)		Emax (% of DAMGO)	EC_{50} (nM)
DAMGO	100	217 ± 82	DAMGO	100	25 ± 4
Morphine	97 ± 4	56 ± 22	Morphine	102 ± 3	20 ± 2
b- Endorphin	81 ± 4	111 ± 8	b- Endorphin	89 ± 5	22 ± 5
Endomorphin1	94 ± 3	123 ± 34	Endomorphin1	109 ± 8	44 ± 16
Endomorphin2	92 ± 6	111 ± 22	Endomorphin2	112 ± 5	105 ± 20
Met-Enk-Arg-Phe	106 ± 6	71 ± 5	Met-Enk-Arg-Phe	97 ± 4	7 ± 0.5
Methadone	188 ± 26	700 ± 71	Methadone	120 ± 14	13 ± 5
Fentanyl	90 ± 6	60 ± 11	Fentanyl	104 ± 2	23 ± 7
Buprenorphine	21 ± 5	0.08 ± 0.01	Buprenorphine	36 ± 10	2 ± 0.2

Table 5 continued. Effects of opioids on [^{35}S]GTPγS binding in MOR-1 splice variants. [^{35}S]GTPγS binding was performed with membranes (200µg) from stable cell lines containing the indicated cDNAs. 6 different C-terminal variants were characterized, mMOR-1, mMOR-1A, mMOR-1B1, mMOR-1C, mMOR-1E and mMOR-1O along with the control receptor MOR-TR-PK which is truncated after exon 3. Ki and EC50 values were calculated on GraphPad Prism using non-linear regression analysis. Analysis of variance followed by Bonferroni's post-hoc test was performed to determine whether there were any significant differences between the receptors for the indicated drug. Results are the mean ± SEM of at least three independent experiments. For each variant, the data was normalized using stimulation of 10µM DAMGO. The data is reported as % Emax DAMGO to normalize for difference in receptor expression level across variants as well as the variability in basal stimulation from assay to assay.

MOR-1O		
Ligands	G protein activation	
	Emax (% of DAMGO)	EC_{50} (nM)
DAMGO	100	166 ± 9
Morphine	66 ± 3	133 ± 46
b- Endorphin	85 ± 2	210 ± 30
Endomorphin1	88 ± 5	342 ± 110
Endomorphin2	61 ± 5	360 ± 83
Met-Enk-Arg-Phe	91 ± 7	84 ± 16
Methadone	101 ± 4	107 ± 36
Fentanyl	112 ± 5	166 ± 24
Buprenorphine	33 ± 2	4 ± 3

Table 6 Significance values for EC50 values of drugs in Table 5. Analysis of variance followed by Bonferroni's post-hoc test was performed to determine whether there were any significant differences between the receptors for the indicated drug.

EC50

	MOR-TR	MOR-1	MOR-1A	MOR-1B	MOR-1C	MOR-1E	MOR-1O
DAMGO							
MOR-TR	-	NS	NS	NS	NS	NS	NS
MOR-1		-	NS	NS	$P \leq 0.05$	NS	NS
MOR-1A			-	NS	$P \leq 0.05$	NS	NS
MOR-1B				-	NS	$P \leq 0.05$	NS
MOR-1C					-	NS	NS
MOR-1E						-	NS
MOR-1O							-

EC50

	MOR-TR	MOR-1	MOR-1A	MOR-1B	MOR-1C	MOR-1E	MOR-1O
Morphine							
MOR-TR	-	NS	NS	NS	NS	NS	$P \leq 0.05$
MOR-1		-	NS	NS	NS	NS	$P \leq 0.01$
MOR-1A			-	NS	NS	NS	$P \leq 0.01$
MOR-1B				-	NS	NS	NS
MOR-1C					-	NS	NS
MOR-1E						-	$P \leq 0.01$
MOR-1O							-

Table 6 continued. Significance values for EC50 values of drugs in Table 5. Analysis of variance followed by Bonferroni's post-hoc test was performed to determine whether there were any significant differences between the receptors for the indicated drug.

EC50

	MOR-TR	MOR-1	MOR-1A	MOR-1B	MOR-1C	MOR-1E	MOR-1O
b-Endorphin							
MOR-TR	-	P ≤ 0.001	P ≤ 0.001	P ≤ 0.001	P ≤ 0.001	P ≤ 0.001	P ≤ 0.001
MOR-1		-	NS	NS	NS	NS	NS
MOR-1A			-	NS	NS	NS	NS
MOR-1B				-	NS	NS	NS
MOR-1C					-	NS	NS
MOR-1E						-	NS
MOR-1O							-

EC50

	MOR-TR	MOR-1	MOR-1A	MOR-1B	MOR-1C	MOR-1E	MOR-1O
Endomorphin 1							
MOR-TR	-	NS	NS	NS	NS	NS	NS
MOR-1		-	NS	NS	NS	NS	P ≤ 0.05
MOR-1A			-	NS	NS	NS	NS
MOR-1B				-	NS	NS	NS
MOR-1C					-	NS	NS
MOR-1E						-	P ≤ 0.05
MOR-1O							-

Table 6 continued Significance values for EC50 values of drugs in Table 5. Analysis of variance followed by Bonferroni's post-hoc test was performed to determine whether there were any significant differences between the receptors for the indicated drug.

EC50

	MOR-TR	MOR-1	MOR-1A	MOR-1B	MOR-1C	MOR-1E	MOR-1O
Endomorphin 2							
MOR-TR	-	NS	NS	P ≤ 0.05	NS	NS	P ≤ 0.05
MOR-1		-	NS	P ≤ 0.05	NS	NS	P ≤ 0.05
MOR-1A			-		NS	NS	NS
MOR-1B				-	NS	NS	NS
MOR-1C					-	NS	NS
MOR-1E						-	NS
MOR-1O							-

EC50

	MOR-TR	MOR-1	MOR-1A	MOR-1B	MOR-1C	MOR-1E	MOR-1O
Met-Enk-Arg-Phe							
MOR-TR	-	P ≤ 0.01	P ≤ 0.01	NS	NS	P ≤ 0.01	NS
MOR-1		-	NS	NS	P ≤ 0.05	NS	P ≤ 0.01
MOR-1A			-	NS	P ≤ 0.01	NS	P ≤ 0.01
MOR-1B				-	NS	NS	P ≤ 0.05
MOR-1C					-	P ≤ 0.01	NS
MOR-1E						-	P ≤ 0.001
MOR-1O							-

Table 6 continued. Significance values for EC50 values of drugs in Table 5. Analysis of variance followed by Bonferroni's post-hoc test was performed to determine whether there were any significant differences between the receptors for the indicated drug.

EC50

	MOR-TR	MOR-1	MOR-1A	MOR-1B	MOR-1C	MOR-1E	MOR-1O
Methadone							
MOR-TR	-	NS	NS	NS	P ≤ 0.001	NS	NS
MOR-1		-	NS	NS	P ≤ 0.0001	NS	NS
MOR-1A			-	NS	P ≤ 0.0001	NS	NS
MOR-1B				-	P ≤ 0.0001	NS	NS
MOR-1C					-	P ≤ 0.0001	P ≤ 0.0001
MOR-1E						-	NS
MOR-1O							-

EC50

	MOR-TR	MOR-1	MOR-1A	MOR-1B	MOR-1C	MOR-1E	MOR-1O
Fentanyl							
MOR-TR	-	NS	NS	NS	NS	NS	NS
MOR-1		-	NS	NS	NS	NS	NS
MOR-1A			-	NS	NS	NS	NS
MOR-1B				-	NS	NS	NS
MOR-1C					-	NS	NS
MOR-1E						-	NS
MOR-1O							-

Table 6 continued. Significance values for EC50 values of drugs in Table 5. Analysis of variance followed by Bonferroni's post-hoc test was performed to determine whether there were any significant differences between the receptors for the indicated drug.

EC50

	MOR-TR	MOR-1	MOR-1A	MOR-1B	MOR-1C	MOR-1E	MOR-1O
Buprenorphine							
MOR-TR	-	NS	NS	NS	NS	NS	NS
MOR-1		-	NS	NS	NS	NS	NS
MOR-1A			-	NS	NS	NS	NS
MOR-1B				-	NS	NS	NS
MOR-1C					-	NS	NS
MOR-1E						-	NS
MOR-1O							-

Table 7 Significance values for Emax values of drugs in Table 5. Analysis of variance followed by Bonferroni's post-hoc test was performed to determine whether there were any significant differences between the receptors for the indicated drug.

Emax

	MOR-TR	MOR-1	MOR-1A	MOR-1B	MOR-1C	MOR-1E	MOR-1O
DAMGO							
MOR-TR	-	NS	NS	NS	NS	NS	NS
MOR-1		-	NS	NS	NS	NS	NS
MOR-1A			-	NS	NS	NS	NS
MOR-1B				-	NS	NS	NS
MOR-1C					-	NS	NS
MOR-1E						-	NS
MOR-1O							-

Emax

	MOR-TR	MOR-1	MOR-1A	MOR-1B	MOR-1C	MOR-1E	MOR-1O
Morphine							
MOR-TR	-	NS	NS	NS	NS	NS	NS
MOR-1		-	NS	NS	NS	NS	$P \leq 0.05$
MOR-1A			-	NS	NS	NS	NS
MOR-1B				-	NS	NS	NS
MOR-1C					-	NS	NS
MOR-1E						-	NS
MOR-1O							-

Table 7 continued. Significance values for Emax values of drugs in Table 5. Analysis of variance followed by Bonferroni's post-hoc test was performed to determine whether there were any significant differences between the receptors for the indicated drug.

Emax

	MOR-TR	MOR-1	MOR-1A	MOR-1B	MOR-1C	MOR-1E	MOR-1O
b-Endorphin							
MOR-TR	-	NS	P ≤ 0.01	P ≤ 0.01	P ≤ 0.01	P ≤ 0.01	P ≤ 0.01
MOR-1		-	NS	NS	NS	NS	NS
MOR-1A			-	NS	NS	NS	NS
MOR-1B				-	NS	NS	NS
MOR-1C					-	NS	NS
MOR-1E						-	NS
MOR-1O							-

Emax

	MOR-TR	MOR-1	MOR-1A	MOR-1B	MOR-1C	MOR-1E	MOR-1O
Endomorphin 1							
MOR-TR	-	NS	NS	NS	NS	NS	NS
MOR-1		-	NS	NS	NS	NS	NS
MOR-1A			-	NS	NS	NS	NS
MOR-1B				-	NS	NS	NS
MOR-1C					-	NS	NS
MOR-1E						-	NS
MOR-1O							-

Table 7 continued. Significance values for Emax values of drugs in Table 5. Analysis of variance followed by Bonferroni's post-hoc test was performed to determine whether there were any significant differences between the receptors for the indicated drug.

Emax

	MOR-TR	MOR-1	MOR-1A	MOR-1B	MOR-1C	MOR-1E	MOR-1O
Endomorphin 2							
MOR-TR	-	NS	NS	NS	NS	NS	NS
MOR-1		-	NS	NS	NS	NS	$P \leq 0.05$
MOR-1A			-		NS	NS	$P \leq 0.001$
MOR-1B				-	NS	NS	$P \leq 0.05$
MOR-1C					-	NS	NS
MOR-1E						-	$P \leq 0.01$
MOR-1O							-

Emax

	MOR-TR	MOR-1	MOR-1A	MOR-1B	MOR-1C	MOR-1E	MOR-1O
Met-Enk-Arg-Phe							
MOR-TR	-	NS	$P \leq 0.05$	$P \leq 0.05$	NS	NS	$P \leq 0.05$
MOR-1		-	NS	NS	NS	NS	NS
MOR-1A			-	NS	NS	NS	NS
MOR-1B				-	NS	NS	NS
MOR-1C					-	NS	NS
MOR-1E						-	NS
MOR-1O							-

Table 7 continued. Significance values for Emax values of drugs in Table 5. Analysis of variance followed by Bonferroni's post-hoc test was performed to determine whether there were any significant differences between the receptors for the indicated drug.

Emax

	MOR-TR	MOR-1	MOR-1A	MOR-1B	MOR-1C	MOR-1E	MOR-1O
Methadone							
MOR-TR	-	NS	NS	NS	NS	NS	NS
MOR-1		-	NS	NS	NS	NS	NS
MOR-1A			-	NS	NS	NS	NS
MOR-1B				-	$P \leq 0.05$	NS	NS
MOR-1C					-	NS	$P \leq 0.01$
MOR-1E						-	NS
MOR-1O							-

Emax

	MOR-TR	MOR-1	MOR-1A	MOR-1B	MOR-1C	MOR-1E	MOR-1O
Fentanyl							
MOR-TR	-	NS	NS	NS	NS	NS	NS
MOR-1		-	NS	NS	NS	NS	NS
MOR-1A			-	NS	NS	NS	NS
MOR-1B				-	NS	NS	NS
MOR-1C					-	NS	NS
MOR-1E						-	NS
MOR-1O							-

Table 7 continued. Significance values for Emax values of drugs in Table 5. Analysis of variance followed by Bonferroni's post-hoc test was performed to determine whether there were any significant differences between the receptors for the indicated drug.

Emax

	MOR-TR	MOR-1	MOR-1A	MOR-1B	MOR-1C	MOR-1E	MOR-1O
Buprenorphine							
MOR-TR	-	NS	NS	NS	NS	NS	NS
MOR-1		-	NS	NS	$P \leq 0.05$	NS	NS
MOR-1A			-	NS	$P \leq 0.05$	NS	NS
MOR-1B				-	NS	NS	NS
MOR-1C					-	NS	NS
MOR-1E						-	NS
MOR-1O							-

Part II - C-terminal splice variants differentially regulate β – arrestin-2 signaling pathways

The recent focus in the opioid field has been on biased agonism to develop opioid drugs that can preferentially activate certain signaling pathways (Bohn et al., 2000; Raehal et al., 2005). As described in Part I, the main purpose of this study is to explore if the differences at the C-terminus of the receptor ultimately lead to differences in signal transduction and its ability to recruit proteins to the receptor complex. We are specifically interested in 2 crucial GPCR signaling pathways – the G protein pathway and the β-arrestin pathway. The opioid response is mediated in conjunction by G protein and β-arrestin signaling pathways and distinct biological functions are often linked to these different pathways. GPCRs adopt multiple conformations and the binding of different ligands to the same receptor can stabilize distinct conformations leading to diverse signaling profiles. For example, an agonist capable of fully stimulating G protein coupling may show very little efficacy in activating the β-arrestin pathway and vice versa. The concept of biased agonism describes this difference in ligand-directed GPCR signaling. Ligands that have the capability of differentially stimulating the canonical and non-canonical transduction pathways are considered biased agonists.

Much of the recent effort in the field has focused on developing biased agonists that activate only the subset of signaling pathways important for the therapeutic effect while limiting the unwanted side effects

(Raehal et al., 2011). However, since receptor internalization by β-arrestins can lead to both desensitization and resensitization pathways, there seems to be a divide in the literature on the precise role of β-arrestins in opioid action. This leads to an evident discord in which signaling bias is therapeutically beneficial. Recently developed G protein biased agonists like, Herkinorin and TRV130, have shown to display enhanced analgesia with reduced side effects like gastrointestinal dysfunction and respiratory depression (DeWire et al., 2013; Groer et al., 2007). However, drugs based on the structure of endomorphins, which are arrestin biased, also appear to have favorable analgesic profile with fewer adverse effects (Varamini et al., 2012; Wilson et al., 2000). Some of these inconsistencies may arise because most of the studies that look at bias among ligands only focus on one receptor variant of Oprm – the MOR-1 receptor. However, more than one receptor subtype exists endogenously. Clinical observations as well as opioid literature support the existence of multiple mu opioid receptors.

In Part I, we established that the different C-terminal splice variants exhibit differences in signaling pattern through the G protein signaling pathway. Here, we wanted to extend this understanding to the β-arrestin-2 signaling pathway. The C-terminal splice variants show a great deal of heterogeneity in their in-vivo expression pattern as well as in-vitro pharmacology. Their expression is known to differ in a regional as well as cell-type specific manner (Abbadie et al., 2000; Abbadie et al., 2004). Studying the biases in the β-arrestin-2 signaling

pathway would further our understanding of how an in-vitro drug profile could translate into endogenous functional effects. This focus on splice variants is complementary to research on ligand bias and hetero-oligomerization as we anticipate that different splice variants are likely to interact with different complement of proteins to mediate their effects.

The μ-OR variants contain serine and threonine residues in their cytoplasmic tails that represent phosphoacceptor sites for GPCR kinases. Earlier studies have demonstrated that the C-terminal receptor variants differ in their agonist selective phosphorylation, internalization and down-regulation. Whole cell phosphorylation studies show that DAMGO induces an increased phosphorylation in the mMOR-1 and mMOR-1D variants in comparison to mMOR-1C and mMOR-1E variants (Koch et al., 2001). Koch et al. also showed that levels of phosphorylation observed in these variants is both agonist dependent as well as variant dependent. In contrast to the pattern observed with DAMGO induced phosphorylation, morphine induced similar levels of phosphorylation in the mMOR-1D and mMOR-1E receptors but markedly low levels of phosphorylation in the mMOR-1 and mMOR-1C receptor. Changing the Thr-394 residue in the exon 4 portion of MOR-1 into alanine results in a reduction of DAMGO-induced phosphorylation and a slower DAMGO-mediated desensitization of the T394A receptor mutant (Wolf et al., 1999; Pak et al., 1997). In addition, the lack of Thr-394 leads to facilitated receptor internalization, enhanced resensitization, and recycling of the T394A

receptor mutant (Koch et al., 1998). This indicates that Thr394 is a potential β–arrestin recruiting site in the exon 4 region of the C-tail. Other studies have shown Ser375 to be another β–arrestin recruiting site present in the exon 3 region of the mu receptor (Lau et al., 2011, Moulédous et al., 2015).

Since phosphorylation of the C-tail is a pre-requisite for β-arrestin recruitment, these studies suggest that there might also be differences in levels of β-arrestin recruitment across these variants. These differences may be due to availability of phosphorylation sites or protein kinases. In addition, different agonists might phosphorylate different Ser/Thr residues through different mechanisms. For example, DAMGO is known to cause receptor phosphorylation through GRKs whereas Morphine is known to recruit PKA.

We used the DiscoverX PathHunter assay with the clonal cell lines described in Part I to study splice variant specific patterns in drug induced β–arrestin-2 recruitment. We studied 6 different splice variants, mMOR-1-PK, mMOR-1A-PK, mMOR-1B1-PK, mMOR-1C-PK, mMOR-1E-PK and mMOR-1O-PK as well as a control receptor mMOR-TR-PK which is truncated after exon 3. We thought it was important to have the control receptor because the conserved part of the C-tail as encoded by exon 3 contains a β–arrestin-2 recruiting phosphorylation site at Ser375 (Lau et al., 2011, Moulédous et al., 2015). Therefore, the C-terminal splice variants with splicing downstream of exon 3, not only contain the Ser375 phosphorylation site but might also contain

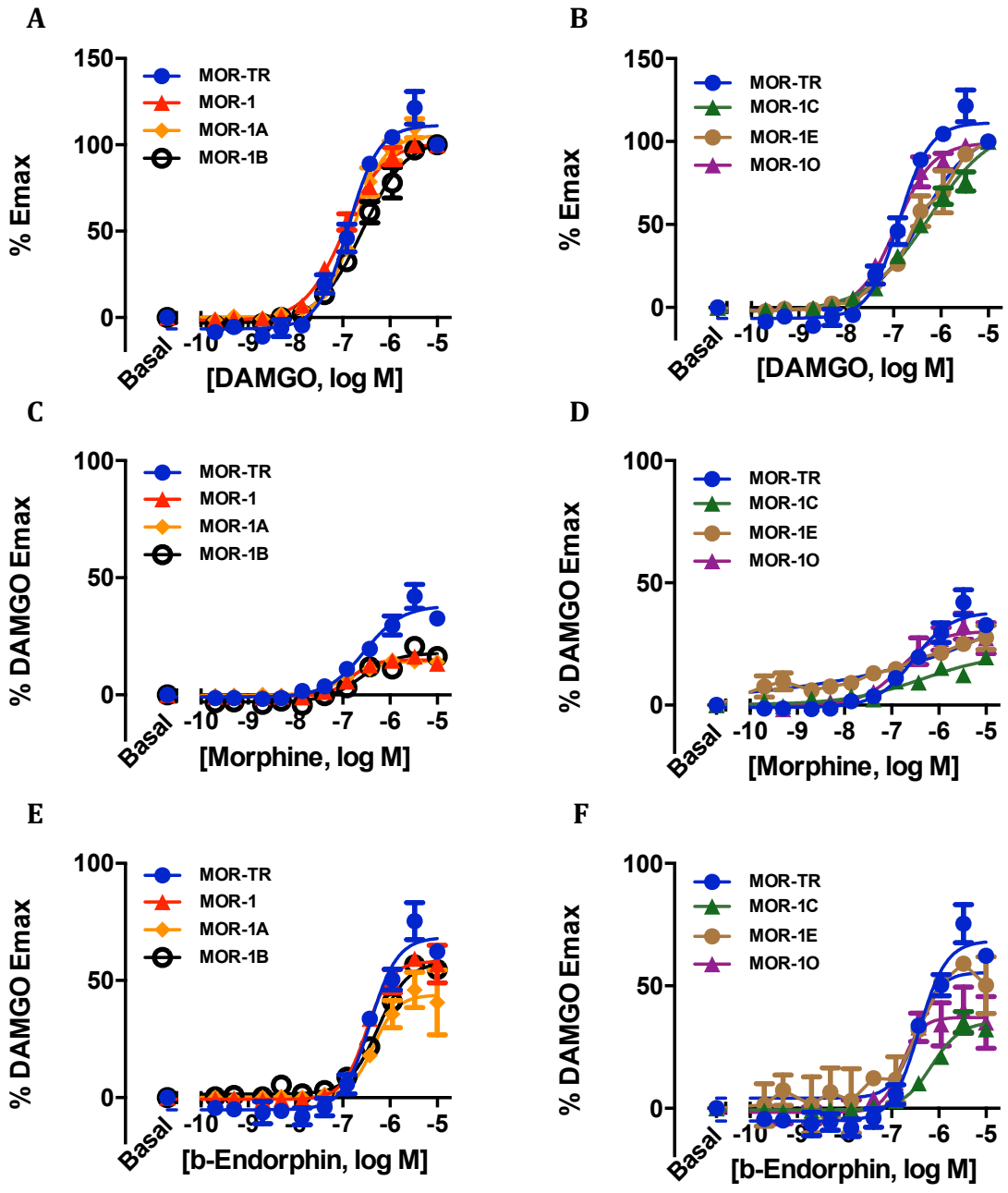

Figure 16 DiscoverX PathHunter assay to measure agonist induced β-arrestin-2 recruitment across the various C-terminal splice variants
Left panel: variants mMOR-TR, mMOR-1, mMOR-1A and mMOR-1B
Right panel: variants mMOR-TR, mMOR-1C, mMOR-1E, mMOR-1O
A comparison of the β-arrestin-2 recruitment curves were generated for 3 mu agonists, **A. and B**. DAMGO, **C. and D.** Morphine, **E. and F.** b-Endorphin. The data was analyzed on GraphPad Prism using non-linear regression analysis. Results are the mean ± S.E. of at least three independent experiments.

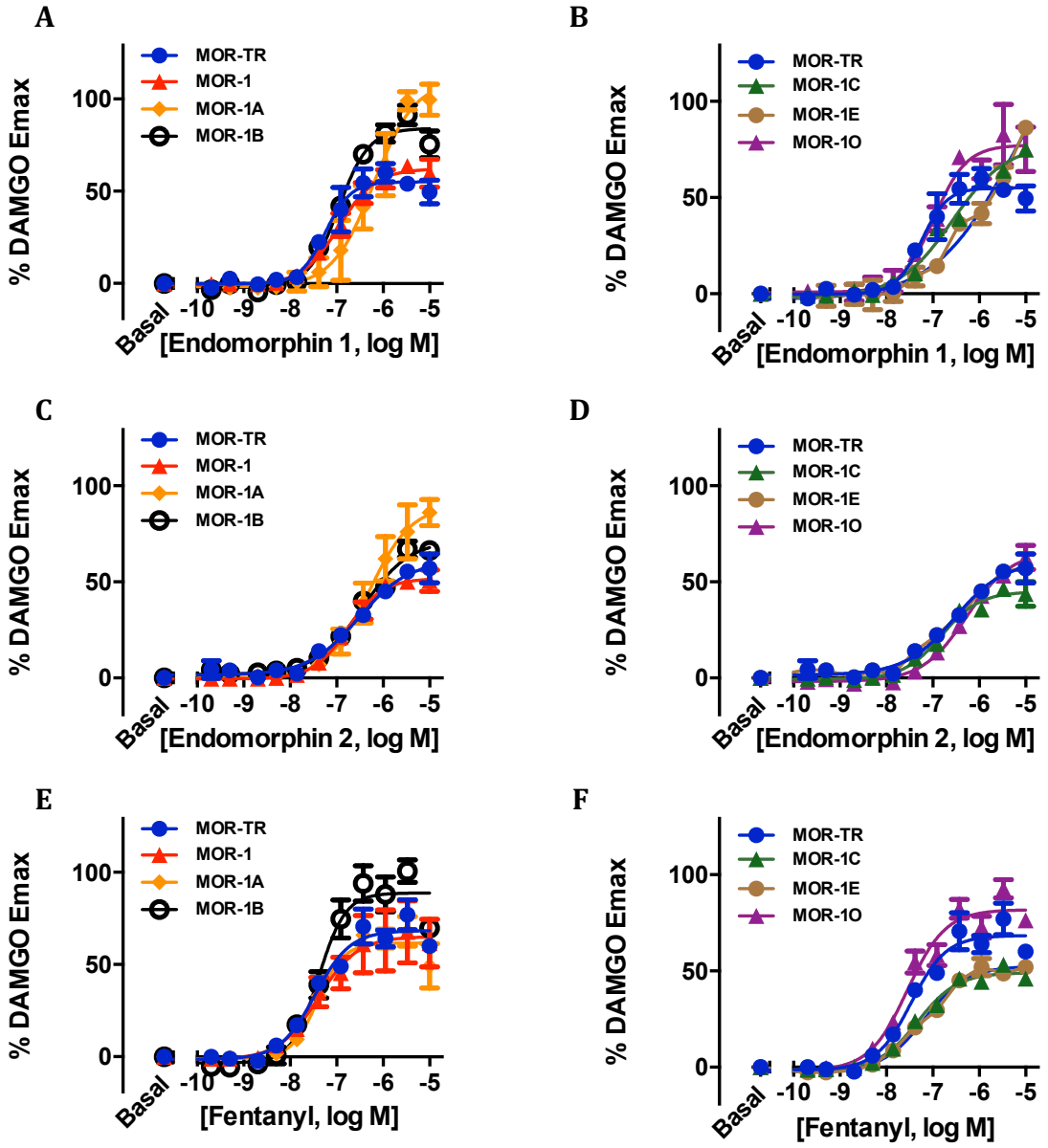

Figure 17 DiscoverX PathHunter assay to measure agonist induced β-arrestin-2 recruitment across the various C-terminal splice variants
Left panel: variants mMOR-TR, mMOR-1, mMOR-1A and mMOR-1B
Right panel: variants mMOR-TR, mMOR-1C, mMOR-1E, mMOR-1O
A comparison of the β-arrestin-2 recruitment curves were generated for 3 mu agonists, **A. and B.** Endomorphin1, **C. and D.** Endomorphin2, **E. and F.** Fentanyl. The data was analyzed on GraphPad Prism using non-linear regression analysis. Results are the mean ± S.E. of at least three independent experiments.

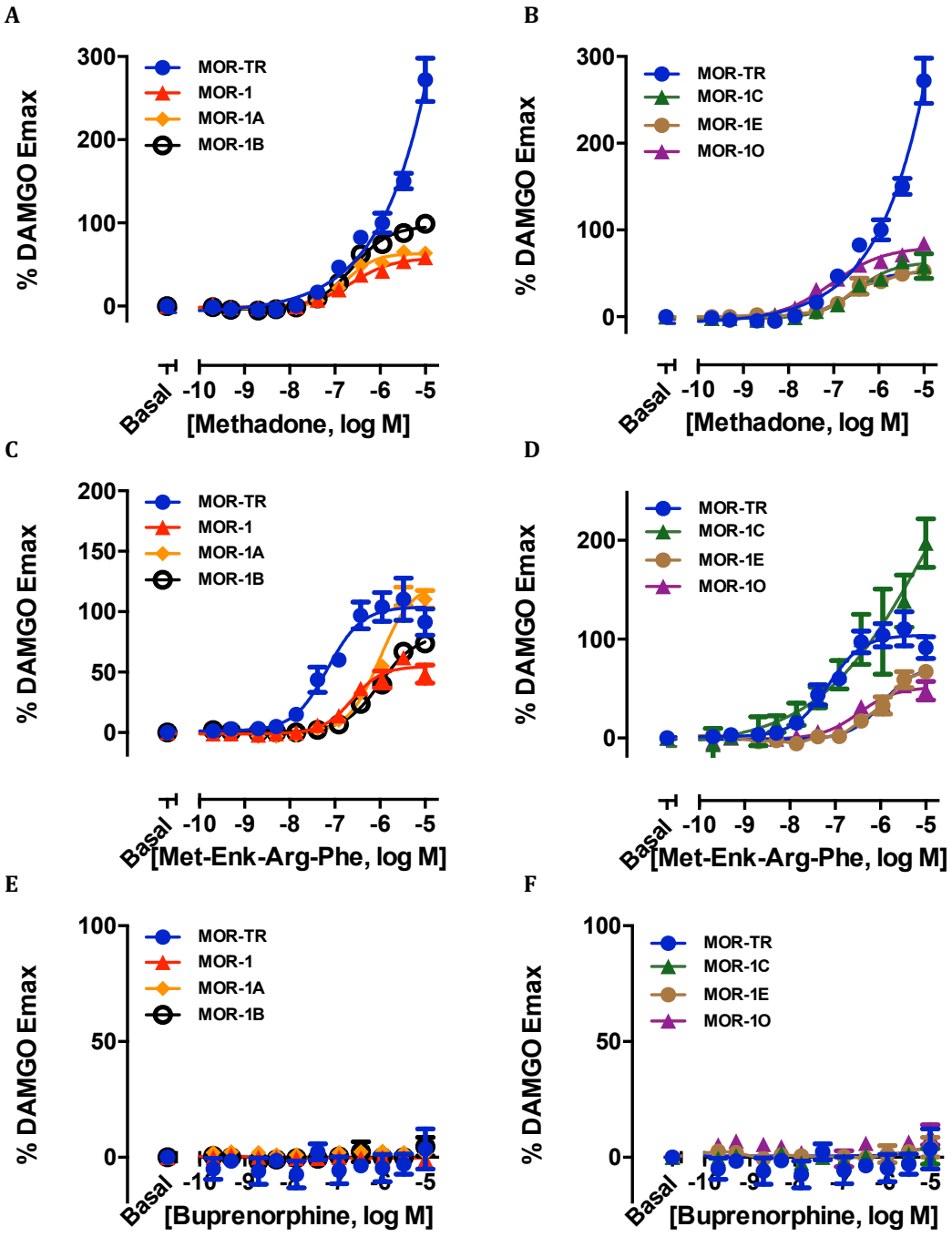

Figure 18 DiscoverX PathHunter assay to measure agonist induced β-arrestin-2 recruitment across the various C-terminal splice variants
Left panel: variants mMOR-TR, mMOR-1, mMOR-1A and mMOR-1B
Right panel: variants mMOR-TR, mMOR-1C, mMOR-1E, mMOR-1O
A comparison of the β-arrestin-2 recruitment curves were generated for 2 mu agonists, **A. and B.** Methadone, **C. and D.** Met-Enk-Arg-Phe, **E. and F.** Buprenorphine. The data was analyzed on GraphPad Prism using non-linear regression analysis. Results are the mean ± S.E. of at least three independent experiments.

additional phosphorylation sites downstream of exon 3. This study would help us determine if the ability of the conserved β–arrestin-2 phosphorylation site may vary across the variants and if adding more amino acids at the C-tail might enhance or impede its ability to recruit arrestins. Figures 16, 17 and 18 depict the arrestin recruitment pattern as seen in these variants in response to a number of mu agonists. The results have been normalized to % DAMGO Emax for every variant in order to eliminate any inherent system bias as a result of difference in expression pattern or basal levels of β–arrestin-2 recruitment.

We screened a panel of peptides and non-peptide opioid agonists and observed differences in both Emax and EC50 values across the different variants tested. The control MOR-TR-PK receptor, which has a truncated C-tail, was significantly more effective at recruiting β–arrestin-2 in comparison to any of the other splice variants. Emax and EC50 values are shown in Table 8. Methadone, a non-peptide agonist, showed a similar trend but a more significant difference between the control receptor and the other splice variants. Methadone stimulated a robust β–arrestin-2 response of Emax - 638% of DAMGO at the mMOR-TR-PK receptor. Adding just 4 amino acids to the control receptor in mMOR-1A-PK significantly impeded its ability to recruit arrestin (Emax – 65% of DAMGO).

The increased efficiency of the mMOR-TR-PK receptor at recruiting β–arrestin-2, however, was not conserved for all the drugs.

Endomorphin1 acted as a partial agonist in the β–arrestin-2 assay at the control receptor (Emax – 66% of DAMGO) but as a full agonist at the mMOR-1A receptor (Emax- 108% of DAMGO). Another peptide agonist, Met-Enk-Arg-Phe was twice as effective at recruiting β–arrestin-2 at the mMOR-1C-PK receptor (Emax- 224% of DAMGO) in comparison to mMOR-TR-PK (Emax - 104% of DAMGO).

mMOR-1C and mMOR-1O variants have exon 7 at the C-tail and overlap in 30 amino acids downstream of exon 3. In addition to exon 7, mMOR-1C also contains exons 8, 9 and an extra 22 amino acids in the C-tail. In spite of the similarity in between these 2 variants, they show significant variations in their agonist induced arrestin recruitment pattern. For example, the two receptors are equally effective in the β – endorphin induced arrestin response, but the mMOR-1O receptor is 8 times more potent in comparison to mMOR-1C. This trend is reversed for Endomorphin 2 and Methadone induced response, where the mMOR-1C receptor is significantly more potent in comparison to the mMOR-1O receptor. One possible reason is that in spite of the sequence similarity, the alternatively spliced sequences contain differential phosphorylation sites that influence their function. mMOR-1C has the longest C-terminal tail across all C-terminal splice variants with 52 amino acids. The long C-terminal tail may modify the structure of the receptor and impact its ability to interact with other protein complexes.

The pattern of β–arrestin-2 recruitment varies across drugs as well as across variants. It is also interesting that in spite of the presence of conserved potential phosphorylation sites in exon 3 part of the C-tail, most of the C-terminal splice variants are less effective at recruiting β-arrestin-2 in comparison to the control mMOR-TR receptor. The response seems to follow a bell curve when correlating the length of the C-tail to arrestin recruitment efficiency, where the mMOR-1C and mMOR-1O receptors with the longer C-tails are much more like the truncated receptor in their ability to recruit arrestin. These assays, however, do not provide sufficient evidence regarding the relevance of these findings in-vivo since β–arrestins can affect a number of downstream pathways. Arrestins have been shown to act as scaffolds for both internalization and ubiquitination machinery.

Alternatively, ERK1/2 activation has also been linked to receptor desensitization through arrestin-dependent and arrestin-independent mechanisms. We measured ERK1/2 activation in two C-terminal variants mMOR-1 and mMOR-1O expressed in HEK cells (Figure 19). Using the drugs that showed us the most differences across variants, we measured ERK1/2 activation as a way to validate our earlier findings. We chose to use western blot analysis as it is a whole cell assay instead of an in vitro assay like the [^{35}S]GTPγS. Additionally, we did this assay in another cell line, HEK cells, to test the applicability of our earlier results. We chose 2 of the C-terminal variants, mMOR-1 and mMOR-1O, that had the most differences from our earlier findings. We compared levels of ERK activation in these variants after

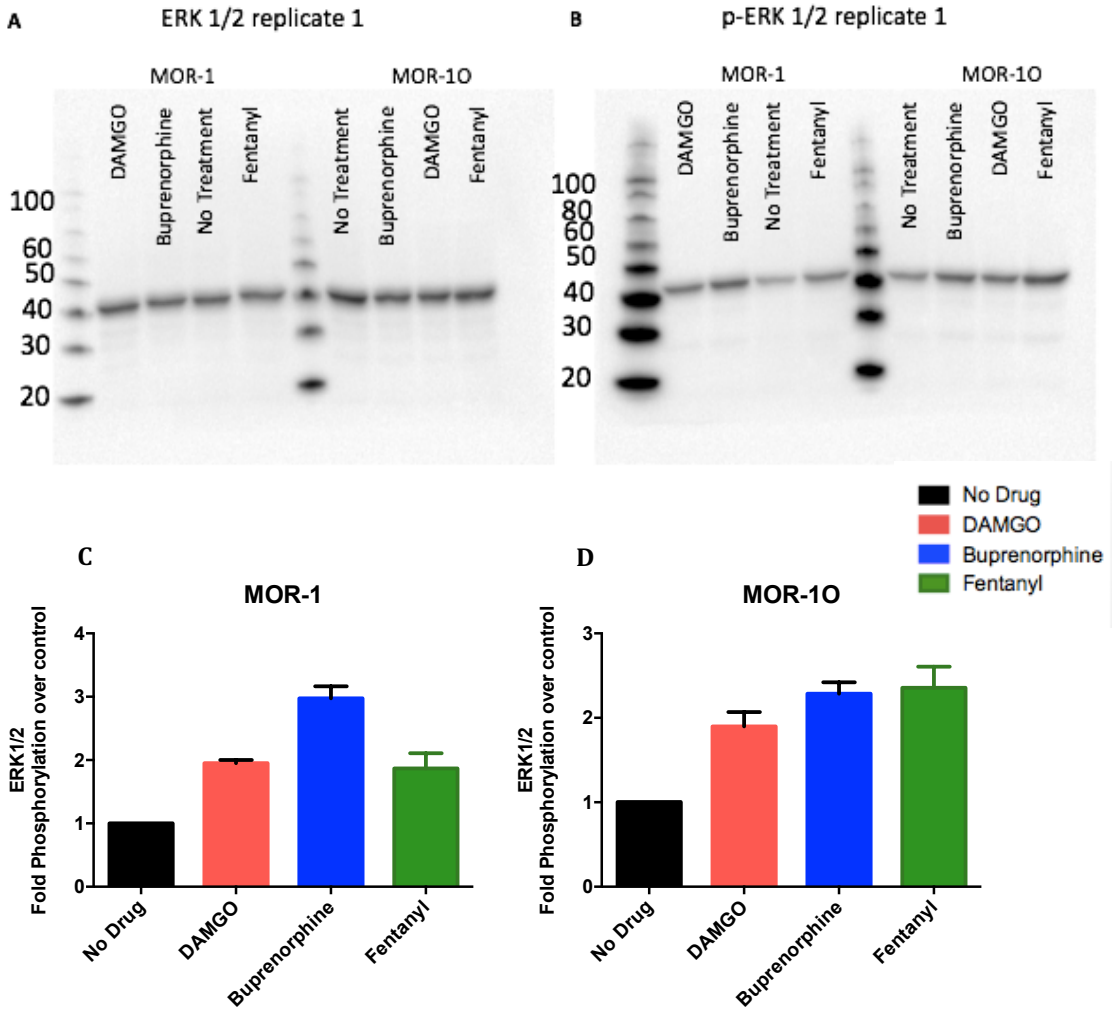

Figure 19 Agonist induced ERK activation in HEK cells expressing MOR-1 and MOR-1O receptor. **A.** Western blot showing total ERK levels in HEK cells expressing the receptor variant after saline, DAMGO, Buprenorphine or Fentanyl treatment. **B.** Western blot showing p-ERK levels in HEK cells expressing the receptor variant after saline, DAMGO, Buprenorphine or Fentanyl treatment. **C.** Fold change in ERK1/2 activation after agonist treatment at MOR-1. The results are from three independent experiments. The p-ERK levels were normalized to total ERK. **D.** Fold change in ERK1/2 activation after agonist treatment at MOR-1O. The results are from three independent experiments. The p-ERK levels were normalized to total ERK.

treatment with 3 different agonists- DAMGO, Buprenorphine and Fentanyl at their equi-active [^{35}S]GTPγS dose. The HEK cell lines expressing the receptor variants showed no significant differences in pERK activation after agonist treatment. ERK results can sometimes be inconclusive because the ERK pathway can be activated through both G protein as well as arrestin dependent mechanism. However, we think that since we used equi-active [^{35}S]GTPγS doses for these assays, the ERK results serve as a validation of our results in the [^{35}S]GTPγS assay. In addition, it also suggests that the cytoplasmic pERK activation we are observing in the western blot assay is primarily through a G protein dependent mechanism.

The differences in β-arrestin activity observed across the variants could be due to several reasons. Firstly, it is possible that the phosphorylation sites in the conserved portion of the exon 3 C-tail are not equally active across the different C-terminal variants. The differences in length and conformation of the C-tail can affect the accessibility of these sites to the GPCR kinases. Secondly, the differences could be due to the differences downstream of exon 3 at the tip of the C-terminus. Some of these variants may potentially have additional phosphorylation and β-arrestin recruiting sites downstream of exon 3. There might also be differences in their ability to interact with other protein kinases. A follow up study should look at the relevance of the Ser375 β-arrestin recruiting site across the different variants and also explore the presence of additional active

phosphorylation sites downstream of exon 3, specifically at variants like MOR-1O which are more effective in recruiting β-arrestin.

Table 8 Effect of mu agonist on β-arrestin-2 recruitment in CHO cells stably transfected with the C-terminal splice variant. A PathHunter β-arrestin-2 assay (DiscoverX) were performed as described in Methods. 6 different C-terminal variants were characterized, mMOR-1, mMOR-1A, mMOR-1B1, mMOR-1C, mMOR-1E and mMOR-1O along with the control receptor MOR-TR-PK which is truncated after exon 3. Ki and EC50 values were calculated on GraphPad Prism using non-linear regression analysis. Analysis of variance followed by Bonferroni's post-hoc test was performed to determine whether there were any significant differences between the receptors for the indicated drug. Results are the mean ± SEM of at least three independent experiments. For each variant, the data was normalized using stimulation of 10μM DAMGO. The data is reported as % Emax DAMGO to normalize for difference in receptor expression level across variants as well as the variability in basal stimulation from assay to assay.

MOR-TR			**MOR-1**		
Ligands	Arrestin activation		Ligands	Arrestin activation	
	Emax (% of DAMGO)	EC_{50} (nM)		Emax (% of DAMGO)	EC_{50} (nM)
DAMGO	100	146 ± 16	DAMGO	100	113 ± 20
Morphine	40 ± 2	350 ± 89	Morphine	15 ± 1	147 ± 19
b- Endorphin	68 ± 5	383 ± 38	b- Endorphin	55 ± 6	315 ± 66
Endomorphin1	66 ± 8	92 ± 14	Endomorphin1	62 ± 6	118 ± 23
Endomorphin2	74 ± 6	75 ± 15	Endomorphin2	52 ± 4	184 ± 37
Met-Enk-Arg-Phe	104 ± 13	78 ± 34	Met-Enk-Arg-Phe	58 ± 5	308 ± 70
Methadone	638 ± 58	97 ± 19	Methadone	59 ± 7	263 ± 59
Fentanyl	69 ± 5	35 ± 4	Fentanyl	65 ± 16	39 ± 5
Buprenorphine	No Signal	No Signal	Buprenorphine	No Signal	No Signal

Table 8 continued. Effect of mu agonist on β-arrestin-2 recruitment in CHO cells stably transfected with the C-terminal splice variant. A PathHunter β-arrestin-2 assay (DiscoverX) were performed as described in Methods. 6 different C-terminal variants were characterized, mMOR-1, mMOR-1A, mMOR-1B1, mMOR-1C, mMOR-1E and mMOR-1O along with the control receptor MOR-TR-PK which is truncated after exon 3. Ki and EC50 values were calculated on GraphPad Prism using non-linear regression analysis. Analysis of variance followed by Bonferroni's post-hoc test was performed to determine whether there were any significant differences between the receptors for the indicated drug. Results are the mean ± SEM of at least three independent experiments. For each variant, the data was normalized using stimulation of 10μM DAMGO. The data is reported as % Emax DAMGO to normalize for difference in receptor expression level across variants as well as the variability in basal stimulation from assay to assay.

MOR-1A			**MOR-1B-1**		
Ligands	Arrestin activation		Ligands	Arrestin activation	
	Emax (% of DAMGO)	EC_{50} (nM)		Emax (% of DAMGO)	EC_{50} (nM)
DAMGO	100	167 ± 2	DAMGO	100	193 ± 40
Morphine	15 ± 0.5	123 ± 4	Morphine	19 ± 2	332 ± 112
b- Endorphin	45 ± 12	462 ± 116	b- Endorphin	62 ± 3	634 ± 47
Endomorphin1	108 ± 7	668 ± 213	Endomorphin1	85 ± 5	115 ± 16
Endomorphin2	92 ± 7	630 ± 183	Endomorphin2	72 ± 4	382 ± 88
Met-Enk-Arg-Phe	125 ± 8	1014 ± 56	Met-Enk-Arg-Phe	83 ± 8	1085 ± 260
Methadone	65 ± 2	200 ± 46	Methadone	98 ± 3	263 ± 43
Fentanyl	62 ± 8	39 ± 7	Fentanyl	89 ± 7	42 ± 5
Buprenorphine	No Signal	No Signal	Buprenorphine	No Signal	No Signal

Table 8 continued. Effect of mu agonist on β-arrestin-2 recruitment in CHO cells stably transfected with the C-terminal splice variant. A PathHunter β-arrestin-2 assay (DiscoverX) were performed as described in Methods. 6 different C-terminal variants were characterized, mMOR-1, mMOR-1A, mMOR-1B1, mMOR-1C, mMOR-1E and mMOR-1O along with the control receptor MOR-TR-PK which is truncated after exon 3. Ki and EC50 values were calculated on GraphPad Prism using non-linear regression analysis. Analysis of variance followed by Bonferroni's post-hoc test was performed to determine whether there were any significant differences between the receptors for the indicated drug. Results are the mean ± SEM of at least three independent experiments. For each variant, the data was normalized using stimulation of 10μM DAMGO. The data is reported as % Emax DAMGO to normalize for difference in receptor expression level across variants as well as the variability in basal stimulation from assay to assay.

MOR-1C			**MOR-1E**		
Ligands	Arrestin activation		Ligands	Arrestin activation	
	Emax (% of DAMGO)	EC_{50} (nM)		Emax (% of DAMGO)	EC_{50} (nM)
DAMGO	100	355 ± 94	DAMGO	100	211 ± 64
Morphine	18 ± 1	195 ± 16	Morphine	28 ± 3	48 ± 6
b- Endorphin	37 ± 2	806 ± 180	b- Endorphin	51 ± 1	326 ± 22
Endomorphin1	72 ± 2	225 ± 23	Endomorphin1	72 ± 3	360 ± 37
Endomorphin2	46 ± 6	163 ± 28	Endomorphin2	61 ± 6	400 ± 217
Met-Enk-Arg-Phe	224 ± 44	494 ± 178	Met-Enk-Arg-Phe	83 ± 4	1951 ± 906
Methadone	67 ± 16	407 ± 182	Methadone	54 ± 2	352 ± 111
Fentanyl	49 ± 2	48 ± 4	Fentanyl	53 ± 2	84 ± 17
Buprenorphine	No Signal	No Signal	Buprenorphine	No Signal	No Signal

Table 8 continued. Effect of mu agonist on β-arrestin-2 recruitment in CHO cells stably transfected with the C-terminal splice variant. A PathHunter β-arrestin-2 assay (DiscoverX) were performed as described in Methods. 6 different C-terminal variants were characterized, mMOR-1, mMOR-1A, mMOR-1B1, mMOR-1C, mMOR-1E and mMOR-1O along with the control receptor MOR-TR-PK which is truncated after exon 3. Ki and EC50 values were calculated on GraphPad Prism using non-linear regression analysis. Analysis of variance followed by Bonferroni's post-hoc test was performed to determine whether there were any significant differences between the receptors for the indicated drug. Results are the mean ± SEM of at least three independent experiments. For each variant, the data was normalized using stimulation of 10μM DAMGO. The data is reported as % Emax DAMGO to normalize for difference in receptor expression level across variants as well as the variability in basal stimulation from assay to assay.

MOR-1O		
Ligands	Arrestin activation	
	Emax (% of DAMGO)	EC_{50} (nM)
DAMGO	100	94 ± 34
Morphine	25 ± 0.5	190 ± 19
b- Endorphin	37 ± 9	159 ± 36
Endomorphin1	78 ± 3	127 ± 4
Endomorphin2	94 ± 17	876 ± 541
Met-Enk-Arg-Phe	56 ± 9	463 ± 163
Methadone	80 ± 2	97 ± 19
Fentanyl	83 ± 1	31 ± 5
Buprenorphine	No Signal	No Signal

Table 9 Significance values for EC50 values of drugs in Table 8. Analysis of variance followed by Bonferroni's post-hoc test was performed to determine whether there were any significant differences between the receptors for the indicated drug.

EC50

	MOR-TR	MOR-1	MOR-1A	MOR-1B	MOR-1C	MOR-1E	MOR-1O
DAMGO							
MOR-TR	-	NS	NS	NS	NS	NS	NS
MOR-1		-	NS	NS	NS	NS	NS
MOR-1A			-	NS	NS	NS	NS
MOR-1B				-	NS	NS	NS
MOR-1C					-	NS	$P \leq 0.05$
MOR-1E						-	NS
MOR-1O							-

EC50

	MOR-TR	MOR-1	MOR-1A	MOR-1B	MOR-1C	MOR-1E	MOR-1O
Morphine							
MOR-TR	-	NS	NS	NS	NS	$P \leq 0.05$	NS
MOR-1		-	NS	NS	NS	NS	NS
MOR-1A			-	NS	NS	NS	NS
MOR-1B				-	NS	NS	NS
MOR-1C					-	NS	NS
MOR-1E						-	NS
MOR-1O							-

Table 9 continued. Significance values for EC50 values of drugs in Table 8. Analysis of variance followed by Bonferroni's post-hoc test was performed to determine whether there were any significant differences between the receptors for the indicated drug.

EC50

	MOR-TR	MOR-1	MOR-1A	MOR-1B	MOR-1C	MOR-1E	MOR-1O
b-Endorphin							
MOR-TR	-	NS	NS	NS	NS	NS	NS
MOR-1		-	NS	NS	P ≤ 0.05	NS	NS
MOR-1A			-	NS	NS	NS	NS
MOR-1B				-	NS	NS	P ≤ 0.05
MOR-1C					-	P ≤ 0.05	P ≤ 0.01
MOR-1E						-	NS
MOR-1O							-

EC50

	MOR-TR	MOR-1	MOR-1A	MOR-1B	MOR-1C	MOR-1E	MOR-1O
Endomorphin 1							
MOR-TR	-	NS	P ≤ 0.01	NS	NS	NS	NS
MOR-1		-	P ≤ 0.01	NS	NS	NS	NS
MOR-1A			-	P ≤ 0.01	P ≤ 0.05	NS	P ≤ 0.01
MOR-1B				-	NS	NS	NS
MOR-1C					-	NS	NS
MOR-1E						-	NS
MOR-1O							-

Table 9 continued. Significance values for EC50 values of drugs in Table 8. Analysis of variance followed by Bonferroni's post-hoc test was performed to determine whether there were any significant differences between the receptors for the indicated drug.

EC50

	MOR-TR	MOR-1	MOR-1A	MOR-1B	MOR-1C	MOR-1E	MOR-1O
Endomorphin 2							
MOR-TR	-	NS	NS	NS	NS	NS	NS
MOR-1		-	NS	NS	NS	NS	NS
MOR-1A			-	NS	NS	NS	NS
MOR-1B				-	NS	NS	NS
MOR-1C					-	NS	NS
MOR-1E						-	NS
MOR-1O							-

EC50

	MOR-TR	MOR-1	MOR-1A	MOR-1B	MOR-1C	MOR-1E	MOR-1O
Met-Enk-Arg-Phe							
MOR-TR	-	NS	NS	NS	NS	NS	NS
MOR-1		-	NS	NS	NS	NS	NS
MOR-1A			-	NS	NS	NS	NS
MOR-1B				-	NS	NS	NS
MOR-1C					-	NS	NS
MOR-1E						-	NS
MOR-1O							-

Table 9 continued. Significance values for EC50 values of drugs in Table 8. Analysis of variance followed by Bonferroni's post-hoc test was performed to determine whether there were any significant differences between the receptors for the indicated drug.

EC50

	MOR-TR	MOR-1	MOR-1A	MOR-1B	MOR-1C	MOR-1E	MOR-1O
Methadone							
MOR-TR	-	P ≤ 0.0001	P ≤ 0.0001	P ≤ 0.0001	P ≤ 0.0001	P ≤ 0.0001	P ≤ 0.0001
MOR-1		-	NS	NS	NS	NS	NS
MOR-1A			-	NS	NS	NS	NS
MOR-1B				-	NS	NS	NS
MOR-1C					-	NS	NS
MOR-1E						-	NS
MOR-1O							-

EC50

	MOR-TR	MOR-1	MOR-1A	MOR-1B	MOR-1C	MOR-1E	MOR-1O
Fentanyl							
MOR-TR	-	NS	NS	NS	NS	P ≤ 0.05	NS
MOR-1		-	NS	NS	NS	P ≤ 0.05	NS
MOR-1A			-	NS	NS	P ≤ 0.05	NS
MOR-1B				-	NS	P ≤ 0.05	NS
MOR-1C					-	NS	P ≤ 0.01
MOR-1E						-	NS
MOR-1O							-

Table 10 Significance values for Emax values of drugs in Table 8. Analysis of variance followed by Bonferroni's post-hoc test was performed to determine whether there were any significant differences between the receptors for the indicated drug.

Emax

	MOR-TR	MOR-1	MOR-1A	MOR-1B	MOR-1C	MOR-1E	MOR-1O
DAMGO							
MOR-TR	-	NS	NS	NS	NS	NS	NS
MOR-1		-	NS	NS	NS	NS	NS
MOR-1A			-	NS	NS	NS	NS
MOR-1B				-	NS	NS	NS
MOR-1C					-	NS	NS
MOR-1E						-	NS
MOR-1O							-

Emax

	MOR-TR	MOR-1	MOR-1A	MOR-1B	MOR-1C	MOR-1E	MOR-1O
Morphine							
MOR-TR	-	$P \leq 0.0001$	$P \leq 0.0001$	$P \leq 0.0001$	$P \leq 0.0001$	$P \leq 0.001$	$P \leq 0.001$
MOR-1		-	NS	NS	NS	$P \leq 0.001$	$P \leq 0.01$
MOR-1A			-	NS	NS	$P \leq 0.001$	$P \leq 0.01$
MOR-1B				-	NS	$P \leq 0.05$	NS
MOR-1C					-	$P \leq 0.01$	NS
MOR-1E						-	NS
MOR-1O							-

Table 10 continued. Significance values for Emax values of drugs in Table 8. Analysis of variance followed by Bonferroni's post-hoc test was performed to determine whether there were any significant differences between the receptors for the indicated drug.

Emax

	MOR-TR	MOR-1	MOR-1A	MOR-1B	MOR-1C	MOR-1E	MOR-1O
b-Endorphin							
MOR-TR	-	NS	NS	NS	NS	NS	NS
MOR-1		-	NS	NS	NS	NS	NS
MOR-1A			-	NS	NS	NS	NS
MOR-1B				-	NS	NS	NS
MOR-1C					-	NS	NS
MOR-1E						-	NS
MOR-1O							-

Emax

	MOR-TR	MOR-1	MOR-1A	MOR-1B	MOR-1C	MOR-1E	MOR-1O
Endomorphin 1							
MOR-TR	-	NS	$P \leq 0.001$	NS	NS	NS	NS
MOR-1		-	$P \leq 0.001$	NS	NS	NS	NS
MOR-1A			-	NS	$P \leq 0.01$	$P \leq 0.01$	$P \leq 0.05$
MOR-1B				-	NS	NS	NS
MOR-1C					-	NS	NS
MOR-1E						-	NS
MOR-1O							-

Table 10 continued. Significance values for Emax values of drugs in Table 8. Analysis of variance followed by Bonferroni's post-hoc test was performed to determine whether there were any significant differences between the receptors for the indicated drug.

Emax

	MOR-TR	MOR-1	MOR-1A	MOR-1B	MOR-1C	MOR-1E	MOR-1O
Endomorphin 2							
MOR-TR	-	NS	NS	NS	NS	NS	NS
MOR-1		-	NS	NS	NS	NS	NS
MOR-1A			-	NS	P ≤ 0.05	NS	NS
MOR-1B				-	NS	NS	NS
MOR-1C					-	NS	P ≤ 0.05
MOR-1E						-	NS
MOR-1O							-

Emax

	MOR-TR	MOR-1	MOR-1A	MOR-1B	MOR-1C	MOR-1E	MOR-1O
Met-Enk-Arg-Phe							
MOR-TR	-	NS	NS	NS	P ≤ 0.01	NS	NS
MOR-1		-	NS	NS	P ≤ 0.001	NS	NS
MOR-1A			-	NS	P ≤ 0.05	NS	NS
MOR-1B				-	P ≤ 0.01	NS	NS
MOR-1C					-	P ≤ 0.01	P ≤ 0.001
MOR-1E						-	NS
MOR-1O							-

Table 10 continued. Significance values for Emax values of drugs in Table 8. Analysis of variance followed by Bonferroni's post-hoc test was performed to determine whether there were any significant differences between the receptors for the indicated drug.

Emax

	MOR-TR	MOR-1	MOR-1A	MOR-1B	MOR-1C	MOR-1E	MOR-1O
Methadone							
MOR-TR	-	P ≤ 0.0001	P ≤ 0.0001	P ≤ 0.0001	P ≤ 0.0001	P ≤ 0.0001	P ≤ 0.0001
MOR-1		-	NS	NS	NS	NS	NS
MOR-1A			-	NS	NS	NS	NS
MOR-1B				-	NS	NS	NS
MOR-1C					-	NS	NS
MOR-1E						-	NS
MOR-1O							-

Emax

	MOR-TR	MOR-1	MOR-1A	MOR-1B	MOR-1C	MOR-1E	MOR-1O
Fentanyl							
MOR-TR	-	NS	NS	NS	NS	NS	NS
MOR-1		-	NS	NS	NS	NS	NS
MOR-1A			-	NS	NS	NS	NS
MOR-1B				-	P ≤ 0.05	NS	NS
MOR-1C					-	NS	NS
MOR-1E						-	NS
MOR-1O							-

Part III – C-terminal splice variants differ in their inherent signaling bias and impact agonist induced therapeutic and side effects in-vivo

β-arrestins are essential for the internalization of the receptor and act as scaffolds for the activation of several downstream effects ranging from desensitization, downregulation, as well as resensitization of the receptor. The functional relevance of β-arrestins has been vigorously explored in the opioid field. A β-arrestin-1 knockout animal is developmentally normal and exhibits normal cardiac parameters. However, the stimulation of the β-adrenergic receptor in this animal produces an exaggerated hemodynamic response (Conner et al., 1997). This indicates that β-arrestin-1 plays a role in cardiac β-adrenergic receptor desensitization.

Bohn et al. used a β-arrestin-2 knockout animal model to understand its relevance in GPCR function in vivo. β-arrestin-2 knockout mice show prolonged morphine analgesia and develop no tolerance in response to acute or chronic morphine treatment (Bohn et al., 1999; Bohn et al., 2000). As shown in Figure 20, wild-type mice exhibited a roughly 50% reduction in morphine responsiveness if they received morphine, as compared to saline, the day before. Whereas, the barr2$^{-/-}$ mice maintained the same degree of responsiveness to morphine, regardless of if they had been treated with saline or morphine on the previous day. This indicates that the barr2$^{-/-}$ mice do not develop acute antinociceptive tolerance to morphine.

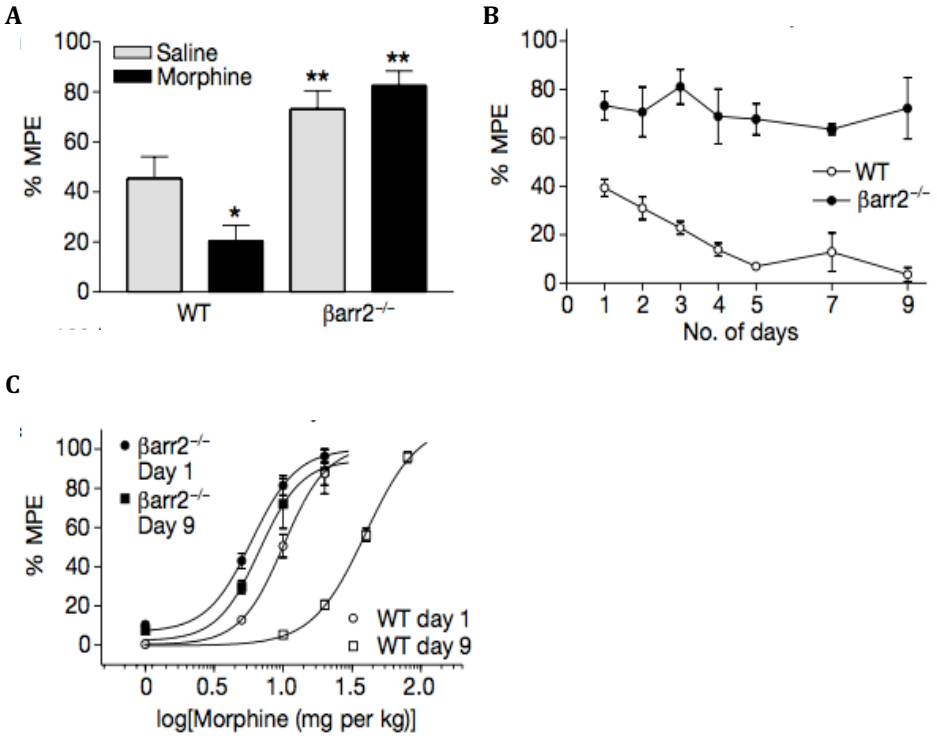

Figure 20 Lack of morphine antinociceptive tolerance in barr2$^{-/-}$ mice. **A.** Paw withdrawal latency after a moderate dose of morphine (10mg per kg, subcutaneously (s.c.) 24h after receiving an injection of either saline or 100 mg per kg morphine. **B.** Paw withdrawal latency after daily administration of morphine. **C.** Dose response curve comparing morphine induced analgesia from day 1 to day 9. (From Bohn et al., 1999)

They also looked at analgesia after chronic morphine treatment, as in the clinical setting, tolerance to morphine's analgesic properties usually develops over continued use of moderate levels of the drug. Mice were injected daily with morphine, and paw-withdrawal latencies were recorded (Fig. 20b). Although the wild-type littermates had significantly diminished responsiveness to the drug by day 5, the knockout mice continued to experience as much antinociception on

day 5 to day 9 as on day 1. Notably, the barr2$^{-/-}$ mice did not experience a shift in their sensitivity to morphine after chronic daily administration, whereas the wild-type mice experienced a significant rightward shift in efficacy after continued treatment (Fig. 20c). In addition, these mice showed no significant difference in comparison to wild type mice in their naloxone induced withdrawal. This was in agreement with earlier studies that have linked physical dependence to a cAMP (G protein pathway) mediated response.

These findings are critical because they link the functional significance of β-arrestin-2 knockdown to prolonged analgesia and tolerance. Consequently, drugs that are endogenously G protein biased as against β-arrestin-2 biased would presumably lead to a more effective analgesic response with limited tolerance side effects. A critical dilemma facing our efforts to discover further examples of β-arrestin biased ligands is how best to detect and quantify bias. In practice, ligand bias is defined operationally by the methods used to characterize receptor functions. For G-protein function, there are many well-established assays with high sensitivity and specificity, and robust high throughput systems are available for any 7TMR of interest. However, there are far fewer methods for assessing β-arrestin efficacy. These include measurements of receptor phosphorylation, β-arrestin translocation to receptors and β-arrestin functions. Measures of β-arrestin functions include receptor desensitization and internalization and β-arrestin-dependent signals such as ERK1/2 activation. Receptor desensitization and internalization can be difficult

to interpret because these effects can occur through both β-arrestin dependent and β-arrestin independent mechanisms. Similarly, ERK1/2 activation can occur through many pathways, necessitating careful controls to ensure reliable measurement of β-arrestin signals. Thus, the simplest assays of β-arrestin efficacy are measures of β-arrestin translocation to receptors.

Much of the recent work in the opioid field has focused on ligand bias at the MOR-1 receptor. However, the inherent endogenous bias of a drug would be the summation of its biases across the different μ-OR variants. The differences in receptor biases among the splice variants of the mu receptor is a previously unexplored subject. Here, we have tried to calculate signal bias across 6 C-terminal splice variants mMOR-1-PK, mMOR-1A-PK, mMOR-1B1-PK, mMOR-1C-PK, mMOR-1E-PK, mMOR-1O-PK and compare how it varies from the control receptor mMOR-TR-PK. We looked at the β-arrestin-2 pathway using DiscoverX PathHunter system and G protein using [^{35}S]GTPγS binding assay as described in Part I and II.

We chose to use the operational model of Black and Leff to quantify the effective signaling by receptors. To compare the relative activity of agonists in the two pathways and identify the bias, we generated concentration response curve for each signaling pathway (Figure 21 – 27). As described in methods, we then compared the log(τ/Ka) value of each test ligand to the log(τ/Ka) of a reference ligand, like DAMGO, for both G protein activation and arrestin recruitment. We used a

reference ligand that has a very similar EC50 value for both the G protein and arrestin pathways and displays full efficacy at both pathways. Ligand bias is quantified by comparing the relative activity of an agonist in one assay to the relative activity in another assay, using the same reference ligand. This method reduces to the observation or the system bias (Kenakin et al., 2013). Transduction coefficients are useful in comparing the relative signaling of ligands, but can be problematic when trying to measure the efficacy of agonists that produce maximal or no effect in a given signaling pathway, like Buprenorphine (Rajagopal, 2013). Due to the limitations of this method, we were not able to quantify bias for Buprenorphine, even though, it is a perfectly β-arrestin biased agonist in our hands that does not recruit β-arrestin at any of the C-terminal splice variants.

After calculating the bias factors using the Black and Leff Operational Model, we used a few different normalization methods to compare differences across variants or across drugs at one variant. We generated a heat map of biased factors (Table 11). The negative (blue) values indicate arrestin bias whereas the positive bias (red) values indicate G protein bias. Table 11a is normalized with respect to DAMGO at every variant and is optimized to compare differences across drugs at a variant. As a proof of concept, we see that the peptides like Endomorphin1 and Endomorphin2 are arrestin biased at mMOR-1, as has been published previously (Rivero et al., 2012). Met-Enk-Arg-Phe is significantly G protein biased at several of the C-terminal splice variants. It can be observed that at each variant,

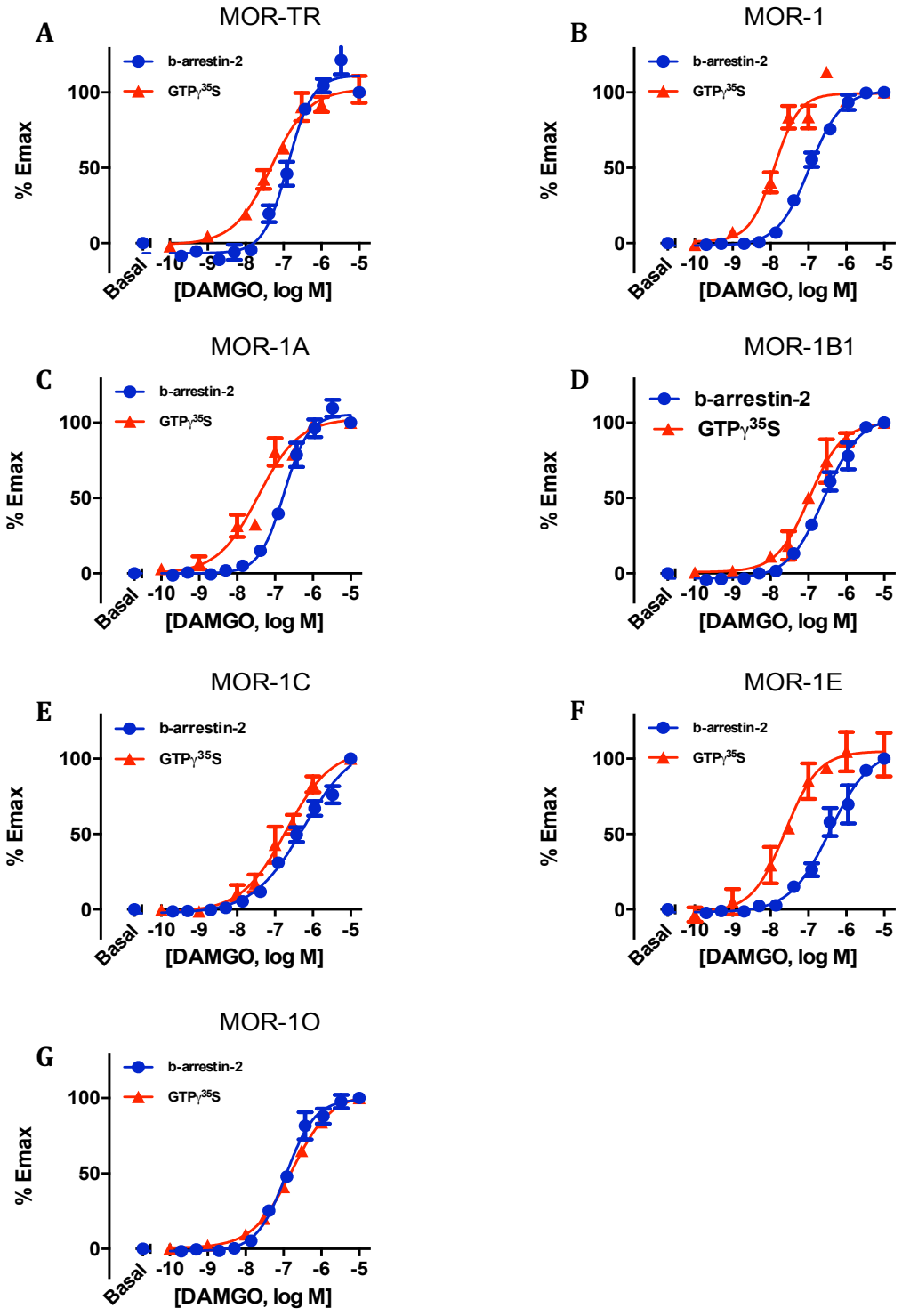

Figure 21 DAMGO induced β-arrestin2 recruitment and G protein activation in CHO cells stably transfected with variants **A.** MOR-TR-PK **B.** MOR-1-PK **C.** MOR-1A-PK **D.** MOR-1B1-PK **E.** MOR-1C-PK **F.** MOR-1E-PK **G.** MOR-1O-PK β-arrestin2 recruitment and G protein activation. A PathHunter β-arrestin2 assay (DiscoverX) and [^{35}S]GTPγS binding assay were performed, as described in Methods. Results are from three independent experiments. Each dose response curve has been normalized to maximal DAMGO stimulation (10μM DAMGO) at the particular receptor variant for comparison across drugs.

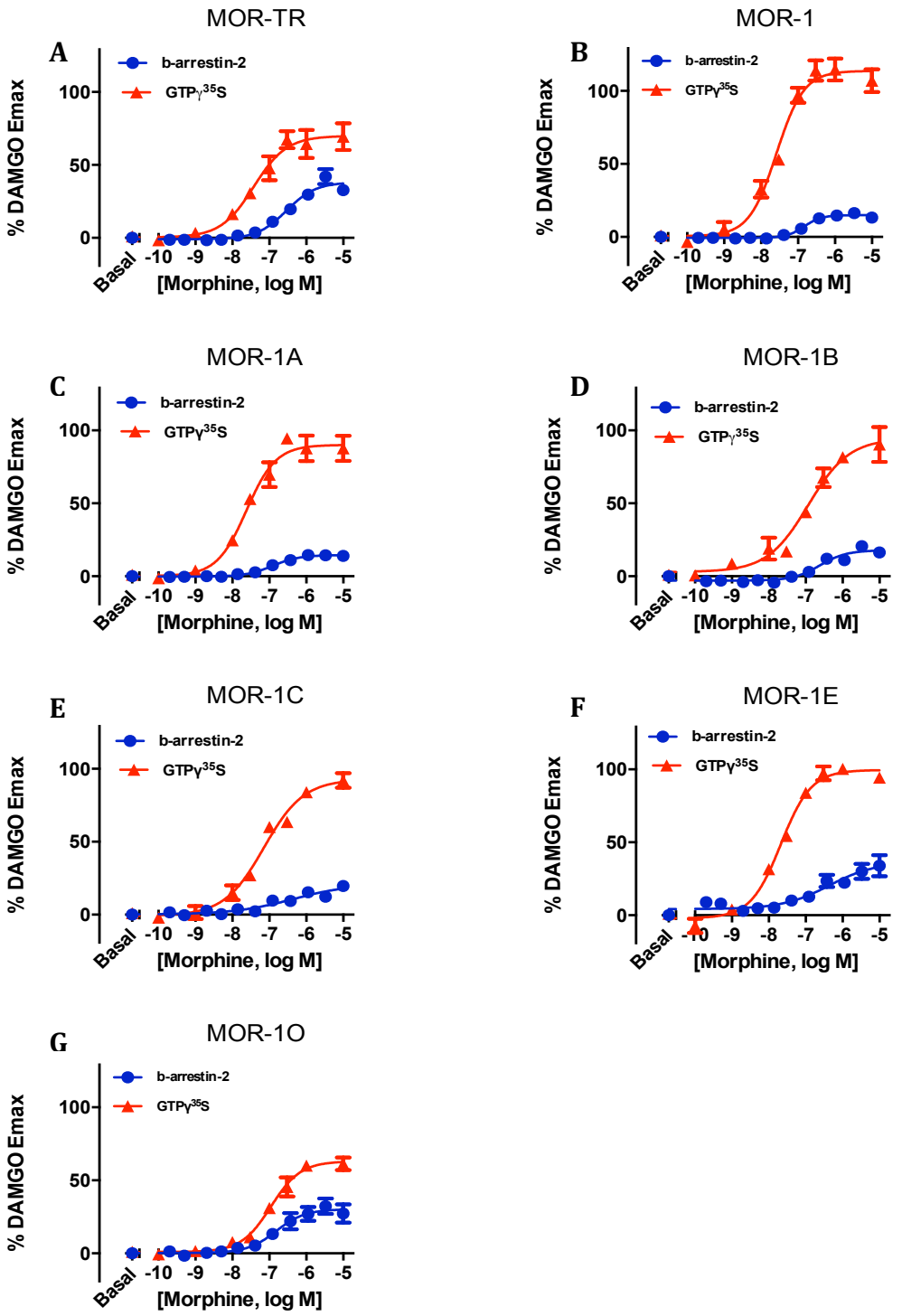

Figure 22 Morphine induced β-arrestin2 recruitment and G protein activation in CHO cells stably transfected with variants **A.** MOR-TR-PK **B.** MOR-1-PK **C.** MOR-1A-PK **D.** MOR-1B1-PK **E.** MOR-1C-PK **F.** MOR-1E-PK **G.** MOR-1O-PK β-arrestin2 recruitment and G protein activation. A PathHunter β-arrestin2 assay (DiscoverX) and [^{35}S]GTPγS binding assay were performed, as described in Methods. Results are from three independent experiments. Each dose response curve has been normalized to maximal DAMGO stimulation (10μM DAMGO) at the particular receptor variant for comparison across drugs.

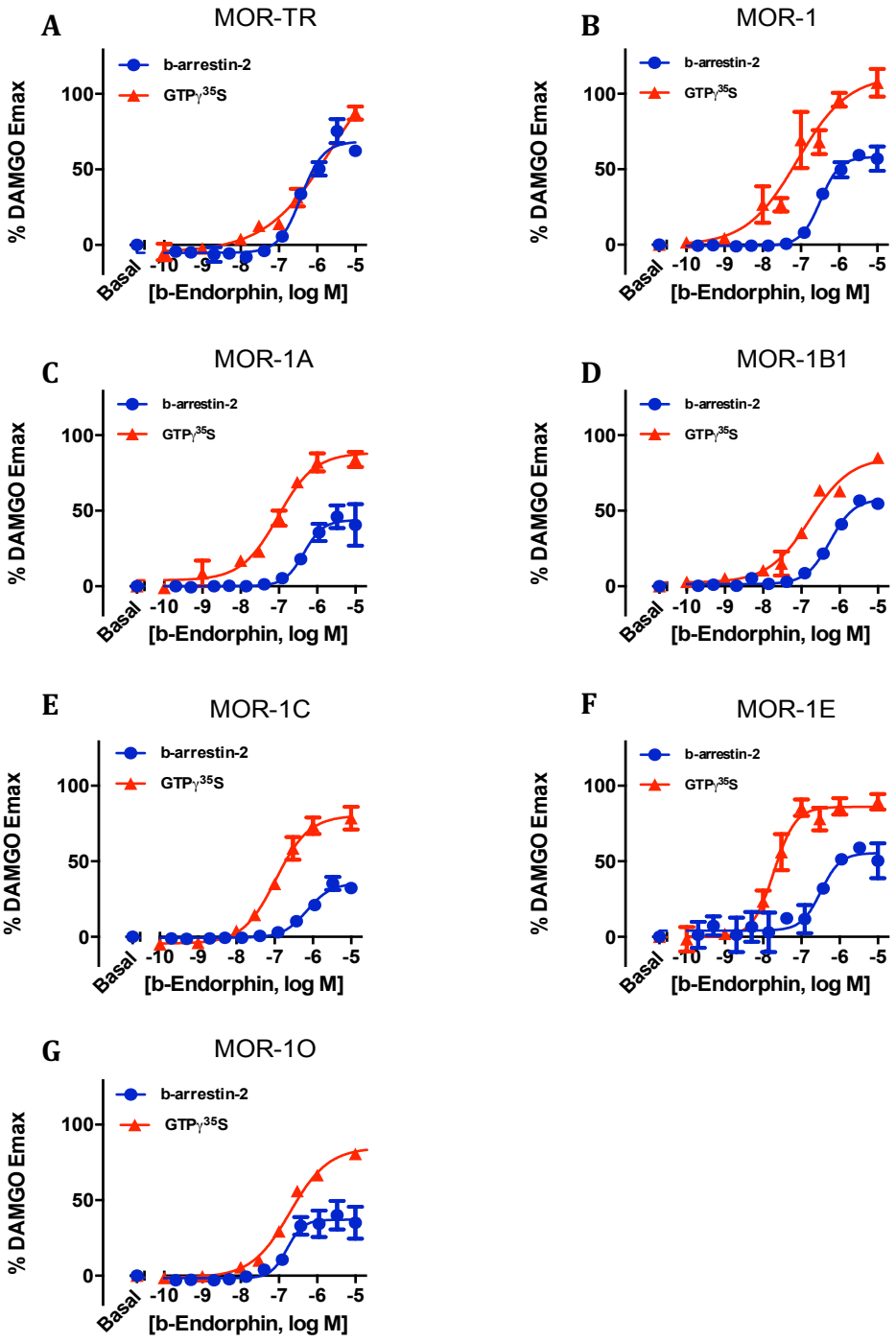

Figure 23 b-Endorphin induced β-arrestin2 recruitment and G protein activation in CHO cells stably transfected with variants **A.** MOR-TR-PK **B.** MOR-1-PK **C.** MOR-1A-PK **D.** MOR-1B1-PK **E.** MOR-1C-PK **F.** MOR-1E-PK **G.** MOR-1O-PK β-arrestin2 recruitment and G protein activation. A PathHunter β-arrestin2 assay (DiscoverX) and [^{35}S]GTPγS binding assay were performed, as described in Methods. Results are from three independent experiments. Each dose response curve has been normalized to maximal DAMGO stimulation (10μM DAMGO) at the particular receptor variant for comparison across drugs.

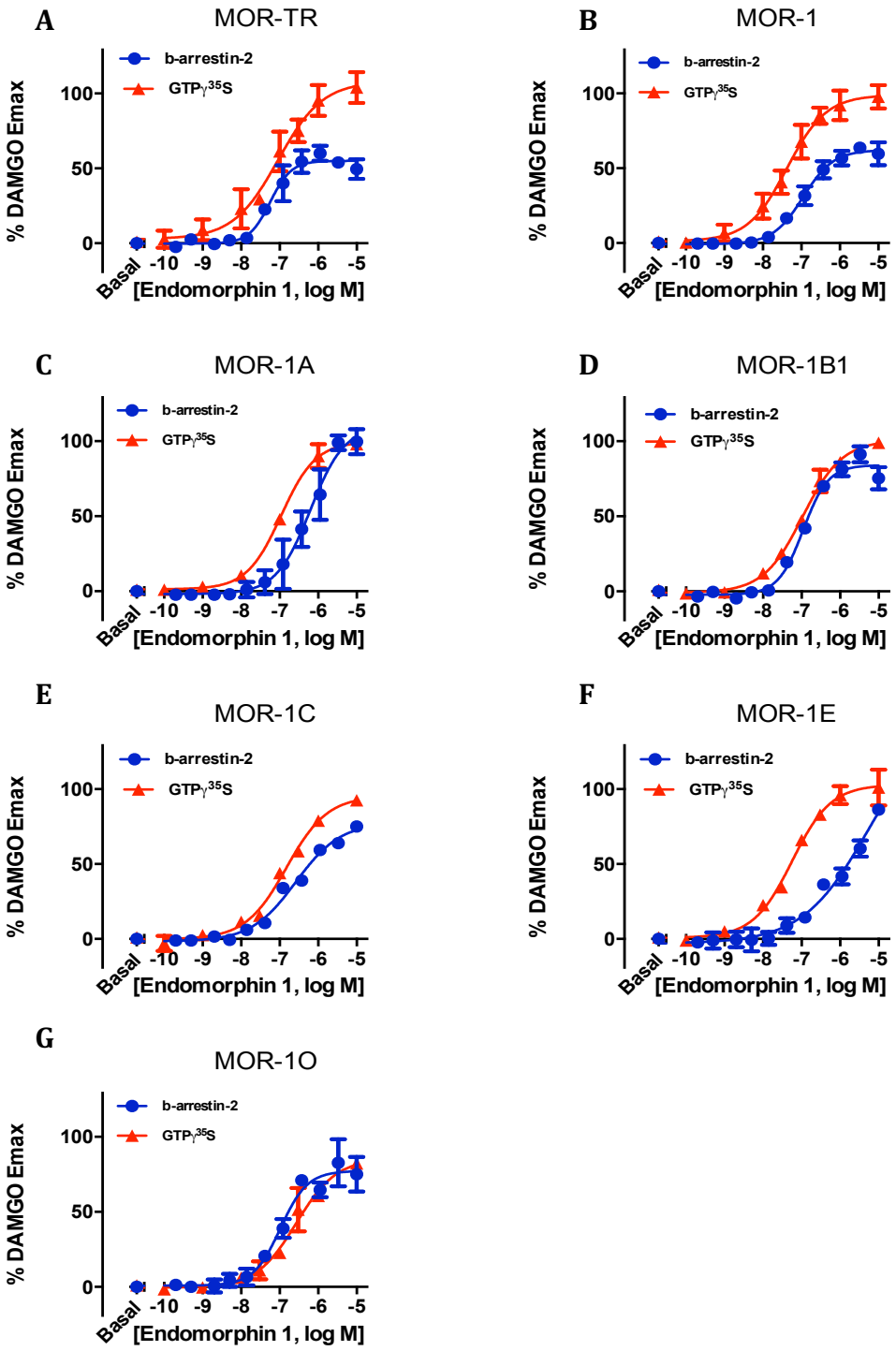

Figure 24 Endomorphin1 induced β-arrestin2 recruitment and G protein activation in CHO cells stably transfected with variants **A.** MOR-TR-PK **B**. MOR-1-PK **C.** MOR-1A-PK **D.** MOR-1B1-PK **E.** MOR-1C-PK **F.** MOR-1E-PK **G.** MOR-1O-PK β-arrestin2 recruitment and G protein activation. A PathHunter β-arrestin2 assay (DiscoverX) and [^{35}S]GTPγS binding assay were performed, as described in Methods. Results are from three independent experiments. Each dose response curve has been normalized to maximal DAMGO stimulation (10μM DAMGO) at the particular receptor variant for comparison across drugs

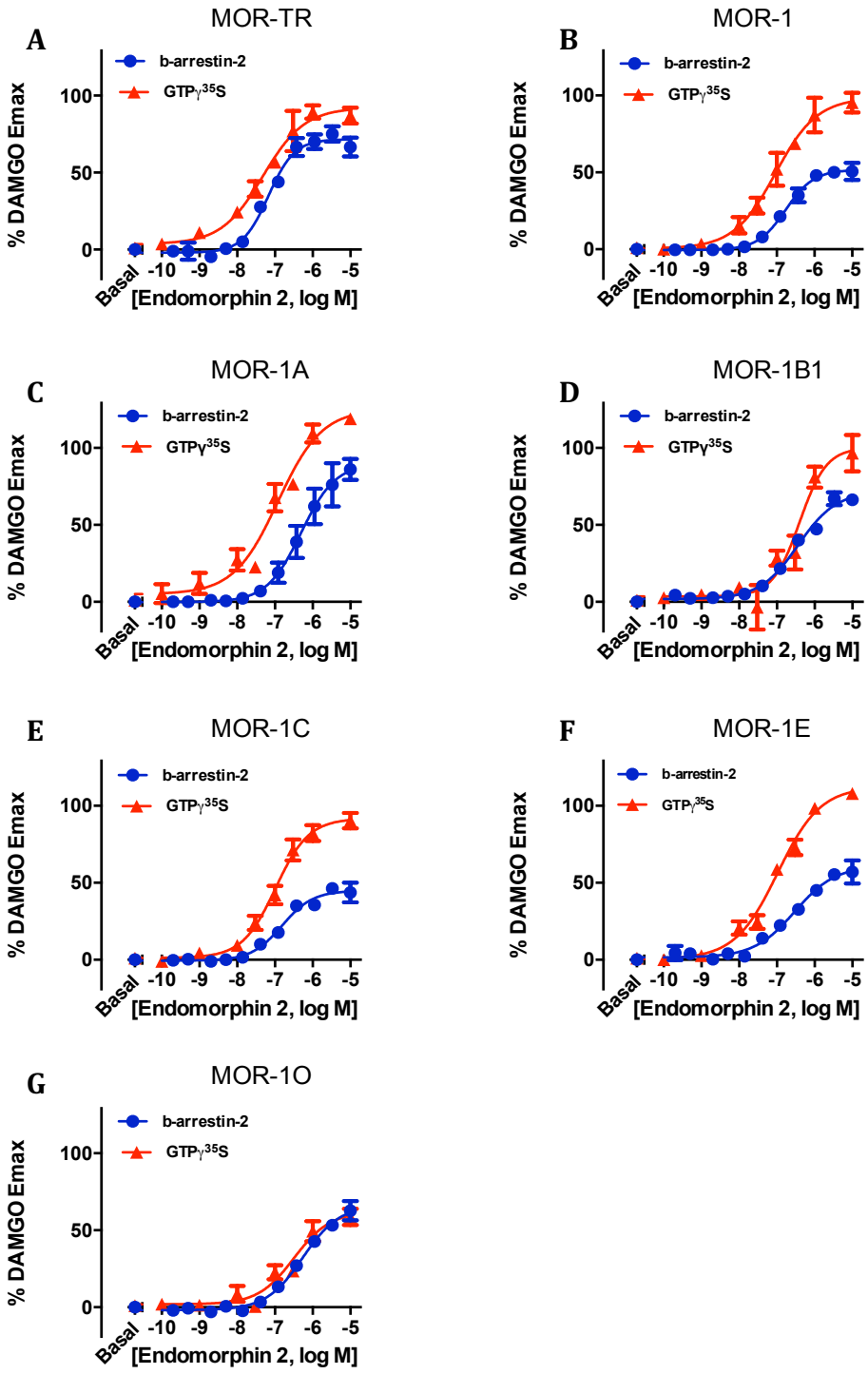

Figure 25 Endomorphin2 induced β-arrestin2 recruitment and G protein activation in CHO cells stably transfected with variants **A**. MOR-TR-PK **B.** MOR-1-PK **C.** MOR-1A-PK **D.** MOR-1B1-PK **E.** MOR-1C-PK **F.** MOR-1E-PK **G.** MOR-1O-PK β-arrestin2 recruitment and G protein activation. A PathHunter β-arrestin2 assay (DiscoverX) and [^{35}S]GTPγS binding assay were performed, as described in Methods. Results are from three independent experiments. Each dose response curve has been normalized to maximal DAMGO stimulation (10μM DAMGO) at the particular receptor variant for comparison across drugs

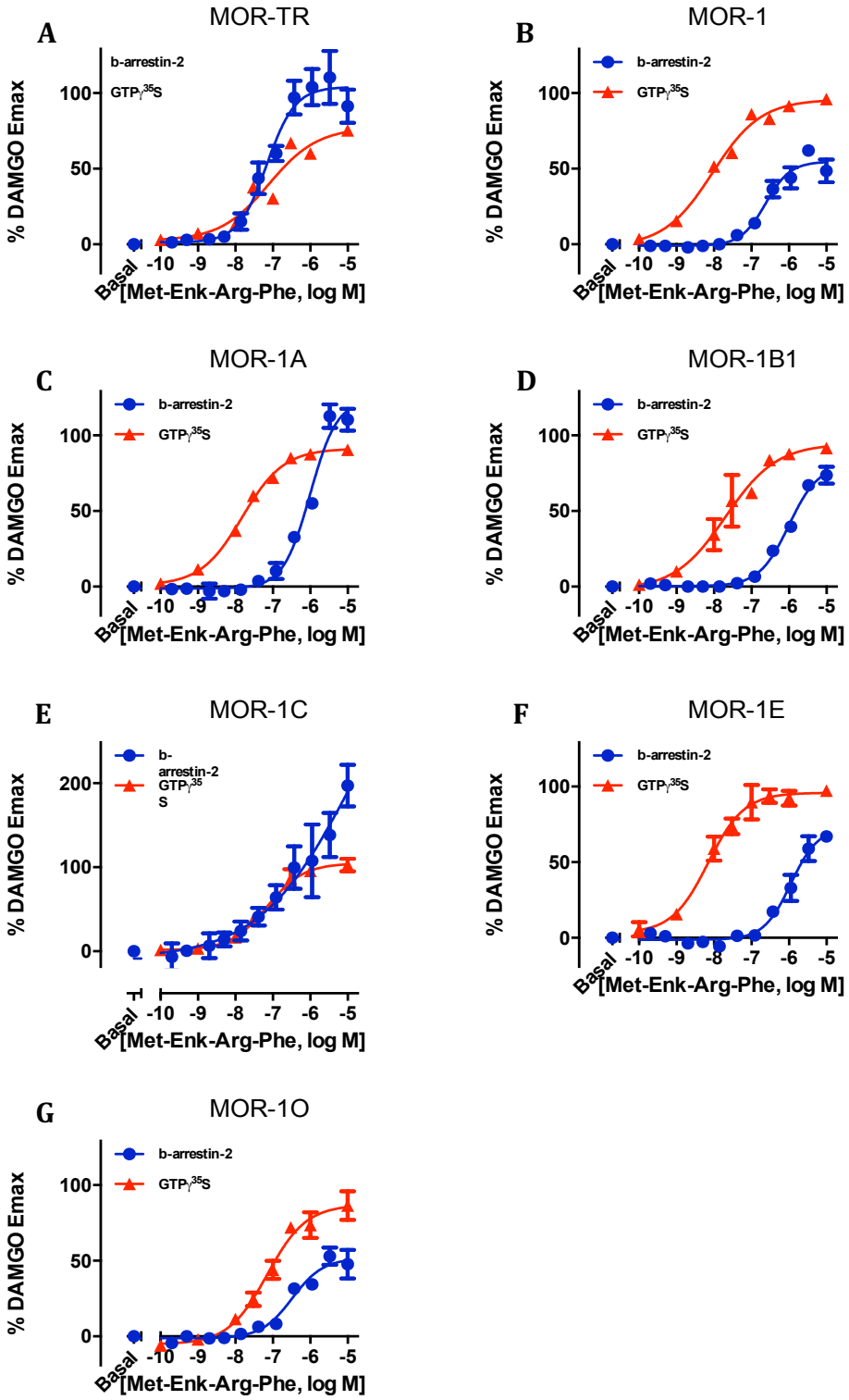

Figure 26 Met-Enk-Arg-Phe induced β-arrestin2 recruitment and G protein activation in CHO cells stably transfected with variants **A.** MOR-TR-PK **B.** MOR-1-PK **C.** MOR-1A-PK **D.** MOR-1B1-PK **E.** MOR-1C-PK **F.** MOR-1E-PK **G.** MOR-1O-PK β-arrestin2 recruitment and G protein activation. A PathHunter β-arrestin2 assay (DiscoverX) and [^{35}S]GTPγS binding assay were performed, as described in Methods. Results are from three independent experiments. Each dose response curve has been normalized to maximal DAMGO stimulation (10μM DAMGO) at the particular receptor variant for comparison across drugs

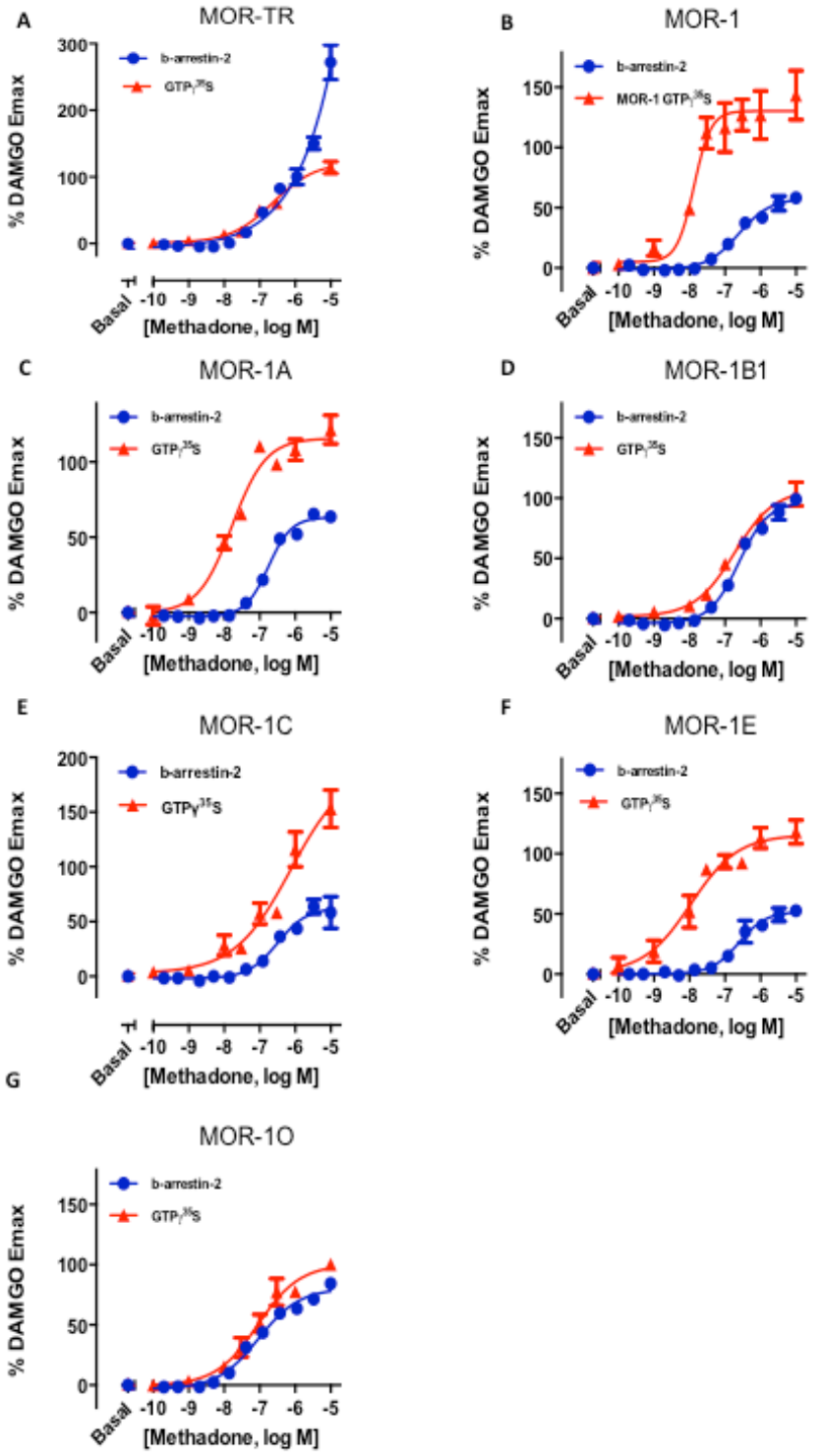

Figure 27 Methadone induced β-arrestin2 recruitment and G protein activation in CHO cells stably transfected with variants **A.** MOR-TR-PK **B.** MOR-1-PK **C.** MOR-1A-PK **D.** MOR-1B1-PK **E.** MOR-1C-PK **F.** MOR-1E-PK **G.** MOR-1O-PK β-arrestin2 recruitment and G protein activation. A PathHunter β-arrestin2 assay (DiscoverX) and [^{35}S]GTPγS binding assay were performed, as described in Methods. Results are from three independent experiments. Each dose response curve has been normalized to maximal DAMGO stimulation (10μM DAMGO) at the particular receptor variant for comparison across drugs

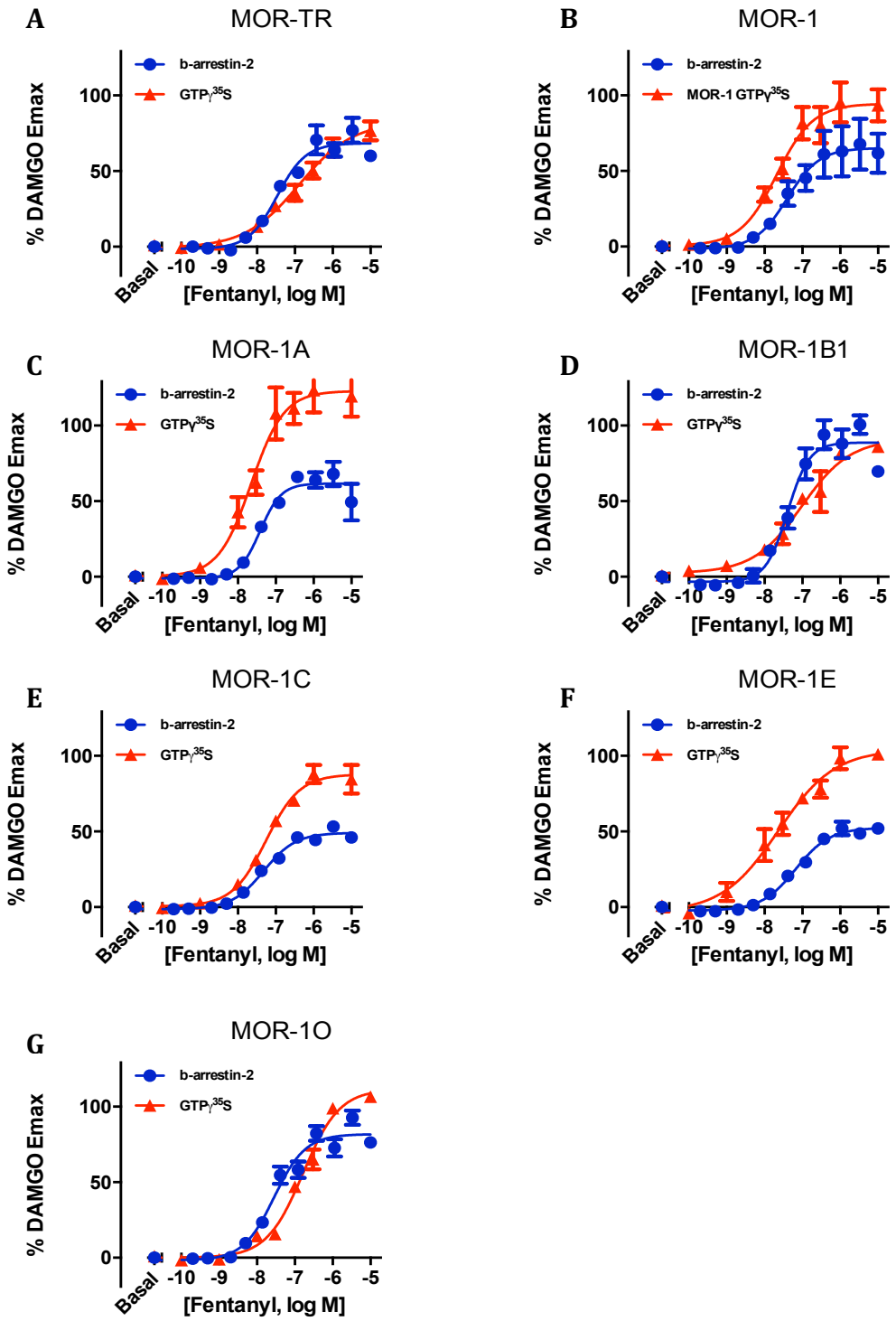

Figure 28 Fentanyl induced β-arrestin2 recruitment and G protein activation in CHO cells stably transfected with variants **A.** MOR-TR-PK **B**. MOR-1-PK **C.** MOR-1A-PK **D.** MOR-1B1-PK **E.** MOR-1C-PK **F.** MOR-1E-PK **G.** MOR-1O-PK β-arrestin2 recruitment and G protein activation. A PathHunter β-arrestin2 assay (DiscoverX) and [^{35}S]GTPγS binding assay were performed, as described in Methods. Results are from three independent experiments. Each dose response curve has been normalized to maximal DAMGO stimulation (10μM DAMGO) at the particular receptor variant for comparison across drugs

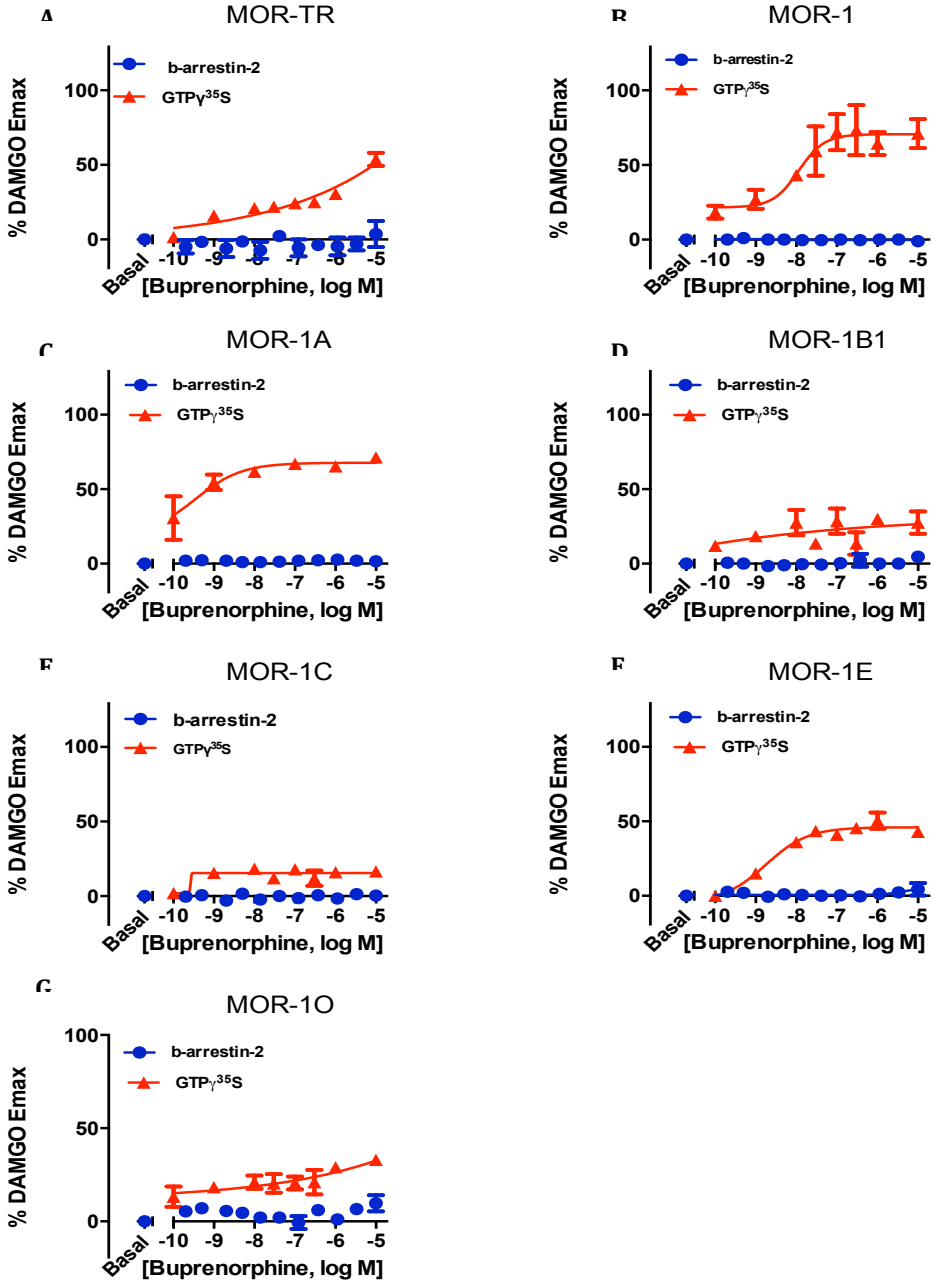

Figure 29 Buprenorphine induced β-arrestin2 recruitment and G protein activation in CHO cells stably transfected with variants **A.** MOR-TR-PK **B.** MOR-1-PK **C.** MOR-1A-PK **D.** MOR-1B1-PK **E.** MOR-1C-PK **F.** MOR-1E-PK **G.** MOR-1O-PK β-arrestin2 recruitment and G protein activation. A PathHunter β-arrestin2 assay (DiscoverX) and [^{35}S]GTPγS binding assay were performed, as described in Methods. Results are from three independent experiments. Each dose response curve has been normalized to maximal DAMGO stimulation (10μM DAMGO) at the particular receptor variant for comparison across drugs

Table 11 Heat map of biased factors. Biased factors were calculated using the Black and Leff Operational Model by using different normalization methods. Results are the mean ± S.E. of at least three independent experiments.**A.** normalized with respect to DAMGO at the variant for a comparison across drugs **B.** normalized with respect to every individual drug at mMOR-TR for a comparison across variants **C.** normalized with respect to drug in mMOR-1 for another comparison across variants **D.** normalized with respect to DAMGO at MOR-1 for a simultaneous comparison between drugs and variants.

A. Normalized to DAMGO at the variant

	MOR-TR	MOR-1	MOR-1A	MOR-1B1	MOR-1C	MOR-1E	MOR-1O
DAMGO	1.0	1.0	1.0	1.0	1.0	1.0	1.0
Morphine	2.8	-1.5	1.2	-1.2	1.5	-11.9	2.1
b-Endorphin	-17.9	-2.1	1.0	1.4	1.5	1.1	1.1
Endomorphin2	-2.1	-4.5	-1.1	-2.7	-2.9	-6.5	2.5
Endomorphin1	-4.6	-3.3	1.3	-2.3	-2.5	-1.4	-1.9
Met-Enk-Arg-Phe	-3.2	3.1	15.0	20.0	40.8	15.7	5.2
Methadone	3.4	2.1	2.5	-1.9	-9.4	1.8	1.7
Fentanyl	-4.2	-4.4	-2.5	-6.0	-5.1	-3.0	-4.3

B. Normalized to drug in MOR -TR

	MOR-TR	MOR-1	MOR-1A	MOR-1B1	MOR-1C	MOR-1E	MOR-1O
DAMGO	1.0	3.1	1.6	-1.1	1.5	4.8	-3.3
Morphine	1.0	-1.4	-1.5	-3.9	-1.2	-6.9	-6.3
b-Endorphin	1.0	25.6	28.8	22.6	40.6	95.9	6.0
Endomorphin2	1.0	1.4	3.0	-1.5	1.1	1.6	1.6
Endomorphin1	1.0	4.3	9.4	1.7	2.8	30.7	-1.4
Met-Enk-Arg-Phe	1.0	29.7	74.1	55.2	197.7	236.6	4.9
Methadone	1.0	1.9	1.2	-7.1	-20.4	2.6	-6.6
Fentanyl	1.0	2.9	2.6	-1.6	1.3	6.8	-3.5

C. Normalized to drug in MOR-1

	MOR-TR	MOR-1	MOR-1A	MOR-1B1	MOR-1C	MOR-1E	MOR-1O
DAMGO	-3.1	1.0	-1.9	-3.5	-2.0	1.6	-10.2
Morphine	1.4	1.0	-1.1	-2.8	1.2	-5.0	-3.3
b-Endorphin	-25.6	1.0	1.1	-1.1	1.6	3.7	-4.3
Endomorphin2	-1.4	1.0	2.1	-2.1	-1.3	1.1	1.1
Endomorphin1	-4.3	1.0	2.2	-2.5	-1.5	3.7	-6.0
Met-Enk-Arg-Phe	-29.7	1.0	2.5	1.9	6.7	8.0	-6.1
Methadone	-1.9	1.0	-1.6	-13.4	-38.5	1.4	-12.4
Fentanyl	-2.9	1.0	-1.1	-4.7	-2.3	2.3	-10.0

D. Normalized to MOR-1 DAMGO

	MOR-TR	MOR-1	MOR-1A	MOR-1B1	MOR-1C	MOR-1E	MOR-1O
DAMGO	-3.1	1.0	-1.9	-3.5	-2.0	1.6	-10.2
Morphine	-1.1	-1.5	-1.7	-4.3	-1.3	-7.6	-5.0
b-Endorphin	-54.8	-2.1	-1.9	-2.4	-1.4	1.7	-9.2
Endomorphin2	-6.5	-4.5	-2.2	-9.5	-5.7	-4.1	-4.1
Endomorphin1	-14.0	-3.3	-1.5	-8.1	-4.9	1.1	-19.4
Met-Enk-Arg-Phe	-9.6	3.1	7.7	5.7	20.5	24.5	-2.0
Methadone	1.1	2.1	1.3	-6.5	-18.6	2.9	-6.0
Fentanyl	-12.8	-4.4	-4.9	-21.0	-10.2	-1.9	-44.3

different drugs show different degrees of bias.

Variants containing exon 7, like MOR-1C and MOR-1O have a higher propensity for β-arrestin2 bias. Table 11b and 11c are optimized to compare differences in biases across variants, and we observed that the mMOR-1O variant demonstrated an inherent and consistent β-arrestin-2 bias across different drugs at the receptor. These findings can be significant since β-arrestin-2 has been previously linked with prolonged analgesic response along with no tolerance side effects.

Calculating bias and using the different normalization methods gave us several additional insights into understanding the differences across these variants. When we looked at morphine activity, it was relatively unbiased with respect to DAMGO at all the variants except for at mMOR-1E where it was significantly β-arrestin biased. This is interesting because Koch et al. have looked at levels of phosphorylation in response to morphine across the different variants and observed high levels of phosphorylation at the mMOR-1E receptor after morphine treatment (Koch et al., 2001). Mu Opiod action is dependent on both biased signaling as well as the splice variant mediating the function.

It also appears that the removal of 12 amino acids encoded by exon 4 shifts the receptor to a β-arrestin bias (Table 11C, 11D). The mMOR-TR response seems much similar to mMOR-1O, in that they are both arrestin biased relative to mMOR-1. Out of all the drug we tested,

methadone and fentanyl showed the most difference across the variants. When normalized to mMOR-1, Fentanyl was relatively unbiased at mMOR-1A, mMOR-1C and mMOR-1E, but significantly arrestin biased at mMOR-1O (10 fold). Methadone was unbiased at MOR-1A and MOR-1E but significantly arrestin biased at MOR-1C (38 fold) and MOR-1O (12 fold).). This was the highest difference we saw across all drugs.

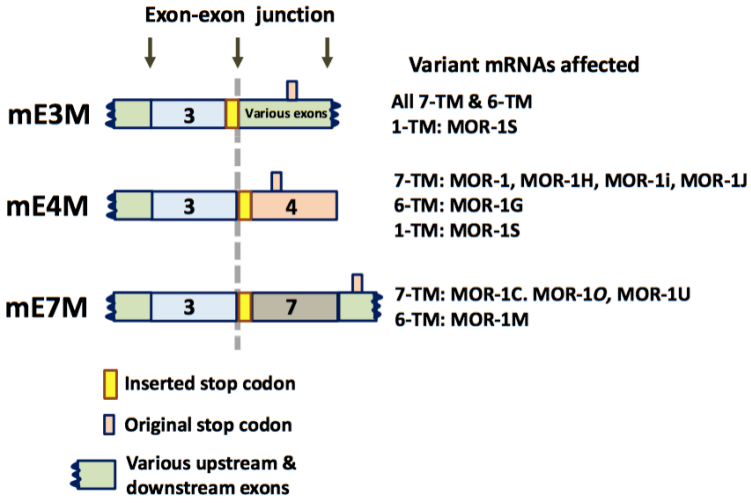

Figure 30 Schematic of the stop codon insertion on variant mRNAs. Three targeted mouse models, mE3M, mE4M and mE7M, were generated by inserting a stop codon at an appropriate site within indicated exons shown by colored boxes. Inserted and original stop codon are indicated by yellow and pink bars, respectively. In mE3M, a stop codon was inserted at the end of exon 3 to eliminate every C-terminal tails of all 7-TM and 6-TM variants, as well as 1-TM mMOR-1S. In mE4M and mE7M, a stop codon was created at the beginning of exon 4 or exon 7 to eliminate individual C-terminal tails encoded by exon 4 or exon 7 of indicated variants, respectively.

These results are crucial in providing some indication of how these drugs would behave endogenously. These results become more significant when comparing the functional significance of alternative

C-termini in-vivo. In our lab, we have generated three mutant mouse models with truncations of the distal end of the C-terminus in two different inbred strains (Work done by Jin Xu and Ying Xian Pan). By truncating either all C-terminal tails or selectively truncating C-terminal tails encoded by exon 4 or exon 7, we were able to show the importance of these C-terminal tails in morphine tolerance and physical dependence, and suggest a mechanism involving interactions between E7-encoded C-terminus and β-arrestin-2 for morphine-induced desensitization and tolerance. The first mouse model (mE3M) was generated by inserting a stop codon at the 3'-end of exon 3 that prevents translation of all exons downstream of exon 3, even though their mRNAs are expressed. Thus, the mE3M homozygous mice express only truncated mu opioid receptors lacking any of distal C-terminal tails. In the other two mouse models (mE4M and mE7M), we introduced a stop codon at the 5'-end of exon 4 (E4) and exon 7 (E7) to stop translation at the end of exon 3 only in those specific variants containing exon 4 or exon 7 in mE4M or mE7M mice, respectively (Figure 30). Based on our results from the in-vitro assays, we were most interested in the mE4M and mE7M mutant mice as they seem to have opposing effects on the receptor's ability to recruit β-arrestin-2.

As shown in Figure 31A, chronic morphine treatment (10mg/kg, twice a day) induced modest tolerance in the respective WT B6 control mice from all mutant mouse models over 5 days. However, in mE3M-B6 and mE4M-B6 homozygous mice, tolerance developed faster and to a greater extent. This enhanced tolerance was even more evident in

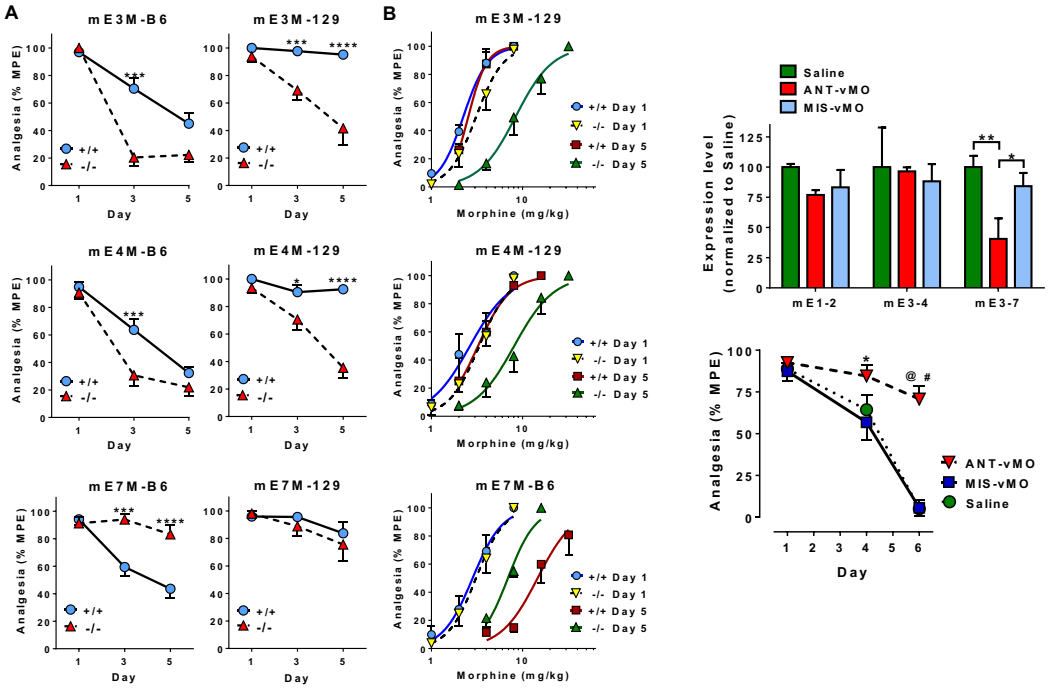

Figure 31 Effect of the C-terminal truncation on morphine tolerance. (A) Morphine tolerance in the mutant mice. Tolerance was induced and assessed as described in Methods. The number of mice used were: mE3M-B6, WT (+/+): 15 & homozygous (-/-): 14 in two independent experiments; mE4M-B6, +/+: 18 & -/-: 17 in two independent experiments; mE7M-B6, +/+: 20 & -/-: 19 in three independent experiments; mE3M-129, +/+: 15 & -/-: 11 in two independent experiments; mE4M-129, +/+ & -/-: 13 in two independent experiments; mE7M-129, +/+ & -/-: 7 in one experiment. *: $p < 0.05$; ***: $p < 0.001$; ****: $p < 0.0001$ (2-way ANOVA with Bonferroni's *post hoc* test). (B) Morphine dose-response curve in the mutant mice. Cumulative dose-response studies were performed before (Day 1) and after (Day 5) morphine treatment (C) Antisense vivo-morpholino oligo (ANT-vMO targeting intron/E7) study in CD-1 mice. Top: mRNA expression. RNAs from the PAG dissected on Day 6 (see bottom panel) were used in RT-qPCRs. MIS-vMO: mismatched oligo; All $2^{-(\Delta Ct)}$ values are normalized with Saline group. Results are the mean ± SEM of at least three individual samples. *: $p < 0.05$; **: $p < 0.01$(1-way ANOVA with Bonferroni's *post hoc* test). Bottom: Morphine tolerance. Group of mice were i.c.v. injected with 10 µg of ANT-vMO (n = 18) or MIS-vMO (n = 16), or Saline (n = 19), for four days (Days 1 – 4). Tolerance was induced by twice-daily morphine injection (10 mg/kg, s.c.) for 5 days (Days 2 – 6). Morphine analgesia was tested on Days 1, 4 and 6. Results are from two independent experiments. 2-way ANOVA with Bonferroni's *post hoc* test was used. # & @: compared to Saline and MIS-vMO, $p < 0.0001$, respectively. *: compared to MIS-vMO, $p < 0.05$.

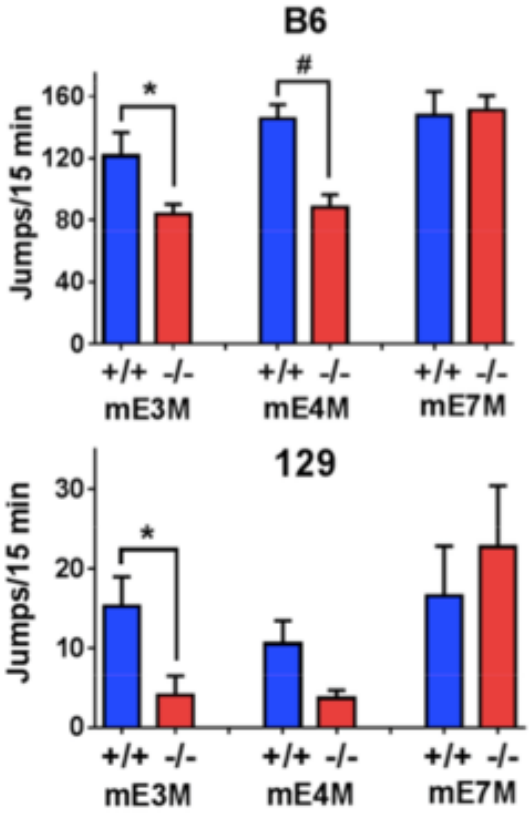

Figure 32 Effect of the C-terminal truncation on morphine physical dependence in the mutant mice. **(A)** Morphine physical dependence. Morphine physical dependence was assessed by naloxone-precipitated withdrawal after chronic morphine treatment in the mutant mice in B6 **(Top)** or 129 **(Bottom)** backgrounds. Results were showed as the number of jumps within 15 min immediately followed naloxone injection. The number of mice used were: mE3M-B6, WT (+/+): 15 & homozygous (-/-): 14 in two independent experiments; mE4M-B6, +/+: 18 & -/-: 17 in two independent experiments; mE7M-B6, +/+ & -/-: 10 in one independent experiments; mE3M-129, +/+: 15 & -/-: 11 in two independent experiments; mE4M-129, +/+ & -/-: 13 in two independent experiments; mE7M-129, +/+ & -/-: 7 in one experiment. 1-way ANOVA with Bonferroni's *post hoc* test was used. Compared to +/+, *: $p < 0.05$; #: $p < 0.0001$. +/+: WT mice; -/-: homozygous mice

mE3M and mE4M homozygous mice on the 129 background. In contrast to the minimal morphine tolerance in the WT 129 mice over the same time period, both mE3M-129 and mE4M-129 homozygous mice developed modest morphine tolerance similar to that seen in the WT B6 mice. mE3M-129 and mE4M-129 homozygous mice, however, developed modest morphine tolerance similar to that seen in the WT B6 mice. Cumulative dose response curve studies before and after chronic morphine administration also gave the same result where chronic morphine significantly shifted the curves to the right with a higher ED50 value in both mE3M-129 and mE4M-129 homozygous mice (Figure 31B). This is consistent with our earlier findings in in-vitro assays, where removal of the 2 amino acids encoded by exon 4 pushed the receptor to a more arrestin recruiting state.

Interestingly, truncating exon 7 (E7)-encoded C-terminal tails in B6 (mE7M-B6 homozygous) mice had an opposite effect. There was little decrease in morphine responses over 5 days compared to the WT B6 littermate controls and the cumulative dose response studies revealed only a slight shift to the right in mE7M-B6 homozygous mice following chronic morphine (2.2-fold) compared to a far greater shift in WT B6 control mice (5.2-fold).

To further investigate the function of exon 7-associated C-terminal variants in morphine tolerance and dependence, we used a knockdown strategy with an antisense vivo-morpholino oligo that targets intron/exon 7 to block splicing from exon 3 (E3) to exon 7 (E7),

eliminating E7-containing transcripts. Mice treated with saline or mis-morpholigo oligo displayed normal morphine tolerance after 5-day morphine treatment. As expected, mice treated with the antisense vivo-morpholino oligo showed little morphine tolerance. These results are similar to those in mE7M-B6 homozygous mice, confirming the involvement of exon 7-associated variants in morphine tolerance. Not surprisingly, if the exon 7 variants are indeed the β-arrestin-2 biased variants, knocking out these mutants would give a phenotype similar to the Bohn et al. β-arrestin-2 knockout mice.

Morphine physical dependence was assessed with naloxone-precipitated withdrawal following 5 days of chronic morphine treatment by measuring jumping, a reliable measure of the physical dependence. Naloxone precipitated significantly less jumping in both mE3M-B6 and mE4M-B6 homozygous mice than their WT B6 control mice (Top panel, Figure 32A), suggesting a diminished level of dependence. There was no significant difference in the jumping frequency between the mE7M-B6 WT and homozygous mice. These results suggest that unlike morphine tolerance, morphine dependence is not influenced by exon 7-associated variants in B6 or CD-1 mice. The WT 129 control mice all showed lower jumping frequencies than the WT B6 control mice (Bottom panel, Figure 32A), consistent with previous observations (Bohn et al., 1999). However, we observed even fewer jumps in E3M-B6 129 homozygous mice. As in the B6 background, the exon 7 truncation in the 129 mice showed no change in jumping, again supporting the hypothesis that knocking out the

exon 7 variants gives a phenotype similar to the β-arrestin-2 knockout mice.

These findings serve to validate our results from the in-vitro assays where we were able to show the MOR-1O receptor variant was relatively more β-arrestin-2 biased. When knocking down this variant, as in the mE7M model, these mice show a phenotype similar to the β-arrestin-2 knockout mice as shown by Bohn et al. This suggests a physical and functional association of E7-encoded C-terminal tails with β-arrestin-2. One caveat with this interpretation is that mE7M model also affects 2 other 7TM receptor variants MOR-1C and MOR-1U, as well as a 6TM variant, MOR-1M. Our follow up study should look at the signaling bias at these other variants in trying to understand the specific moiety in the C-tail that encourages the receptor interaction with β-arrestin-2.

Chapter IV – Discussion

The C-terminal tail is the intracellular part of the receptor that interacts with other proteins and signaling complexes to trigger downstream signaling pathways. Alternative splicing of the cytoplasmic tail has been observed for a number of G protein-coupled receptors including the sst2A somatostatin receptor (Vanetti et al., 1992), the D2 dopamine receptor (Guiramand et al., 1995), the EP3 prostaglandin receptor (Namba et al., 1993), and a number of serotonin receptor subtypes (Lucas et al., 1995). C-terminal splicing is thought to modulate several aspects of G protein coupled receptor physiology, like cell and tissue-specific expression, subcellular targeting, coupling to specific G proteins as well as β-arrestin recruitment.

The μ-OR shows extensive alternative splicing. Over the years, more than 60 splice variants have been isolated (Pasternak and Pan, 2013). These receptor variants show a lot of heterogeneity in their expression pattern in the brain, their localization in the cell (pre- vs post-synaptic), their phosphorylation as well as internalization pattern. The μ-OR variants have been detected in different regions of rodent brain at the protein level, immunohistochemically and by Western blot, and at the mRNA level using RT-PCR (Abbadie et al., 2000a,b, 2001; Pan et al., 1999, 2000, 2001, 2003). Antisense mapping studies have constantly implicated that all the variants are functionally relevant (Pan et al., 1999, 2000, 2001).

In this report, we have demonstrated for the first time that the C-terminal splice variants of the μ-OR show differences in their signaling bias. Until recently, a drug's efficacy for β-arrestin recruitment was believed to be proportional to its efficacy for G-protein activities. This paradigm restricts 7TMR drug effects to a linear spectrum of responses, ranging from inhibition of all responses to stimulation of all responses. We tested 6 different C-terminal splice variants, mMOR-1, mMOR-1A, mMOR-1B1, mMOR-1C, mMOR-1E and mMOR-1O receptor and compared it to the control receptor mMOR-TR which is truncated at exon 3. Using the [^{35}S]GTPγS and DiscoverX PathHunter assay, we were able to quantify agonist induced stimulation in these pathways across the different C-terminal variants and observe clear differences. One caveat of the DiscoverX PathHunter assay is that these constructs have an additional 4kDa prolink fragment at the C-terminus. However, in spite of the limitations, the DiscoverX assay seemed a more reasonable choice in comparison to the other available assays Translator™ β-arrestin-GFP, TANGO or FRET assays for reading arrestin recruitment. These other assays involve a more substantive manipulation of the C-terminus in comparison to the DiscoverX assay and are relatively less high-throughput.

All of these C-terminal splice variants are 7TM receptors that contain the same binding pocket. As expected, they have similar binding affinity for the different mu agonists. Despite the similar affinity for these agonists, the C-terminal variants are significantly different in their agonist induced effects. For example, in response to DAMGO,

mMOR-TR, mMOR-1C and mMOR-1O receptors are equi-effective as well as equi-potent in both the β-arrestin and [^{35}S]GTPγS pathways. Whereas, some other variants, mMOR-1, mMOR-1A and mMOR-1E receptors show a right shift of the arrestin dose response curve. Morphine is a full agonist in the [^{35}S]GTPγS assay across most C-terminal variants, however, it is only a partial agonist in the β-arrestin assay. For b-Endorphin, the MOR-TR receptor was similarly effective and potent in both pathways which wasn't true for any of the other C-terminal variants.

Agonists like Met-Enk-Arg-Phe and Methadone showed a lot of variability in their response at the different receptor variants. Both these agonists were more effective in the β-arrestin recruitment assay in comparison to the [^{35}S]GTPγS at the control mMOR-TR receptor. Similar to the truncated receptor, mMOR-1A and mMOR-1C were also more effective in the β-arrestin pathway. However, in spite of the higher Emax, the mMOR-1A β-arrestin curve was significantly right shifted. For Methadone, mMOR-1B and mMOR-1O receptors were equi-effective and equi-potent in both the assays. But, mMOR-1 and mMOR-1C had a significant difference where the agonists were more effective than DAMGO in the [^{35}S]GTPγS assay and acted as partial agonists (Emax ~50% DAMGO) in the β-arrestin recruitment assay.

Calculating bias and using the different normalization methods gave us several additional insights into understanding the differences across these variants. At each variant, different drugs show different

degrees of bias. We saw that the peptides like Endomorphin1 and Endomorphin2 are arrestin biased at mMOR-1, as has been published previously (Rivero et al., 2012). We observed differences in both the magnitude of the bias as well as the directionality of the bias across variants. Methadone was seen to be a mild G protein biased agonist as mMOR-1 (Bias factor 2.1) but was a strong arrestin biased agonist at mMOR-1C (Bias factor -9.4). Met-Enk-Arg-Phe was also a mild G protein biased agonist at mMOR-1 (Bias factor 3.1) but was a much stronger G protein biased agonist at mMOR-1C (Bias factor 41). This suggests that mu opioid action is dependent on both biased signaling and the splice variant mediating the function.

When comparing mMOR-1 to the truncated receptor mMOR-TR, we also observed that the removal of 12 amino acids encoded by exon 4 shifts the receptor to a β-arrestin-2 bias. These observations are critical because the truncated receptor, mMOR-TR contains exon 3 which is shared by all C-terminal variants. As a result, the potential phosphorylation sites (Ser/ Thr residues like Ser375) present in the exon 3 region of the receptor are conserved across all of the receptor variants. Despite the availability of these conserved sites, the C-terminal variants show differences in their β-arrestin recruitment pattern. This suggests that the addition of only a few amino acids, as in MOR-1A, can significantly impact the ability of the C-tail to interact with other kinases and signaling complexes leading to differences in signaling pattern and ultimately, signal bias. Furthermore, in addition to these conserved sites, some of the C-terminal splice variants may

have additional active phosphorylation sites downstream of exon 3. Exon 7 containing variants, like mMOR-1C and mMOR-1O, have several additional potential phosphorulation sites downstream of exon 3 and were seen to have a higher propensity for β-arrestin-2 recruitment.

Mu agonist-induced receptor phosphorylation and subsequent β-arrestin binding that restrains further coupling of the receptor with the G proteins has been postulated as one mechanism of receptor desensitization and mu opioid tolerance (Raehal et al., 2011; Willliams et al., 2013). Earlier studies have shown morphine to induce different levels of receptor phosphorylation, internalization and desensitization among several C-terminal splice variants, including the E4-associated mMOR-1 and E7-associated mMOR-1C in HEK293 cells (Koch et al., 1998). mMOR-1C, but not mMOR-1, is internalized in vivo by morphine administration (Abbadie et al., 2001). Our in-vitro findings suggest differences in arrestin recruitment pattern across the C-terminal variants. On quantification, we see that the mMOR-1O variant, which has an additional 30 amino acids from exon 7 downstream of exon 3, is significantly β-arrestin biased relative to the other C-terminal variants. The exon 7 associated C-terminal tail has been postulated to have a number of additional phosphorylation sites for various protein kinases, such as GRKs (Figure 6), raising the hypothesis that E7-associated C-terminal variants favor morphine-induced phosphorylation by GRKs, leading to increased β-arrestin recruitment and facilitated receptor desensitization.

In addition to the [^{35}S]GTPγS assay, we also used pERK activation as a validation of our previous results and a further indication of the agonist induced bias. ERK activation can sometimes be inconclusive as the ERK activation can be a result of either G protein or β-arrestin activation. We used western blot analysis in another cell line, HEK cells, to test 2 of the C-terminal variants, MOR-1 and MOR-1O. The HEK cell lines expressing the receptor variants showed no significant differences in pERK activation after agonist treatment. This result serves as a validation of our results in the [^{35}S]GTPγS assay because we used 3 different agonists at their equi-active [^{35}S]GTPγS dose. In addition, it also suggests that the cytoplasmic pERK activation we are observing in a western blot assays is primarily coming from the G protein pathway.

These findings, although significant, come with the caveat that these pathways have been studied in a system that is significantly dependent on the assay conditions, cell lines used, levels of other kinases and G proteins expressed in the system. Another limitation with our current method is that it studies one receptor in isolation from all the other receptor variants. While this is useful to study the individual receptor pharmacology, these receptors exist in a very heterogeneous fashion in the brain. Endogenously, different combination of receptor variants might be expressed in a cell. The expression of different receptor combinations might lead to different

homo/ heterodimers, in which case, their signaling bias might be completely different than what we observe individually.

Another caveat is the difference in signal amplification observed in the two assays. The [^{35}S]GTPγS assay has a 1 : many signal amplification ratio, where one receptor can activate more than one G protein. However, the β-arrestin assay has a 1 : 1 signal amplification, such that one receptor can only recruit one β-arrestin-2 unit. Such differences in signal amplification, if not carefully monitored, can lead to false interpretation of bias as the receptors would seem more effective in the [^{35}S]GTPγS assay.

Our studies explored the difference in the mouse mu opioid receptor variants. This was done to facilitate further studies using mouse in-vivo models. However, significant overlap has been shown between the mouse and the human receptor variants. With reference to our findings, both the mouse and the human mu receptor gene contain exon 4 with high consensus in their sequence. Both mouse and humans express the MOR-1O receptor variant. The MOR-1O receptor variant is encoded by exon 7ab in mouse and exon O in humans. Both the mouse and human receptor variants contain 30 amino acids downstream of exon 3 with significant overlap in the specific amino acid residues present at the tip of the C-tail.

The predominant 7TM variant is MOR-1, which contains 12 exon 4-encoded amino acids. Removal of those 12 amino acids facilitated

morphine tolerance in mE4M homozygous mice on both B6 and 129 backgrounds, implying that expression of the E4-encoded C-terminal sequences impedes the development of morphine tolerance. In contrast, truncation of E7-associated C-terminal tails attenuated morphine tolerance, implying that those sequences facilitate the development of morphine tolerance. The importance of E7-associated variants was further supported by the antisense model where downregulation of the variants led to similar responses. Our in vitro observation suggest that several mu agonists stimulate β-arrestin2 biased signaling relative to G protein coupling, with an E7-associated 7TM variant, mMOR-1O in comparison to the E4-associated C-terminal 7TM mMOR-1. This also provides a strong support for the functional interaction between the E7-associated C-terminal tails and β-arrestin-2.

	mE4M Truncation of E4-encoded C-termini		mE7M Truncation of E7-encoded C-termini		β-arrestin-2 KO
Strain	129	B6	129	B6	B6/129svJ
Morphine Analgesia	No change	No change	No change	No change	Enhanced
Locomotor Activity	No change	Reduced	No change	Reduced	Reduced
Tolerance	Developed	Enhances	No change	Attenuated	Attenuated
Physical Dependence	No change	Reduced	No change	No change	No change
Reward (CPP)	No change	No change	No change	Reduced	Enhanced
Inhibition of GI transit	No change	Reduced	No change	No change	No change
Receptor desensitization in brainstem			No change	Lost	Lost

Figure 33 Comparison of behavioral and biochemical studies in targeted mice

More interestingly, mE7M mice showed a phenotype similar to the β-arrestin-2 KO mice. These mE7M mice had no substantial difference in analgesic sensitivity or physical dependence but developed no

tolerance. Similarity in several morphine-induced behaviors between these mE7M-B6 homozygous and β-arrestin-2 KO mice suggests a physical and functional association of E7-encoded C-terminal tails with β-arrestin-2, a hypothesis further supported by our in vitro data that several mu agonists displayed more bias toward arrestin binding on E7-associated variants, particularly mMOR-1O. Furthermore, the ability to modulate morphine tolerance by down-regulating the E7-associated variants with an antisense vivo-morpholino oligo illustrated the therapeutic potential of targeting E7-associated variants.

The in-vivo data shows that the distal C-terminal sequences significantly impacted morphine tolerance, with opposite effects seen between E4- and E7-associated C-terminal truncation models. Exon 4 facilitates tolerance whereas, exon 7 diminishes tolerance. Similarity between the Exon 7 truncation and β-arrestin2 KO model confirms a physical and functional link between exon 7 containing variants and β-arrestin-2. The mE7 mice show a difference in their reward behavior in comparison to the β-arrestin2 KO studies by Bohn et al. These differences could be a result of the strain differences between the two models. β-arrestin2 KO mice from Bohn studies were on a mixed B6/129svj background.

Additionally, the exon 7-encoded C-terminal sequences contain a consensus β-arrestin-2 binding motif, PxPxxE or PxxPxxE that interacts with positively charged residues at the N-terminus of β-

arrestin-2, predicted mainly based on the recent crystal structure of rhodopsin-β-arrestin2 complex. It will be interesting to further explore the role of these phosphorylation or negatively charged sites on the E7-encoded C-terminal tail in β-arrestin-2 binding and receptor signaling.

While these results clearly show the importance of individual C-termini in morphine actions, attributing these actions to a specific variant is not yet possible since the current truncation model impacts on more than one variant. E4-associated C-terminal tails are present in the 7TM variants mMOR-1, mMOR-1H, mMOR-1i and mMOR-1J, and the 6TM variant mMOR-1G. E7-associated C-terminal tails are also present in the 7TM variants mMOR-1C, mMOR-1*O* and mMOR-1U, as well as the 6TM variant mMOR-1M. We anticipate that since morphine has a far greater affinity for 7TM receptor in binding assays, it seems likely that the truncation phenotypes involve 7TM variants. Future experiments will be necessary to follow up on these other receptor variants and their signaling bias.

The involvement of E7-associated C-terminal tails in promoting morphine tolerance raises the possibility that E7-associated C-terminal variants may be potential targets for therapeutic intervention

to alleviate these morphine effects, as shown by our antisense vivo-morpholino oligo study. This oligo markedly reduced E3/E7 splicing and expression of E7-associated variants and attenuated morphine tolerance without affecting morphine dependence, mimicking the effect of truncation of E7-associated C-terminal tails in mE7M-B6 homozygous mice. Antisense morpholino oligos have been successfully used to correct aberrant splicing in a growing number of animal models for several human diseases. Our results provide another example where in vivo antisense morpholino approach might be of value one day clinically. In spite of the caveats of our approach, our findings establish that different C-terminal splice variants, through differences in biases, affect different functional aspects of the drug. Mu opioid actions are dependent on both biased signaling as well as the splice variant mediating the function.

Reference:

Abbadie, C., Pan, Y. X., Drake, C. T., & Pasternak, G. W. (2000). Comparative immunohistochemical distributions of carboxy terminus epitopes from the mu-opioid receptor splice variants MOR-1D, MOR-1 and MOR-1C in the mouse and rat CNS. Neuroscience, 100(1), 141-153. Chicago

Abbadie, C., & Pasternak, G. W. (2001). Differential in vivo internalization of MOR-1 and MOR-1C by morphine. Neuroreport, 12(14), 3069-3072.

Abbadie, C., Rossi, G. C., Orciuolo, A., Zadina, J. E., & Pasternak, G. W. (2002). Anatomical and functional correlation of the endomorphins with mu opioid receptor splice variants. European Journal of Neuroscience, 16(6), 1075-1082.

Abbadie, C., Pan, Y.-X., & Pasternak, G. W. (2004). Immunohistochemical study of the expression of exon11-containing mu opioid receptor variants in mouse brain. Neuroscience, 127(2), 419–30.

Arden, J. R., Segredo, V., Wang, Z., Lameh, J., & Sadée, W. (1995). Phosphorylation and Agonist-Specific Intracellular Trafficking of an Epitope-Tagged μ-Opioid Receptor Expressed in HEK 293 Cells. Journal of neurochemistry, 65(4), 1636-1645.

Attwood, T. K., Eliopoulos, E. E., & Findlay, J. B. (1991). Multiple sequence alignment of protein families showing low sequence homology: a

methodological approach using database pattern-matching discriminators for G-protein-linked receptors. Gene, 98(2), 153-159.

Bare, L. A., Mansson, E., & Yang, D. (1994). Expression of two variants of the human μ opioid receptor mRNA in SK-N-SH cells and human brain. FEBS letters, 354(2), 213-216.

Beckett, A. H., & Casy, A. F. (1954). Synthetic analgesics: stereochemical considerations. Journal of Pharmacy and Pharmacology, 6(1), 986-1001.

Beckett, A. H., Casy, A. F., Harper, N. J., & Phillips, P. M. (1956). Analgesics and their antagonists: Some steric and chemical considerations. Journal of Pharmacy and Pharmacology, 8(1), 860-873.

Benovic, J. L., Kühn, H., Weyand, I., Codina, J., Caron, M. G., & Lefkowitz, R. J. (1987). Functional desensitization of the isolated beta-adrenergic receptor by the beta-adrenergic receptor kinase: potential role of an analog of the retinal protein arrestin (48-kDa protein). Proceedings of the National Academy of Sciences, 84(24), 8879-8882.

Bohn, L. M., Lefkowitz, R. J., Gainetdinov, R. R., Peppel, K., Caron, M. G., & Lin, F. T. (1999). Enhanced morphine analgesia in mice lacking β-arrestin 2. Science, 286(5449), 2495-2498.

Bokoch M.P., Zou Y., Rasmussen S.G., Liu C.W., Nygaard R., Rosenbaum D.M., Fung J.J., Choi H.J., Thian F.S., Kobilka T.S., (2010) Ligand-specific

regulation of the extracellular surface of a G-protein-coupled receptor. Nature 463:108–112.

Bolan, E. A., Pan, Y. X., & Pasternak, G. W. (2004). Functional analysis of MOR-1 splice variants of the mouse mu opioid receptor gene Oprm. Synapse, 51(1), 11-18.

Bohn, L. M., Lefkowitz, R. J., Gainetdinov, R. R., Peppel, K., Caron, M. G., & Lin, F. T. (1999). Enhanced morphine analgesia in mice lacking β-arrestin 2. Science, 286(5449), 2495-2498.

Bohn, L. M., Gainetdinov, R. R., Lin, F. T., Lefkowitz, R. J., & Caron, M. G. (2000). μ-Opioid receptor desensitization by β-arrestin-2 determines morphine tolerance but not dependence. Nature, 408(6813), 720-723.

Bohn, L. M., Dykstra, L. A., Lefkowitz, R. J., Caron, M. G., & Barak, L. S. (2004). Relative opioid efficacy is determined by the complements of the G protein-coupled receptor desensitization machinery. Molecular pharmacology, 66(1), 106-112.

Bjarnadóttir, T. K., Fredriksson, R., Höglund, P. J., Gloriam, D. E., Lagerström, M. C., & Schiöth, H. B. (2004). The human and mouse repertoire of the adhesion family of G-protein-coupled receptors. Genomics, 84(1), 23-33.

Burbach, J. P. H., & Meijer, O. C. (1992). The structure of neuropeptide receptors. European Journal of Pharmacology: Molecular Pharmacology, 227(1), 1-18.

Cadet, P., Mantione, K. J., & Stefano, G. B. (2003). Molecular identification and functional expression of μ3, a novel alternatively spliced variant of the human μ opiate receptor gene. The Journal of Immunology, 170(10), 5118-5123.

Chakrabarti, S., Law, P. Y., & Loh, H. H. (1998). Distinct Differences Between Morphine-and [d-Ala2, N-MePhe4, Gly-ol5]-Enkephalin-μ-Opioid Receptor Complexes Demonstrated by Cyclic AMP-Dependent Protein Kinase Phosphorylation. Journal of neurochemistry, 71(1), 231-239.

Chakrabarti, S., Regec, A., & Gintzler, A. R. (2005). Biochemical demonstration of mu-opioid receptor association with Gsα: enhancement following morphine exposure. Molecular brain research, 135(1), 217-224.

Changeux, J. P., Kasai, M., & Lee, C. Y. (1970). Use of a snake venom toxin to characterize the cholinergic receptor protein. Proceedings of the National Academy of Sciences of the United States of America, 67, 1241–1247.

Chen, Y., Mestek, A. N. T. O. N., Liu, J. I. A. N., Hurley, J. A., & Yu, L. (1993). Molecular cloning and functional expression of a mu-opioid receptor from rat brain. Molecular Pharmacology, 44(1), 8-12.

Cherny, N., Ripamonti, C., Pereira, J., Davis, C., Fallon, M., McQuay, H., & Expert Working Group of the European Association of Palliative Care Network. (2001). Strategies to manage the adverse effects of oral morphine: an evidence-based report. Journal of Clinical Oncology, 19(9), 2542-2554.

Choi, H. S., Kim, C. S., Hwang, C. K., Song, K. Y., Wang, W., Qiu, Y., & Loh, H. H. (2006). The opioid ligand binding of human μ-opioid receptor is modulated by novel splice variants of the receptor. Biochemical and biophysical research communications, 343(4), 1132-1140.

Chou, K. C., Carlacci, L., Maggiora, G. M., Parodi, L. A., & Schulz, M. W. (1992). An energy-based approach to packing the 7-helix bundle of bacteriorhodopsin. Protein Science, 1(6), 810-827.

Clark, J. A., Liu, L., Price, M., Hersh, B., Edelson, M., & Pasternak, G. W. (1989). Kappa opiate receptor multiplicity: evidence for two U50, 488-sensitive kappa 1 subtypes and a novel kappa 3 subtype. Journal of Pharmacology and Experimental Therapeutics, 251(2), 461-468.

Collier, H. O. J., & Roy, A. C. (1974). Morphine-like drugs inhibit the stimulation by E prostaglandins of cyclic AMP formation by rat brain homogenate. Nature, 248, 24-27.

Collier, H. O. (1980). Cellular site of opiate dependence. Nature.

Conner, D. A., Mathier, M. A., Mortensen, R. M., Christe, M., Vatner, S. F., Seidman, C. E., & Seidman, J. G. (1997). β-Arrestin1 knockout mice appear normal but demonstrate altered cardiac responses to β-adrenergic stimulation. Circulation research, 81(6), 1021-1026.

Cronet, P., Sander, C., & Vriend, G. (1993). Modeling of transmembrane seven helix bundles. Protein engineering, 6(1), 59-64.

Daaka, Yehia, Louis M. Luttrell, and Robert J. Lefkowitz. "Switching of the coupling of the β2-adrenergic receptor to different G proteins by protein kinase A." Nature 390.6655 (1997): 88-91.

De Vries, L., Zheng, B., Fischer, T., Elenko, E., & Farquhar, M. G. (2000). The regulator of G protein signaling family. Annual review of pharmacology and toxicology, 40(1), 235-271.

Deng, H. B., Yu, Y., Pak, Y., O'Dowd, B. F., George, S. R., Surratt, C. K., & Wang, J. B. (2000). Role for the C-terminus in agonist-induced μ opioid receptor phosphorylation and desensitization. Biochemistry, 39(18), 5492-5499.

DeWire, S. M., Yamashita, D. S., Rominger, D. H., Liu, G., Cowan, C. L., Graczyk, T. M., & Koblish, M. (2013). A G protein-biased ligand at the μ-opioid receptor is potently analgesic with reduced gastrointestinal and respiratory dysfunction compared with morphine. Journal of Pharmacology and Experimental Therapeutics, 344(3), 708-717.

Donnelly, D., Johnson, M. S., Blundell, T. L., & Saunders, J. (1989). An analysis of the periodicity of conserved residues in sequence alignments of G-protein coupled receptors. FEBS letters, 251(1-2), 109-116.

Doyle, G. A., Sheng, X. R., Schwebel, C. L., Ferraro, T. N., Berrettini, W. H., & Buono, R. J. (2006). Identification and functional significance of polymorphisms in the μ-opioid receptor gene (Oprm) promoter of C57BL/6 and DBA/2 mice. Neuroscience research, 55(3), 244-254.

Doyle, G. A., Sheng, X. R., Lin, S. S., Press, D. M., Grice, D. E., Buono, R. J., & Berrettini, W. H. (2007). Identification of five mouse μ-opioid receptor (MOR) gene (Oprm1) splice variants containing a newly identified alternatively spliced exon. Gene, 395(1), 98-107.

Doyle, G. A., Sheng, X. R., Lin, S. S., Press, D. M., Grice, D. E., Buono, R. J., & Berrettini, W. H. (2007). Identification of three mouse μ-opioid receptor (MOR) gene (Oprm1) splice variants containing a newly identified alternatively spliced exon. Gene, 388(1), 135-147.

Ehlert, F. J. (2008). On the analysis of ligand-directed signaling at G protein-coupled receptors. Naunyn-Schmiedeberg's archives of pharmacology, 377(4-6), 549-577.

El Kouhen, R., Maestri-El Kouhen, O., Law, P. Y., & Loh, H. H. (1999). The absence of a direct correlation between the loss of [D-Ala2, MePhe4, Gly5-ol]

Enkephalin inhibition of adenylyl cyclase activity and agonist-induced μ-opioid receptor phosphorylation. Journal of Biological Chemistry, 274(14), 9207-9215.

El Kouhen, R., Burd, A. L., Erickson-Herbrandson, L. J., Chang, C. Y., Law, P. Y., & Loh, H. H. (2001). Phosphorylation of Ser363, Thr370, and Ser375 residues within the carboxyl tail differentially regulates μ-opioid receptor internalization. Journal of Biological Chemistry, 276(16), 12774-12780.

Eppler, C. M., Hulmes, J. D., Wang, J. B., Johnson, B., Corbett, M., Luthin, D. R., ... & Linden, J. (1993). Purification and partial amino acid sequence of a mu opioid receptor from rat brain. Journal of Biological Chemistry, 268(35), 26447-26451.

Ferguson SS, Z hang J, Barak L S, C aron MG (1998) Molecular mecha- nisms of G protein-coupled receptor desensitization and resensitiza- tion. Life Sci 62:1561–1565.

Ferguson, S. S. (2001). Evolving concepts in G protein-coupled receptor endocytosis: the role in receptor desensitization and signaling. Pharmacological reviews, 53(1), 1-24.

Figueroa, K. W., Griffin, M. T., & Ehlert, F. J. (2009). Selectivity of agonists for the active state of M1 to M4 muscarinic receptor subtypes. Journal of Pharmacology and Experimental Therapeutics, 328(1), 331-342.

Findlay, J. B., & Pappin, D. J. (1986). The opsin family of proteins. Biochemical Journal, 238(3), 625.

Foley, K. M. (1985). The treatment of cancer pain. New England Journal of Medicine, 313(2), 84-95.

Foley, K. M. (1996). Controlling the pain of cancer. Scientific American, 275(3), 164.

Freedman, N. J., Ament, A. S., Oppermann, M., Stoffel, R. H., Exum, S. T., & Lefkowitz, R. J. (1997). Phosphorylation and desensitization of human endothelin A and B receptors Evidence for G protein-coupled receptor kinase specificity. Journal of Biological Chemistry, 272(28), 17734-17743.

Fukuda, K., Kato, S., Mori, K., Nishi, M., Takeshima, H., Iwabe, N., & Sugimoto, T. (1994). cDNA cloning and regional distribution of a novel member of the opioid receptor family. FEBS letters, 343(1), 42-46.

Gainetdinov, R. R., Bohn, L. M., Walker, J. K., Laporte, S. A., Macrae, A. D., Caron, M. G. & Premont, R. T. (1999). Muscarinic supersensitivity and impaired receptor desensitization in G protein–coupled receptor kinase 5–deficient mice. Neuron, 24(4), 1029-1036.

Gainetdinov, R. R., Bohn, L. M., Sotnikova, T. D., Cyr, M., Laakso, A., Macrae, A. D., ... & Premont, R. T. (2003). Dopaminergic supersensitivity in G protein-coupled receptor kinase 6-deficient mice. Neuron, 38(2), 291-303.

Gesty-Palmer D., Flannery P., Yuan L., Corsino L., Spurney R., Lefkowitz R.J., Luttrell L.M. (2009) A beta-arrestin-biased agonist of the parathyroid hormone receptor (PTH1R) promotes bone formation independent of G protein activation. Sci. Transl. Med. 1:1ra1.

Gomes, I., Gupta, A., Filipovska, J., Szeto, H. H., Pintar, J. E., & Devi, L. A. (2004). A role for heterodimerization of μ and δ opiate receptors in enhancing morphine analgesia. Proceedings of the National Academy of Sciences of the United States of America, 101(14), 5135-5139.

Gomes, I., Fujita, W., Gupta, A., Saldanha, S. A., Negri, A., Pinello, C. E., & Devi, L. A. (2013). Identification of a μ-δ opioid receptor heteromer-biased agonist with antinociceptive activity. Proceedings of the National Academy of Sciences, 110(29), 12072-12077.

Goodman, R. R., Adler, B. A., & Pasternak, G. W. (1985). Regional differences in μ1-binding of [3H][d-Ala2, d-Leu5]-enkephalin: Comparisons of thalamus and cortex in the rat. Neuroscience letters, 59(2), 155-158.

Goodman, R. R., & Pasternak, G. W. (1985). Visualization of mu1 opiate receptors in rat brain by using a computerized autoradiographic subtraction technique. Proceedings of the National Academy of Sciences, 82(19), 6667-6671.

Gilman, A. G. (1987). G proteins: transducers of receptor-generated signals. Annual review of biochemistry, 56(1), 615-649.

Gregory, K. J., Hall, N. E., Tobin, A. B., Sexton, P. M., & Christopoulos, A. (2010). Identification of orthosteric and allosteric site mutations in M2 muscarinic acetylcholine receptors that contribute to ligand-selective signaling bias. Journal of Biological Chemistry, 285(10), 7459-7474.

Groer, C. E., Tidgewell, K., Moyer, R. A., Harding, W. W., Rothman, R. B., Prisinzano, T. E., & Bohn, L. M. (2007). An Opioid Agonist that Does Not Induce μ-Opioid Receptor—Arrestin Interactions or Receptor Internalization. Molecular pharmacology, 71(2), 549-557.

Guiramand, J., Montmayeur, J. P., Ceraline, J., Bhatia, M., & Borrelli, E. (1995). Alternative splicing of the dopamine D2 receptor directs specificity of coupling to G-proteins. Journal of Biological Chemistry, 270(13), 7354-7358.

Haberstock-Debic, H., Wein, M., Barrot, M., Colago, E. E., Rahman, Z., Neve, R. L., & Svingos, A. L. (2003). Morphine acutely regulates opioid receptor trafficking selectively in dendrites of nucleus accumbens neurons. The Journal of neuroscience, 23(10), 4324-4332.

Haga, T. A. T. S. U. Y. A., Haga, K., & Gilman, A. G. (1977). Hydrodynamic properties of the B-adrenergic receptor and adenylate cyclase from wild type and variant S49 lymphoma cells. J. biol. Chem, 252(5776), l977.

Harding, W. W., Tidgewell, K., Byrd, N., Cobb, H., Dersch, C. M., Butelman, E. R., ... & Prisinzano, T. E. (2005). Neoclerodane diterpenes as a novel

scaffold for μ opioid receptor ligands. Journal of medicinal chemistry, 48(15), 4765-4771.

Herrero-Turrion, M. J., & Rodríguez, R. E. (2008). Bioinformatic analysis of the origin, sequence and diversification of μ opioid receptors in vertebrates. Molecular Phylogenetics and Evolution, 49, 877–892.

Huang, W., Manglik, A., Venkatakrishnan, A. J., Laeremans, T., Feinberg, E. N., Sanborn, A. L., & Granier, S. (2015). Structural insights into mu-opioid receptor activation. Nature, 524(7565), 315-321.

Hwang, C.K., et al. Epigenetic programming of mu-opioid receptor gene in mouse brain is regulated by MeCP2 and Brg1 chromatin remodelling factor. Journal of cellular and molecular medicine 13, 3591-3615 (2009).

Hwang, C.K., et al. Evidence of endogenous mu opioid receptor regulation by epigenetic control of the promoters. Molecular and cellular biology 27, 4720-4736 (2007).

Iwata, K., Luo, J., Penn, R. B., & Benovic, J. L. (2005). Bimodal regulation of the human H1 histamine receptor by G protein-coupled receptor kinase 2. Journal of Biological Chemistry, 280(3), 2197-2204.

Jordan, B. A., & Devi, L. A. (1999). G-protein-coupled receptor heterodimerization modulates receptor function. Nature, 399(6737), 697–700. http://doi.org/10.1038/21441

Kahsai A.W., Xiao K., Rajagopal S., Ahn S., Shukla A.K., Sun J., Oas T.G., Lefkowitz R.J. (2011) Multiple ligand-specific conformations of the β2-adrenergic receptor. Nat. Chem. Biol. 7:692–700.

Keith, D. E., Murray, S. R., Zaki, P. A., Chu, P. C., Lissin, D. V., Kang, L., & von Zastrow, M. (1996). Morphine activates opioid receptors without causing their rapid internalization. Journal of Biological Chemistry, 271(32), 19021-19024.

Kenakin, T., Watson, C., Muniz-Medina, V., Christopoulos, A., & Novick, S. (2012). A simple method for quantifying functional selectivity and agonist bias. ACS chemical neuroscience, 3(3), 193-203.

Kenakin, T., & Christopoulos, A. (2013). Signalling bias in new drug discovery: detection, quantification and therapeutic impact. Nature Reviews Drug Discovery, 12(3), 205-216.

Kim, J., Ahn, S., Ren, X. R., Whalen, E. J., Reiter, E., Wei, H., & Lefkowitz, R. J. (2005). Functional antagonism of different G protein-coupled receptor kinases for β-arrestin-mediated angiotensin II receptor signaling. Proceedings of the National Academy of Sciences of the United States of America, 102(5), 1442-1447.

Kirchhausen, T. (1999). Adaptors for clathrin-mediated traffic. Annual review of cell and developmental biology, 15(1), 705-732.

Klein, G., Rossi, G. C., Waxman, A. R., Arout, C., Juni, A., Inturrisi, C. E., & Kest, B. (2009). The contribution of MOR-1 exons 1–4 to morphine and heroin analgesia and dependence. Neuroscience letters, 457(3), 115-119.

Kobilka, B. (1992). Adrenergic receptors as models for G protein-coupled receptors. Annual review of neuroscience, 15(1), 87-114.

Koch, T., Schulz, S., Schröder, H., Wolf, R., Raulf, E., & Höllt, V. (1998). Carboxyl-terminal splicing of the rat μ opioid receptor modulates agonist-mediated internalization and receptor resensitization. Journal of Biological Chemistry, 273(22), 13652-13657.

Koch, T., Schulz, S., Schröder, H., Wolf, R., Raulf, E., & Höllt, V. (1998). Carboxyl-terminal splicing of the rat μ opioid receptor modulates agonist-mediated internalization and receptor resensitization. Journal of Biological Chemistry, 273(22), 13652-13657.

Koch, T., Schulz, S., Pfeiffer, M., Klutzny, M., Schröder, H., Kahl, E., & Höllt, V. (2001). C-terminal splice variants of the mouse μ-opioid receptor differ in morphine-induced internalization and receptor resensitization. Journal of Biological Chemistry, 276(33), 31408-31414.

Kochanek, K. D., Murphy, S. L., & Xu, J. (2015). Deaths: Final Data for 2011. National vital statistics reports: from the centers for disease control and prevention, national center for health statistics, National Vital Statistics System, 63(3), 1-120.

Kohout, T. A., Lin, F. T., Perry, S. J., Conner, D. A., & Lefkowitz, R. J. (2001). β-Arrestin 1 and 2 differentially regulate heptahelical receptor signaling and trafficking. Proceedings of the National Academy of Sciences, 98(4), 1601-1606.

Krupnick JG, Benovic JL (1998) The role of receptor kinases and arrestins in G protein-coupled receptor regulation. Annu Rev Pharmacol Toxicol 38:289–319.

Lau, E. K., Trester-Zedlitz, M., Trinidad, J. C., Kotowski, S. J., Krutchinsky, A. N., Burlingame, A. L., & von Zastrow, M. (2011). Quantitative encoding of a partial agonist effect on individual opioid receptors by multi-site phosphorylation and threshold detection. Science signaling, 4(185), ra52.

Law, P. Y., Erickson, L. J., El-Kouhen, R., Dicker, L., Solberg, J., Wang, W., & Loh, H. H. (2000). Receptor density and recycling affect the rate of agonist-induced desensitization of μ-opioid receptor. Molecular pharmacology, 58(2), 388-398.

Lefkowitz RJ (1998) G protein-coupled receptors. III. New roles for receptor kinases and beta-arrestins in receptor signaling and desensi- tization. J Biol Chem 273:18677–18680.

Lefkowitz, R. J. (2000). The superfamily of heptahelical receptors. Nature Cell Biology, 2(7), E133-E136.

Limbird, L. E., & Lefkowitz, R. J. (1977). Resolution of beta-adrenergic receptor binding and adenylate cyclase activity by gel exclusion chromatography. Journal of Biological Chemistry, 252(2), 799-802.

Limbird, L. E., & Lefkowitz, R. J. (1978). Agonist-induced increase in apparent β-adrenergic receptor size. Proceedings of the National Academy of Sciences, 75(1), 228-232.

Lohse, M. J., Andexinger, S., Pitcher, J., Trukawinski, S., Codina, J., Faure, J. P., ... & Lefkowitz, R. J. (1992). Receptor-specific desensitization with purified proteins. Kinase dependence and receptor specificity of beta-arrestin and arrestin in the beta 2-adrenergic receptor and rhodopsin systems. Journal of Biological Chemistry, 267(12), 8558-8564.

Lucas, J. J., & Hen, R. (1995). New players in the 5-HT receptor field: genes and knockouts. Trends in pharmacological sciences, 16(7), 246-252.

Manglik, A., Kruse, A. C., Kobilka, T. S., Thian, F. S., Mathiesen, J. M., Sunahara, R. K. & Granier, S. (2012). Crystal structure of the [micro]-opioid receptor bound to a morphinan antagonist. Nature, 485(7398), 321-326.

McPherson, J., Rivero, G., Baptist, M., Llorente, J., Al-Sabah, S., Krasel, C., & Henderson, G. (2010). μ-Opioid receptors: correlation of agonist efficacy for signalling with ability to activate internalization. Molecular pharmacology, 78(4), 756-766.

McWilliams, L. A., Cox, B. J., & Enns, M. W. (2003). Mood and anxiety disorders associated with chronic pain: An examination in a nationally representative sample. Pain, 106, 127–133.

Molinari, P., Vezzi, V., Sbraccia, M., Grò, C., Riitano, D., Ambrosio, C., & Costa, T. (2010). Morphine-like opiates selectively antagonize receptor-arrestin interactions. Journal of biological chemistry, 285(17), 12522-12535.

Moore, C. A., Milano, S. K., & Benovic, J. L. (2007). Regulation of receptor trafficking by GRKs and arrestins. Annu. Rev. Physiol., 69, 451-482.

Moulédous, L., Froment, C., Burlet-Schiltz, O., Schulz, S., & Mollereau, C. (2015). Phosphoproteomic analysis of the mouse brain mu‐opioid (MOP) receptor. FEBS letters, 589(18), 2401-2408.

Namba, T., Sugimoto, Y., Negishi, M., Irie, A., Ushikubi, F., Kakizuka, A., & Narumiya, S. (1993). Alternative splicing of C-terminal tail of prostaglandin E receptor subtype EP3 determines G-protein specificity. Nature, 365(6442), 166-170.

Nordström, K. J., Lagerström, M. C., Wallér, L. M., Fredriksson, R., & Schiöth, H. B. (2009). The Secretin GPCRs descended from the family of Adhesion GPCRs. Molecular biology and evolution, 26(1), 71-84.

Oakley, R. H., Laporte, S. A., Holt, J. A., Barak, L. S., & Caron, M. G. (1999). Association of β-arrestin with G protein-coupled receptors during clathrin-mediated endocytosis dictates the profile of receptor resensitization. Journal of Biological Chemistry, 274(45), 32248-32257.

Oakley, R. H., Laporte, S. A., Holt, J. A., Caron, M. G., & Barak, L. S. (2000). Differential affinities of visual arrestin, βarrestin1, and βarrestin2 for G protein-coupled receptors delineate two major classes of receptors. Journal of Biological Chemistry, 275(22), 17201-17210

Oakley, R. H., Laporte, S. A., Holt, J. A., Barak, L. S., & Caron, M. G. (2001). Molecular determinants underlying the formation of stable intracellular G protein-coupled receptor-β-arrestin complexes after receptor endocytosis. Journal of Biological Chemistry, 276(22), 19452-19460.

Oldfield, S., Braksator, E., Rodriguez-Martin, I., Bailey, C. P., Donaldson, L. F., Henderson, G., & Kelly, E. (2008). C-terminal splice variants of the μ-opioid receptor: existence, distribution and functional characteristics. Journal of neurochemistry, 104(4), 937-945.

Overington, J., Donnelly, D., Johnson, M. S., Šali, A., & Blundell, T. L. (1992). Environment-specific amino acid substitution tables: tertiary templates and prediction of protein folds. Protein Science, 1(2), 216-226.

Pan, L., Xu, J., Yu, R., Xu, M.M., Pan, Y.X., Pasternak, G.W., 2005a. Identification and characterization of six new alternatively spliced variants of the human mu opioid receptor gene. Oprm. Neurosci. 133, 209e220.

Pan, Y.-X., Xu, J.Y., Xu, M.M., Yu, R., Bolan, E., Gilbert, A.K., Pasternak, G.W., 2009a. Isolation and expression of three new splice variants, mMOR-1A, mMOR-1O and mMOR-1P, from mouse mu opioid receptor gene. Oprm. submitted for publication.

Pan, Y.X., 2005. Diversity and complexity of the mu opioid receptor gene: alter- native pre-mRNA splicing and promoters. DNA Cell. Biol. 24, 736e750.

Pan, Y.X., Xu, J., Bolan, E., Chang, A., Mahurter, L., Rossi, G., Pasternak, G.W., 2000. Isolation and expression of a novel alternatively spliced mu opioid receptor isoform, MOR-1F. FEBS Lett. 466, 337e340.

Pan, Y.X., Xu, J., Bolan, E.A., Abbadie, C., Chang, A., Zuckerman, A., Rossi, G.C., Pasternak, G.W., 1999. Identification and characterization of three new alter- natively spliced mu opioid receptor isoforms. Mol. Pharmacol. 56, 396e403.

Pan, Y.-X., 2000. Identification and characterization of a novel promoter of a mouse mu opioid receptor gene (Oprm) that generates eight splice variants. Gene 295, 97e108.

Pan, Y.-X., Xu, J., Mahurter, L., Bolan, E., Xu, M., & Pasternak, G. W. (2001). Generation of the mu opioid receptor (MOR-1) protein by three new splice variants of the Oprm gene. Proceedings of the National Academy of

Sciences of the United States of America, 98(24), 14084–9. http://doi.org/10.1073/pnas.241296098

Pan, Y.X., Xu, J., Mahurter, L., Xu, M., Gilbert, A.K., Pasternak, G.W., 2003. Identification and characterization of two new human mu opioid receptor splice variants, hMOR-1O and hMOR-1X. Biochem. Biophys. Res. Commun. 301, 1057e1061.

Pan, Y., Xu, J., Bolan, E., Moskowitz, H. S., Xu, M., & Pasternak, G. W. (2005). Identification of Four Novel Exon 5 Splice Variants of the Mouse -Opioid Receptor Gene: Functional Consequences of C-Terminal Splicing, 68(3), 866–875. http://doi.org/10.1124/mol.105.011858.

Pan, Y.-X., Xu, J., Xu, M., Rossi, G. C., Matulonis, J. E., & Pasternak, G. W. (2009). Involvement of exon 11-associated variants of the mu opioid receptor MOR-1 in heroin, but not morphine, actions. Proceedings of the National Academy of Sciences, 106(12), 4917–4922.

Pak, Y., O'Dowd, B. F., & George, S. R. (1997). Agonist-induced desensitization of the μ opioid receptor is determined by threonine 394 preceded by acidic amino acids in the COOH-terminal tail. Journal of Biological Chemistry, 272(40), 24961-24965.

Pasternak, G. W., Gintzler, A. R., Houghten, R. A., Ling, G. S. F., Goodman, R. R., Spiegel, K., ... & Recht, L. D. (1983). Biochemical and pharmacological

evidence for opioid receptor multiplicity in the central nervous system. Life sciences, 33, 167-173.

Pasternak, G. W., & Wood, P. J. (1986). Minireview: Multiple mu opiate receptors. Life sciences, 38(21), 1889-1898.

Pasternak, G. W., Bodnar, R. J., Clark, J. A., & Inturrisi, C. E. (1987). Morphine-6-glucuronide, a potent mu agonist. Life sciences, 41(26), 2845-2849.

Pasternak, D. A., Pan, L., Xu, J., Yu, R., Xu, M. M., Pasternak, G. W., & Pan, Y. X. (2004). Identification of three new alternatively spliced variants of the rat mu opioid receptor gene: dissociation of affinity and efficacy. Journal of neurochemistry, 91(4), 881-890.

Pert, C. B., & Snyder, S. H. (1973). Opiate receptor: demonstration in nervous tissue. Science, 179(4077), 1011-1014.

Pert, C. B., Pasternak, G., & Snyder, S. H. (1973). Opiate agonists and antagonists discriminated by receptor binding in brain. Science 182, 1359-1361 (1973).

Pierce, K. L., Premont, R. T., & Lefkowitz, R. J. (2002). Seven-transmembrane receptors. Nature Reviews Molecular Cell Biology, 3(9), 639-650.

Portoghese, P. S. (1966). Stereochemical factors and receptor interactions associated with narcotic analgesics. Journal of pharmaceutical sciences, 55(9), 865-887.

Raehal, K. M., Walker, J. K., & Bohn, L. M. (2005). Morphine side effects in β-arrestin 2 knockout mice. Journal of Pharmacology and Experimental Therapeutics, 314(3), 1195-1201.

Raehal, K. M., Schmid, C. L., Groer, C. E., & Bohn, L. M. (2011). Functional selectivity at the μ-opioid receptor: implications for understanding opioid analgesia and tolerance. Pharmacological Reviews, 63(4), 1001-1019.

Rajagopal, S., Ahn, S., Rominger, D. H., Gowen-MacDonald, W., Lam, C. M., DeWire, S. M., & Lefkowitz, R. J. (2011). Quantifying ligand bias at seven-transmembrane receptors. Molecular pharmacology, 80(3), 367-377.

Rajagopal, S. (2013). Quantifying biased agonism: understanding the links between affinity and efficacy. Nature Reviews Drug Discovery, 12(6), 483-483.

Ren, X. R., Reiter, E., Ahn, S., Kim, J., Chen, W., & Lefkowitz, R. J. (2005). Different G protein-coupled receptor kinases govern G protein and β-arrestin-mediated signaling of V2 vasopressin receptor. Proceedings of the National Academy of Sciences of the United States of America, 102(5), 1448-1453.

Rivero, G., Llorente, J., McPherson, J., Cooke, A., Mundell, S. J., McArdle, C. A., & Henderson, G. (2012). Endomorphin-2: a biased agonist at the μ-opioid receptor. Molecular pharmacology, 82(2), 178-188.

Rodbell, M., Birnbaumer, L., Pohl, S. L., & Krans, H. M. J. (1971). The glucagon-sensitive adenyl cyclase system in plasma membranes of rat liver V. An obligatory role of guanyl nucleotides in glucagon action. Journal of Biological Chemistry, 246(6), 1877-1882.

Ross, E. M., & Wilkie, T. M. (2000). GTPase-activating proteins for heterotrimeric G proteins: regulators of G protein signaling (RGS) and RGS-like proteins. Annual review of biochemistry, 69(1), 795-827.

Rossi, G., Pan, Y. X., Cheng, J., & Pasternak, G. W. (1994). Blockade of morphine analgesia by an antisense oligodeoxynucleotide against the mu receptor. Life sciences, 54(21), PL375-PL379.

Rossi, G. C., Pan, Y. X., Brown, G. P., & Pasternak, G. W. (1995). Antisense mapping the MOR-1 opioid receptor: evidence for alternative splicing and a novel morphine-6β-glucuronide receptor. FEBS letters, 369(2-3), 192-196.

Rossi, G. C., Standifer, K. M., & Pasternak, G. W. (1995). Differential blockade of morphine and morphine-6β-glucuronide analgesia by antisense oligodeoxynucleotides directed against MOR-1 and G-protein α subunits in rats. Neuroscience letters, 198(2), 99-102.

Rossi, G. C., Brown, G. P., Leventhal, L., Yang, K., & Pasternak, G. W. (1996). Novel receptor mechanisms for heroin and morphine-6β-glucuronide analgesia. Neuroscience letters, 216(1), 1-4.

Saidak, Z., Blake-Palmer, K., Hay, D. L., Northup, J. K., & Glass, M. (2006). Differential activation of G-proteins by μ-opioid receptor agonists. British journal of pharmacology, 147(6), 671-680.

Sanchez-Blazquez, P., DeANTONIO, I., RODRÍGUEZ-DÍAZ, M., & Garzon, J. (1999). Antisense oligodeoxynucleotides targeting distinct exons of the cloned mu-opioid receptor distinguish between endomorphin-1 and morphine supraspinal antinociception in mice. Antisense and Nucleic Acid Drug Development, 9(3), 253-260.

Schiöth, H. B., Nordström, K. J. V., & Fredriksson, R. (2007). Mining the gene repertoire and ESTs for G protein-coupled receptors with evolutionary perspective. Acta physiologica, 190(1), 21-31.

Schulz, S., Mayer, D., Pfeiffer, M., Stumm, R., Koch, T., & Höllt, V. (2004). Morphine induces terminalμ-opioid receptor desensitization by sustained phosphorylation of serine-375. The EMBO journal, 23(16), 3282-3289.

Shapira, M. A., Vogel, Z., & Sarne, Y. (2000). Opioid and cannabinoid receptors share a common pool of GTP-binding proteins in cotransfected cells, but not in cells which endogenously coexpress the receptors. Cellular and molecular neurobiology, 20(3), 291-304.

Sharma, S. K., Nirenberg, M., & Klee, W. A. (1975). Morphine receptors as regulators of adenylate cyclase activity. Proceedings of the National Academy of Sciences, 72(2), 590-594.

Shorr, R. G., Lefkowitz, R. J., & Caron, M. G. (1981). Purification of the beta-adrenergic receptor. Identification of the hormone binding subunit. Journal of Biological Chemistry, 256(11), 5820-5826.

Shorr, R. G., Strohsacker, M. W., Lavin, T. N., Lefkowitz, R. J., & Caron, M. G. (1982). The beta 1-adrenergic receptor of the turkey erythrocyte. Molecular heterogeneity revealed by purification and photoaffinity labeling. Journal of Biological Chemistry, 257(20), 12341-12350.

Sibley, D. R., Strasser, R. H., Benovic, J. L., Daniel, K., & Lefkowitz, R. J. (1986). Phosphorylation/dephosphorylation of the beta-adrenergic receptor regulates its functional coupling to adenylate cyclase and subcellular distribution. Proceedings of the National Academy of Sciences, 83(24), 9408-9412.

Simon, E. J., Hiller, J. M., & Edelman, I. (1973). Stereospecific binding of the potent narcotic analgesic [3H] etorphine to rat-brain homogenate. Proceedings of the National Academy of Sciences, 70(7), 1947-1949.

Soergel, D. G., Subach, R. A., Burnham, N., Lark, M. W., James, I. E., Sadler, B. M., & Webster, L. R. (2014). Biased agonism of the μ-opioid receptor by TRV130 increases analgesia and reduces on-target adverse

effects versus morphine: a randomized, double-blind, placebo-controlled, crossover study in healthy volunteers. PAIN®, 155(9), 1829-1835.

Standifer, K. M., Cheng, J., Brooks, A. I., Honrado, C. P., Su, W., Visconti, L. M., & Pasternak, G. W. (1994). Biochemical and pharmacological characterization of mu, delta and kappa 3 opioid receptors expressed in BE (2)-C neuroblastoma cells. Journal of Pharmacology and Experimental Therapeutics, 270(3), 1246-1255.

Standifer, K. M., Rossi, G. C., & Pasternak, G. W. (1996). Differential blockade of opioid analgesia by antisense oligodeoxynucleotides directed against various G protein alpha subunits. Molecular pharmacology, 50(2), 293-298.

Strader, C. D., Fong, T. M., Tota, M. R., Underwood, D., & Dixon, R. A. (1994). Structure and function of G protein-coupled receptors. Annual review of biochemistry, 63(1), 101-132.

Stryer, L. (1986). Cyclic GMP cascade of vision. Annual review of neuroscience, 9(1), 87-119.

Sutherland, E. W. In Cyclic AMP 5–13 (Academic Press, NewYork, 1971).

Swaminath G., Xiang Y., Lee T.W., Steenhuis J., Parnot C., Kobilka B.K. (2004) Sequential binding of agonists to the beta2 adrenoceptor. Kinetic evidence for intermediate conformational states. J. Biol. Chem. 279:686–691.

Tanowitz, M., Hislop, J. N., & von Zastrow, M. (2008). Alternative splicing determines the post-endocytic sorting fate of G-protein-coupled receptors. Journal of Biological Chemistry, 283(51), 35614-35621.

Terenius, L. (1973). Stereospecific interaction between narcotic analgesics and a synaptic plasma membrane fraction of rat cerebral cortex. Acta pharmacologica et toxicologica, 32(3–4), 317-320.

Thompson, R. C., Mansour, A., Akil, H., & Watson, S. J. (1993). Cloning and pharmacological characterization of a rat μ opioid receptor. Neuron, 11(5), 903-913.

Traynor, J. R., Clark, M. J., & Remmers, A. E. (2002). Relationship between rate and extent of G protein activation: comparison between full and partial opioid agonists. Journal of Pharmacology and Experimental Therapeutics, 300(1), 157-161.

van der Westhuizen, E. T., Breton, B., Christopoulos, A., & Bouvier, M. (2014). Quantification of ligand bias for clinically relevant β2-adrenergic receptor ligands: implications for drug taxonomy. Molecular pharmacology, 85(3), 492-509.

Vanetti, M., Kouba, M., Wang, X., Vogt, G., & Höllt, V. (1992). Cloning and expression of a novel mouse somatostatin receptor (SSTR2B). FEBS letters, 311(3), 290-294.

Viscusi, E. R., Webster, L., Kuss, M., Daniels, S., Bolognese, J. A., Zuckerman, S., & Skobieranda, F. (2016). A randomized, phase 2 study investigating TRV130, a biased ligand of the μ-opioid receptor, for the intravenous treatment of acute pain. Pain, 157(1), 264-272.

Walters R.W., Shukla A.K., Kovacs J.J., Violin J.D., DeWire S.M., Lam C.M., Chen J.R., Muehlbauer M.J., Whalen E.J., Lefkowitz R.J. (2009) β-Arrestin1 mediates nicotinic acid-induced flushing, but not its antilipolytic effect, in mice. J. Clin. Invest. 119:1312–1321.

Wang, J. B., Imai, Y., Eppler, C. M., Gregor, P., Spivak, C. E., & Uhl, G. R. (1993). mu opiate receptor: cDNA cloning and expression. Proceedings of the National Academy of Sciences, 90(21), 10230-10234.

Ward, S. J., Portoghese, P. S., & Takemori, A. E. (1982). Pharmacological characterization in vivo of the novel opiate, beta-funaltrexamine. Journal of Pharmacology and Experimental Therapeutics, 220(3), 494-498.

Whistler, J. L., & Von Zastrow, M. (1998). Morphine-activated opioid receptors elude desensitization by β-arrestin. Proceedings of the National Academy of Sciences, 95(17), 9914-9919.

White, K. L., Scopton, A. P., Rives, M. L., Bikbulatov, R. V., Polepally, P. R., Brown, P. J., & Roth, B. L. (2014). Identification of novel functionally selective κ-opioid receptor scaffolds. Molecular pharmacology, 85(1), 83-90.

Williams, J. T., Ingram, S. L., Henderson, G., Chavkin, C., von Zastrow, M., Schulz, S., & Christie, M. J. (2013). Regulation of μ-opioid receptors: Desensitization, phosphorylation, internalization, and tolerance. Pharmacological reviews, 65(1), 223-254.

Wolf, R., Koch, T., Schulz, S., Klutzny, M., Schröder, H., Raulf, E., ... & Höllt, V. (1999). Replacement of threonine 394 by alanine facilitates internalization and resensitization of the rat μ opioid receptor. Molecular pharmacology, 55(2), 263-268.

Wolozin, B.L. & Pasternak, G.W. (1981). Classification of multiple morphine and enkephalin binding sites in the central nervous system. Proceedings of the National Academy of Sciences of the United States of America 78, 6181-6185.

Wu, H. E., Mizoguchi, H., Terashvili, M., Leitermann, R. J., Hung, K. C., Fujimoto, J. M., & Tseng, L. F. (2002). Spinal pretreatment with antisense oligodeoxynucleotides against exon-1,-4, or-8 of μ-opioid receptor clone leads to differential loss of spinal endomorphin-1-and endomorphin-2-induced antinociception in the mouse. Journal of Pharmacology and Experimental Therapeutics, 303(2), 867-873.

Xu, J., Xu, M., Hurd, Y.L., Pasternak, G.W. & Pan, Y.X. (2009). Isolation and characterization of new exon 11-associated N-terminal splice variants of the human mu opioid receptor gene. Journal of neurochemistry 108, 962-972.

Xu, J., Xu, M., Rossi, G.C., Pasternak, G.W. & Pan, Y.X. (2011). Identification and characterization of seven new exon 11-associated splice variants of the rat mu opioid receptor gene, OPRM1. Molecular pain 7, 9

Xu, Y. & Carr, L.G. (2001). Functional characterization of the promoter region of the human mu opioid receptor (hMOR) gene: identification of activating and inhibitory regions. Cellular and molecular biology 47 Online Pub, OL29-38

Xu, Y. & Carr, L.G. (2001). Transcriptional regulation of the human mu opioid receptor (hMOR) gene: evidence of positive and negative cis-acting elements in the proximal promoter and presence of a distal promoter. DNA and cell biology 20, 391-402.

Yekkirala, A. S., Kalyuzhny, A. E., & Portoghese, P. S. (2009). Standard opioid agonists activate heteromeric opioid receptors: Evidence for morphine and [D-Ala2-MePhe4-Glyol5] enkephalin as selective μ− δ agonists. ACS chemical neuroscience, 1(2), 146-154.

Yu, Y., Zhang, L., Yin, X., Sun, H., Uhl, G. R., & Wang, J. B. (1997). μ Opioid receptor phosphorylation, desensitization, and ligand efficacy. Journal of Biological Chemistry, 272(46), 28869-28874.

Zamah, A. M., Delahunty, M., Luttrell, L. M., & Lefkowitz, R. J. (2002). Protein Kinase A-mediated Phosphorylation of the β2-Adrenergic Receptor Regulates Its Coupling to Gs and Gi DEMONSTRATION IN A

RECONSTITUTED SYSTEM. Journal of Biological Chemistry, 277(34), 31249-31256.

Zhang, L., Yu, Y., Mackin, S., Weight, F. F., Uhl, G. R., & Wang, J. B. (1996). Differential opiate receptor phosphorylation and desensitization induced by agonists and phorbol esters. Journal of Biological Chemistry, 271(19), 11449-11454.

Zhang, J., Ferguson, S. S., Barak, L. S., Bodduluri, S. R., Laporte, S. A., Law, P. Y., & Caron, M. G. (1998). Role for G protein-coupled receptor kinase in agonist-specific regulation of μ-opioid receptor responsiveness. Proceedings of the National Academy of Sciences, 95(12), 7157-7162.

Zimmerman B., Beautrait A., Aguila B., Charles R., Escher E., Claing A., Bouvier M., Laporte S.A. (2012) Differential β-arrestin-dependent conformational signaling and cellular responses revealed by angiotensin analogs. Sci. Signaling 5:ra33.

Zimprich, A., Simon, T., & Höllt, V. (1995). Cloning and expression of an isoform of the rat μ opioid receptor (rMOR1B) which differs in agonist induced desensitization from rMOR1. FEBS letters, 359(2), 142-146.

Supplemental Figure:

Copyright permission to reproduce Figure

Title:	The superfamily of heptahelical receptors
Author:	Robert J. Lefkowitz
Publication:	Nature Cell Biology
Publisher:	Nature Publishing Group
Date:	Jul 1, 2000

Logged in as:
Ankita Narayan

LOGOUT

Order Completed

Thank you for your order.

This Agreement between Ankita Narayan ("You") and Nature Publishing Group ("Nature Publishing Group") consists of your license details and the terms and conditions provided by Nature Publishing Group and Copyright Clearance Center.

Your confirmation email will contain your order number for future reference.

Printable details.

License Number	4021430438341
License date	Jan 03, 2017
Licensed Content Publisher	Nature Publishing Group
Licensed Content Publication	Nature Cell Biology
Licensed Content Title	The superfamily of heptahelical receptors
Licensed Content Author	Robert J. Lefkowitz
Licensed Content Date	Jul 1, 2000
Licensed Content Volume	2
Licensed Content Issue	7
Type of Use	reuse in a dissertation / thesis
Requestor type	academic/educational
Format	print and electronic
Portion	figures/tables/illustrations
Number of figures/tables/illustrations	1
Figures	7 transmembrane structure of the receptor
Author of this NPG article	no
Your reference number	
Title of your thesis / dissertation	C-TERMINAL SPLICE VARIANTS OF THE MU OPIOID RECEPTOR DIFFERENTIALLY REGULATE SIGNAL TRANSDUCTION AND LIGAND BIAS
Expected completion date	Jan 2017
Estimated size (number of pages)	200
Requestor Location	Ankita Narayan 1330 1st Avenue NEW YORK, NY 10021 United States Attn: Ankita Narayan
Billing Type	Invoice
Billing address	Ankita Narayan 1330 1st Avenue NEW YORK, NY 10021